universität wien

DISSERTATION

Titel der Dissertation

„The role of Ca^{2+} Dependent Protein Kinase 3 in *Arabidopsis thaliana* during salt stress acclimation“

Verfasser

Mag.rer.nat. Bernhard Wurzinger

angestrebter akademischer Grad

Doktor der Naturwissenschaften (Dr. rer. nat.)

Dissertationsgebiet (lt. Studienblatt): Studienkennzahl:	Dr.-Studium der Naturwissenschaften Genetik - Mikrobiologie (Stzw) A 091 441
Betreuer:	Dr. Markus Teige
Wien 2011	

Intelligent ist alles was dem Zufall zuvorkommt
(Intelligent is everything that comes in advance to chance)
Bernie

TABLE OF CONTENTS

1. Introduction

In order to successfully grow, plants have to adapt to their continuously changing environment. For spontaneous changes in the environment the classical paradigm of information processing holds true; Sensing of a stimulus initiates signal transduction processes which subsequently allow the cell to generate an appropriate response to the initial stimulus. Considering the myriad of different stimuli one may ask how a cell achieves an appropriate response?

One common way how organisms translate an extracellular stimulus into an intracellular chemical signal is the use of so called second messengers (eg. Ca^{2+}, cAMP, cGMP and many other small molecules). Amongst these, Ca^{2+} ions are probably the most versatile second messengers in plant cells.

1.1. Ca^{2+} as second messenger

Ca^{2+} is unequally distributed throughout the different compartments of a plant cell. The most favoured explanation for this is, that the cytosolic metabolism of a plant cell requires high concentrations of orthophosphate (P_i), which would form insoluble complexes with Ca^{2+} at millimolar concentrations. Therefore, during evolution of the cell, systems evolved to actively maintain the concentration of free Ca^{2+} in the cytosol at sub micromolar levels (~200 nM) [1,2,84]. The main storage compartments for free Ca^{2+} in the plant cell are the vacuole, the apoplast, the ER and the mitochondria. In all these compartments the concentration of free Ca^{2+} is at least 10 times higher than in the cytosol. The resulting electrochemical potential difference for Ca^{2+} across the membrane allows then for rapid changes in cytosolic free Ca^{2+} concentration, as desired for a signalling molecule.

Two of the most intriguing aspects of Ca^{2+} are its complex spatial and temporal concentration patterns evoked by a wide variety of biotic as well as abiotic stimuli. Attack by herbivores, pathogen elicitors, different hormones, salt, osmotic and drought stress, temperature changes as well as circadian changes are a few examples of stimuli that each lead to a distinct Ca^{2+} signal [3-6].

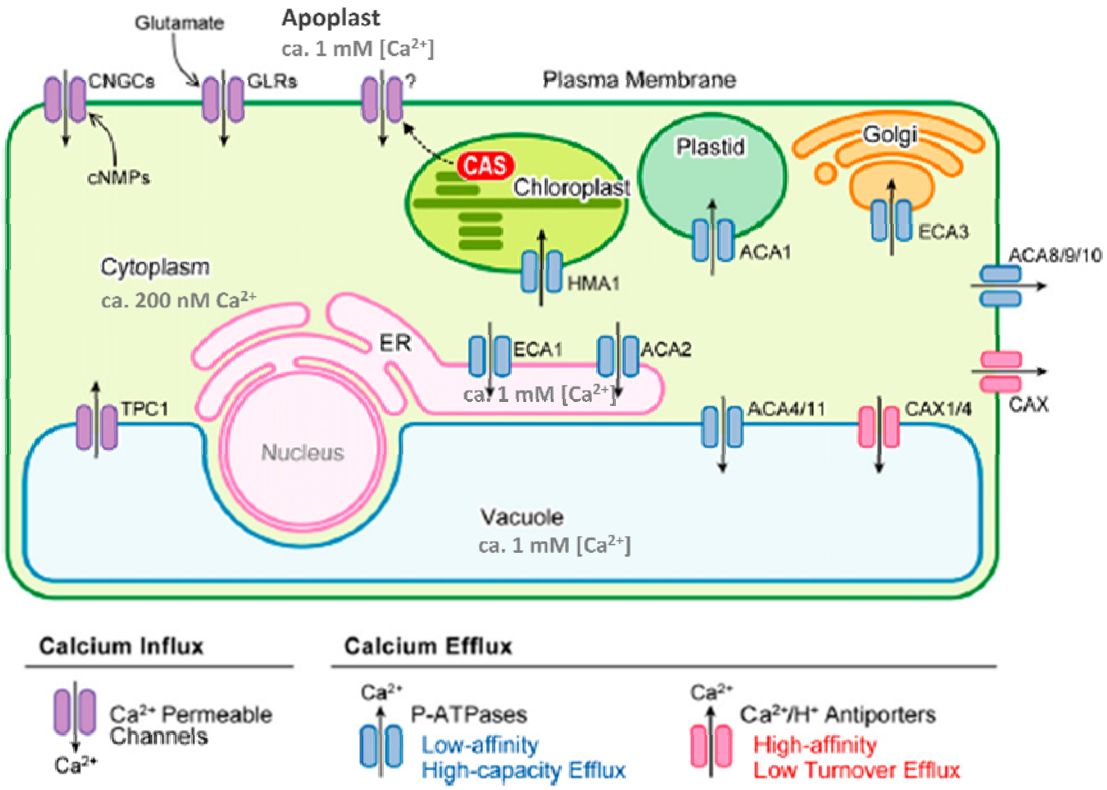

Fig1. Ca^{2+} transport systems in the plant cell, adapted from [3]. Shown are Ca^{2+} transport systems that are characterized so far. CNGC, cyclic nucleotide channel; GLR, glutamate receptor; TPC, two pore channel; CAS, Ca^{2+} sensing receptor; ACA autoinhibited calcium ATPase; ECA, ER type calcium ATPase; HMA, heavy metal ATPase; CAX, cation exchanger;

1.2. Ca^{2+} perception in the plant cell

However, sticking to the scheme of information processing free Ca^{2+} ions are only the first part in a signal transduction cascade leading to physiological adaptation of the cell to the initial stimulus. On the second position in the Ca^{2+} signalling cascade are Ca^{2+}-sensors. In plants three main classes of protein Ca^{2+} sensors are found, which are further involved in the Ca^{2+} dependent signal transduction process: Calmodulins (CaM), calmodulin like proteins (CML) and calcineurin B like protein (CBL).

1.2.1. CaM and CML

CaMs are ubiquitous proteins in all eukaryotes analyzed so far. They form complexes with Ca^{2+} via so called "EF hand" motives, where a calcium binding loop is flanked by an E and a F helix [7]. The canonical CaM sequence contains 4 of such EF hands. Upon binding of Ca^{2+} CaMs change their conformation in a way that a larger hydrophobic domain of the protein gets exposed at its surface. This domain then interacts with other proteins in the cell thereby

altering their enzymatic activity. In the *Arabidopsis thaliana (A.thaliana)* genome 7 CaMs are encoded which belong to only 4 protein isoforms [8].

CMLs are proteins that, like CaMs, only contain EF hand motives, lacking any additionally known functional domain on their poly peptide chain. In *A.thaliana* 50 proteins fall into the family of CMLs. As the name suggests CML amino acid sequences differ up to 84 % and they contain a variable number of EF hand motives (1 - 6 EF hands in *A.thaliana*) [8].

The function of CaMs and CMLs in the cell seems to be as versatile as the whole Ca^{2+} response. Proteins of both families participate in biotic as well as abiotic responses. Furthermore CaMs and CMLs target proteins in different functional categories ranging from cytoskeleton proteins, channels and pumps, metabolic enzymes to transcription factors [9]. Interestingly, for AtCaM7, it was shown that calmodulin itself, regulates transcription by direct interaction with the DNA promoter of light inducible genes [10]. One further fascinating fact is, that the protein family of CaMKs, which seems to be ubiquitous in animals, is missing or largely underrepresented in plants.

1.2.3. CBL

CBLs in plants consist of 4 EF hand domains, like CaMs. However, their overall sequence is not identical to the one of CaM. So far CBLs have been found to interact with a protein kinase family termed CIPKs in plants. This is particularly interesting as calcineurin B in animals interacts with a protein phosphatase. Based on sequence homology search 10 CBLs are present in the *A.thaliana* genome. Together with the calcineurin B interacting protein kinases (CIPKs) the CBLs build up a complex signalling network. [11, 12]

1.3. Ca^{2+} regulated protein kinases

All together there are 67 CaMs, CMLs and CBLs encoded in the *A.thaliana* genome. Nevertheless, an almost equally large group of 60 protein kinases, which are directly regulated in a calcium dependent manner, is present in the *A.thaliana* genome also. Considering the fact that CBLs seem to exclusively regulate CIPKs, the Ca^{2+} regulated protein kinases most likely make up for the functionally most versatile block in the Ca^{2+} signal transduction network in *A.thaliana* in terms of posttranslational modification. A little bit surprising, at least to the author of this thesis, is the fact that all Ca^{2+} regulated protein kinases in plants, characterized so far, belong to the "super-group" of yeast SnF1 related S/T kinases [15]. According to sequence similarity data three main groups of these protein kinases are present in plants. As a common feature, CPKs and CCaMKs encode Ca^{2+} binding

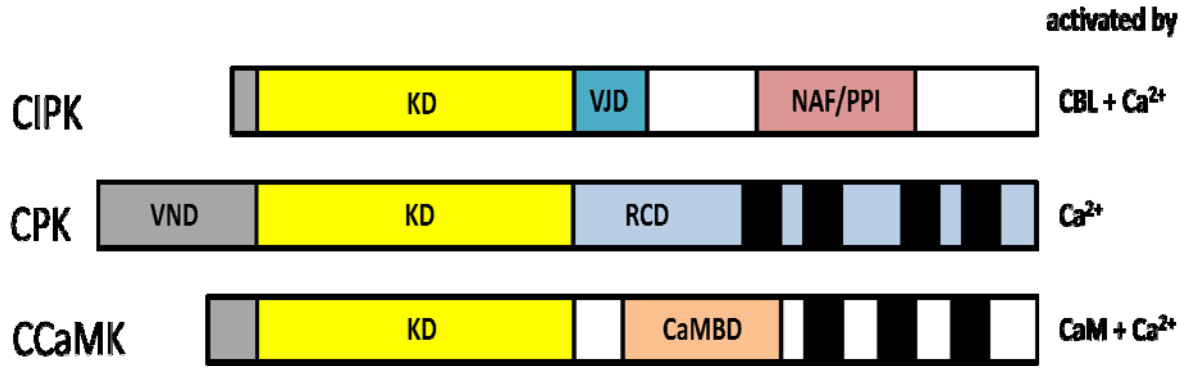

Fig2. The three families of Ca^{2+} regulated protein kinases in plants. The column on the right indicates which factors are needed for kinase activation by Ca^{2+}. KD, conserved SNF1 related S/T kinase domain; VND, variable N-terminal domain; VJD, variable junction domain; NAF/PPI, CBL/PP2C interaction domain; RCD, regulatory C-terminal domain; CaMBD, calmodulin binding domain; black boxes symbolize EF hand structures.

motives and the kinase domain on the same polypeptide chain. In the case of CIPKs the binding motives for CBLs "replace" the Ca^{2+} binding motives of the other two groups. (Figure 2)

1.3.1. CIPK (calcineurin B like protein interacting protein kinase)

CIPKs consist of a conserved, yeast SNF1 related S/T kinase domain at the N-terminal part of the protein. Via a variable junction domain it is linked to a weakly conserved C-terminal regulatory domain containing a NAF and PPI motive. The NAF domain is responsible for binding CBLs which are required to activate the kinase. On the other hand the PPI motive allows interaction with PP2C type phosphatases [13,14]. Genome sequence data accumulated so far suggests that, CIPKs are exclusively present in plants and some protozoa but they do not appear in animals.

Through forward and reverse genetic analysis different physiological functions have been assigned to CBLs and CIPKs. The well understood function of AtCIPK24 (SOS2) in salt stress will be discussed later in the text. Besides that it has been shown that CBL9 k.o. mutants are hypersensitive to ABA [16] and CBL9 acts via interaction with CIPK1 and CIPK3 in the ABA response [17,18]. CIPK23 was identified as regulatory element in K^+ and ABA homeostasis [19,20]. Adding up to the complexity of CIPK23 signalling, a role in nitrate uptake regulation for this kinase was observed too [21].

1.3.2. CPK (calcium dependent protein kinase)

In *A.thaliana* the CPK family with its 34 members forms the largest group of Ca^{2+} regulated protein kinases. Based on sequence alignments the 34 CPKs can be clustered in 4 subgroups (Fig 3). Similar to the CBL/CIPK network also CPKs seem to be exclusive to plants and some protozoa including the malaria parasite. There it has been shown that *Pf*CDPKs 1 and 4 play crucial roles in the lifecycle of *Plasmodium falciparum* [22,23]. The canonical *A.thaliana* CPK sequence consists of a highly variable N-terminal domain followed by the S/T kinase domain which is linked to the C-terminal part of the polypeptide chain containing the Ca^{2+} binding domain. Except *At*CPK25, which has a short C-terminus, all *At*CPKs contain 4 EF hand motives in their C-terminus [24]. Recently, X-ray structures of three apicomplexan CPKs have been obtained leading to a better understanding of the activation and deactivation of CPKs in general [25]. Basically, the C-terminal domain acts as regulatory unit within the protein. In the inactive state, a Lys or Arg in the first helix of the regulatory domain interacts with the conserved Glu and Asp residues in the kinase domain. This basic residue serves then as a pseudo substrate for the kinase, similar to the mechanism observed in CamKs. Additionally three more interactions between hydrophobic residues were found to stabilize the regulatory domain in its position in the inactive form of the kinase. Upon binding of Ca^{2+} the regulatory C-terminal domain refolds and relocates relative to the position of the kinase

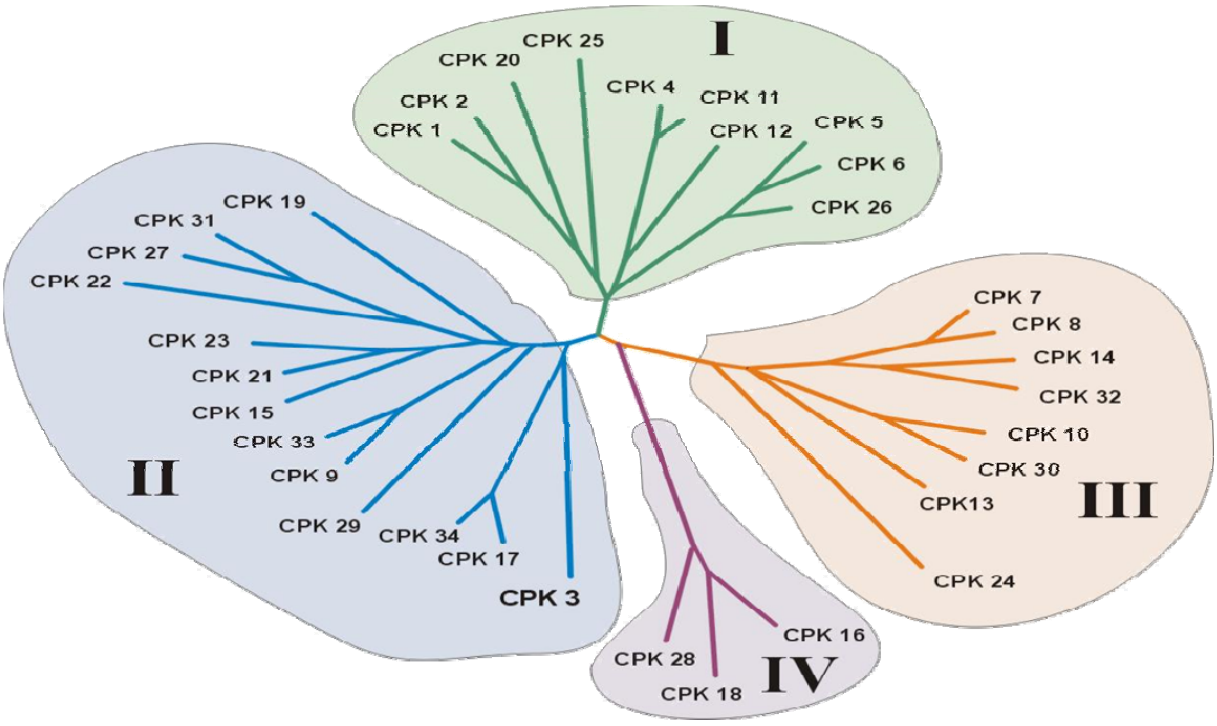

Fig3. Tree of *At*CPKs based on sequence homology [tree is kindly provided by Markus Teige]. The four different subgroups are differentially coloured.

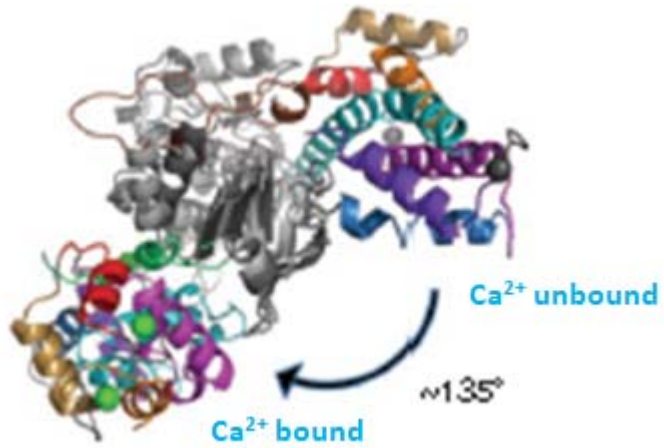

Fig4. Structural change of CPK between Ca^{2+} bound and unbound state [25]. The kinase domain is depicted in grey and the regulatory domain is coloured. The arrow indicates the movement of the C-terminal regulatory domain between Ca^{2+} unbound and Ca^{2+} bound state relative to the kinase domain.

domain. This relocation is extensive as the regulatory domain flaps around the kinase domain by almost 135° clockwise from its Ca^{2+} unbound position (Fig 4). Thereby the substrate recognition site and the catalytic site of the kinase domain get exposed to the surface. The regulatory domain is, at the same time, stabilized at its new position by a combination of ionic and hydrophobic interactions between the amino acid side-chains of the kinase- and regulatory-domain of the protein. Figure 4 shows a picture illustrating the activation process. Ca^{2+} alone was found to be sufficient to activate CPKs [25]. However, recent studies show that the concentration of Ca^{2+} which are necessary for the activation of single CPKs differ within the family of *At*CPKs [26]. So far, little is known about the processes involved in inactivating CPKs. In some cases simple depletion of Ca^{2+} in the reaction buffer turned out to be sufficient to render CPKs inactive but this holds not true for every CPK as observed recently [25]. A reason for this could be the fact that autophosphorylation during activation of the CPK is frequently observed [27,28,33] and removal of this phosphate group is likely to be necessary for complete inactivation of the kinase [25]. This fact makes it interesting to search for protein phosphatases as possible interaction partners of CPKs as well. About a common function of the N-terminal variable domain in *At*CPKs not much is known so far. Most CPKs in plants contain consensus sequences for myristoylation and palmitoylation. In some cases it has also been shown that plant CPKs are indeed myristoylated at their N-terminus and that this modification is crucial for their subcellular localization [29-31]. Unfortunately, so far there are no data available for CPKs to what extent they are acylated in vivo, leaving the question of alcylation as sole "localization signal" still open to be answered. An additional function of the N-terminal domain in the substrate recognition process of CPKs was shown recently [32]. In this study it was demonstrated that *Nt*CPK1 interacts with the transcription factor RSG via the N-terminal domain of the *Nt*CPK1. Furthermore the authors identified an arginine at position 10 of the CPK which is crucial for the interaction. They also observed that

this interaction was Ca^{2+} independent. In a next step the N-terminus of *At*CPK9, a non RSG interacting CPK, was replaced by the N-terminus of *Nt*CPK1. That was sufficient to make *At*CPK9 a full replacement of *Nt*CPK1 in terms of RSG phosphorylation. However, to formulate a general paradigm of CPK - substrate recognition via the kinases N-terminus, more biochemical evidence on a broader range of CPKs and their substrates has to be collected.

Ever since the discovery of CPKs in plants a lot of attention has been brought to elucidate their physiological functions. It is remarkable that up to date no CPK has been assigned to a physiological function through a forward genetic screen. This could be explained by, at least partly, a redundant function of single CPKs with other CPKs or even kinases of other families. Never the less a lot of data accumulated connecting CPKs to distinct physiological pathways occurring in the plant.

CPKs have been identified to take part in abiotic stress signalling, where most data has been gathered on the role of CPKs during the ABA mediated drought stress response. The phytohormone ABA induces closure of stomata in response to drought stress. Recently ABA signalling was reconstituted in vitro by the use of its core components, ABA receptors of the PYR/PYL family, transducing SnRK2 type protein kinases phosphorylating ABF/AREBs (transcription factors) and PP2C type protein phosphatases negatively regulating SnRK2 activity [34]. Nevertheless there is clear evidence for further tuning of the ABA response by CPKs. Knock-out mutants of *Atcpk3* and *Atcpk6* in guard cells exhibited partial impairment of ABA activation of S-type anion channels and plasma membrane Ca^{2+} channels [36]. Furthermore it was observed that *Atcpk3* and *Atcpk6* knock-out lines were partially inhibited in ABA induced stomatal closure [36]. For *At*CPK4 and *At*CPK11 it was reported that their protein content but not their mRNA levels were enhanced after ABA treatment [35]. The authors also showed that *Atcpk4* and *Atcpk11* knock-out plants were less sensitive to ABA and over expressing lines of both kinases were hypersensitive to ABA. In addition the transcription factors ABF1 and ABF4 were shown to be directly phosphorylated by *At*CPK4 and *At*CPK11 in vitro [35]. *At*CPK32 was demonstrated to directly phosphrylate ABF4 and it also interacts with the ABFs 1, 2, 3 and 4 in a yeast two hybrid system [37]. *At*CPK32 overexpressing plants were observed to be slightly more sensitive to ABA during germination [37]. For *Atcpk23* loss of function mutants a stomatal closure phenotype under water stress was reported in *A.thaliana* [38]. In BIFC assays it was also shown that *At*CPK23 directly interacts witch the guard cell anion channel SLAC1 in *A.thaliana* [38]. It is interesting to note, that SLAC1 is also regulated by the OST1 kinase in the same way as by *At*CPK23 and that both kinases interact with ABI1 protein phosphatase which abolishes their regulatory

impact on SLAC1 [26]. Taken together these data show that CPKs play a considerable role in ABA mediated drought stress response, still, more experiments directed towards CPK - target interaction are needed to understand their role in the ABA response. So far only CPK single and double mutants have been analyzed in the context of ABA signalling. Considering the high sequence homology within the CPK families it might be necessary to take a look at higher number parallel CPK knock-out mutants to overcome functional redundancy effects. In addition to the function of CPKs during draught stress response, differences in the phospho-proteome between a line with inhibited *At*CPK1 and a non-inhibited control line were observed by 2-D-gelelectrophoresis after cold stress treatment [46].

Further information on functionality of CPKs has been gathered in experiments regarding biotic stress response pathways. Data was obtained from *N.benthamiana* were *Nt*CPK2 silenced and tomato-CF9 expressing plants exhibited a delayed and reduced hyper sensitive response upon elicitation by Avr9 [39]. It was also shown that *Nt*CPK2 gets activated upon exposure of tobacco to Avr9 [40]. Furthermore it was demonstrated that *Nt*CPK2 is linked to the MAPK pathogen response pathway via ethylene mediated signalling [41]. Recently in a study on elicitor based Ca^{2+} signalling in *A.thalina* it was shown that over expressed *At*CPKs 3, 4, 5, 6, 11 and 26, lacking their regulatory C-terminal domain, were the only ones amongst the 25 CPKs tested that activated a NHL10 reporter construct in protoplasts [42]. Interestingly the closest *A.thaliana* homologs to *Nt*CPK2, *At*CPK1 and *At*CPK2 did not activate the NHL10 reporter [42]. RNA profiling with whole genome chips revealed large functional redundancy on the transcriptional response of transiently expressed *At*CPK5 and *At*CPK11 lacking their regulatory domain [42]. Surprisingly no significant marker genes for ABA, methyljasmonate, ethylene or salicylate were found to be regulated by *At*CPK5, or *At*CPK11 in this study[42]. RT-PCR studies on selected target genes of the FLG22 response revealed different degrees of connection between MAPK and CPK signal transduction pathways. The authors grouped the observed responses into MAPK-specific effects (eg FRK1), CPK-specific effects (eg PHI-1), CPK-MAPK synergistic effects (eg NHL10) and MAPK-dominant effects (FOX) [42]. In addition the involvement of CPK3 and CPK13 in the herbivore attack response had been reported [43]. There, it was observed that upon treatment with the herbivore *Spodoptera littoralis, Atcpk3* and *Atcpk13* k.o. plants had reduced mRNA levels of PDF1.2 compared to the *wild type* control. Under the conditions tested no changes in JA, ethylene and ABA levels were observed by the authors [43]. Most interestingly the authors also showed that cytosolic free Ca^{2+} levels were higher in leaves of *Atcpk3* k.o. plants than compared to leaves of wild type plants after herbivore attack [43], suggesting a role of *At*CPK3 in Ca^{2+}

homeostasis. Recently it was shown that *At*CPK1 also has a role in biotic stress signalling. *At*CPK1 was revealed to be induced on transcript level upon treatment with fungal elicitors [62]. In addition it was demonstrated that *Atcpk1* k.o. lines are less resistant to fungal attack [62]. The authors furthermore showed that SA pathway activation is partially inhibited while JA/ethylene pathways seem not to be affected in *Atcpk1* k.o. plants [62]. Rapid generation of reactive oxygen species (ROS), the so called "oxidative burst", is an important feature of plant innate immune response against pathogens [160]. In potato it was demonstrated that *St*CPK4 and *St*CPK5 are able to phosphorylate and thereby regulate *St*NADPH oxidases which are crucial for generation of ROS at the plasma membrane during the innate immune response [44].

Reflecting the versatility of Ca^{2+} signalling, CPKs have been found to be involved in developmental processes as well. In *A.thaliana* there is genetic evidence that *At*CPK17 and *At*CPK34 are essential for proper pollen tube growth [45]. In *cpk17* and *cpk34* double k.o. mutants a huge reduction in pollen tube growth and pollen fitness had been observed and the phenotype could be rescued by over expressing *At*CPK34 [45]. Unfortunately, as in biotic stress response pathways, little is known about direct interaction partners of CPK17 and CPK34 which could explain the observed phenotypes. Furthermore CPKs in *Medicago truncatula (M.truncatula)* were demonstrated to be regulators in the microbial symbiosis. *Mt*CPK1 function has been demonstrated to be crucial for cell-wall biosynthesis and symbiosis [47]. It was also observed that root nodule number is increased in *Mt*CPK3 RNAi lines [48].

A lot of *in-vitro* data has been gathered so far concerning CPK involvement in carbon and nitrogen metabolism. For nitrate reductase of spinach it was observed that a CPK dependent phosphorylation of a Ser in a canonical 14-3-3 site leads to binding of a 14-3-3 protein which subsequently leads to a steep decrease in nitrate reductase activity [49-53]. Also sucrose synthase (SuSy) and sucrose phosphate synthase (SPS), both key enzymes in the carbon metabolism, have been demonstrated to be targets of CPKs [54,55]. However, it is interesting to note that despite these potential targets of CPKs mentioned above, no convincing *in-vivo* data exists so far, demonstrating the regulatory impact of CPKs on either carbon or nitrogen metabolism. Evidence for specificity of CPK interaction with the three aforementioned metabolic enzymes is also largely missing and only slowly starting to accumulate [53].

1.3.3. CCaMK (calcium binding calmodulin interacting protein kinase)

CCaMKs shall be described very briefly here, as they are not present in *A.thaliana* and other members of the *brassica* family sequenced so far. These kinases feature a visinin-like Ca^{2+} binding domain with 3 EF hands. In addition a calmodulin binding domain is present on the polypeptide chain. The kinases of this family seem to be most active when Ca^{2+} and CaM is bound at the same time [56]. CCaMKs have been found to be essential in *Lotus japonicus* (*L.japonicus), M.truncatula, Sesbania rostrata (S.rostrata)* and *Oryza sativa* (*O.sativa)* for forming symbiotic relationships in roots [57-61].

1.3.4. Localization of Ca^{2+} regulated protein kinases

As mentioned in the beginning, Ca^{2+} signals are distinct in time and space within the plant on a tissue level as well as on a sub-cellular level. Therefore knowledge on localization of the different Ca^{2+} regulated protein kinases is crucial for understanding Ca^{2+} signal transduction pathways. For the CBL/CIPK module the localization of all ten *A.thaliana* CBLs has been described by the use of microscopic- and biochemical fractionation techniques [63,64]. CBLs 1 and 9 were found to localize at the plasma membrane, CBLs 2, 3, 6 and 10 are localized at the vacuolar membrane, CBLs 4 and 5 have been observed in the cytosol as well as at the plasma membrane and CBLs 7 and 8 are localized in the nucleus as well as in the cytosol [63,64]. For proper localization of the membrane targeted CBLs dual lipid modification at the N-terminus, as well as the N-terminal sequence itself were shown to be important [63,64]. Concerning the localization of the corresponding CIPK it has been shown that multiple interactions between one CIPK and different CBLs occur at the same time in one cell and that spatial decoding of Ca^{2+} signals by the CBL/CIPK module is mediated by the CBLs [63,65].
By now the localization of many CPKs in *A.thaliana* has been determined via microscopy and biochemical fractionation experiments (see table 1). As for the CIPKs complex localization patterns within a cell can be observed for CPKs. Interestingly the majority of CPKs have predicted N-terminal acylation signals as it is also observed for CBLs. Several studies already demonstrated that acylation at the N-terminus of CPKs can be achieved in *in vitro* experiments and that it is of importance for proper localization and function [29,30]. It is notable that the majority of CPKs analyzed so far, are indeed found to be localized at different membrane systems. This indicates that CPKs likely act as initial Ca^{2+} signal decoders at the membrane were Ca^{2+} signals are first generated. For this fact it is reasonable to search CPK substrates among membrane proteins. However, for the majority of CPKs, their localization

has only been confirmed through over expressed, tagged variants of the kinases, what could be misleading. Therefore a parallel biochemical localization analysis of endogenous levels of CPKs needs to be done in order to get a more reliable picture of the sub-cellular localization of CPKs. Furthermore, nothing is known so far if any CPK has the ability to change its sub-cellular localization upon binding of calcium which would add another level of complexity in CPK signalling.

CPK #	**sub-cellular localization**	**Ref**
CPK1	peroxisomes, oilbodies	62, 66, 46
CPK2	membranes	30
CPK3	cytosol, nucleus, vacuole, plasma membrane	66, 29
CPK4	cytosol, nucleus	66, 42
CPK5	cytosol nucleus	42
CPK6	plasma membrane, nucleus, cytosol	29, 42
CPK7	plasma membrane	66
CPK8	plasma membrane	66
CPK9	plasma membrane	30
CPK11	cytosol, nucleus	42
CPK13	plasma membrane	30, 43
CPK16	plasma membrane	66
CPK17	plasma membrane (only expressed in pollen)	45
CPK21	plasma membrane	66
CPK23	plasma membrane	26
CPK28	plasma membrane	66
CPK32	nucleus, cytosol	37
CPK34	plasma membrane (only expressed in pollen)	45

Table1. Overview on sub-cellular localization of CPKs in *A.thaliana*.

1.4. Salt stress

Plants are always in contact with soil and the salts therein via their root system. Periods of drought and rain lead to differences of in the soil humidity, directly resulting in changes of the salt concentration around the roots. Plants are capable to adapt to these changes, however, some plant species, or even ecotypes within a species, grow better under higher salt concentrations than others do [67]. Understanding the processes that render plants resistant towards salt stress is not only crucial for understanding the basic functions of a plant but also for designing more flexibly usable cultivars.

Of all soluble salts, NaCl is the most widespread one affecting plant growth. High levels of salt effect plants in two ways. First, it hampers water acquisition via the roots as salt ions compete for H_2O with the water uptake mechanism of roots. Second, high concentrations of free Na^+ ions are toxic to the plant cell [67].

For plants grown on soil, the osmotic effect is the first signal sensed by plants exposed to salt stress [67,68]. This also accounts for the first phenotypic response observed in salt stressed plants, which is the loss of water in the plant tissue as well as stomatal closure. The decrease in water availability for the plant is similar to other abiotic stresses like drought stress. Therefore salt stress response and drought response share similar components and mechanisms in plants. One strategy for the plant to keep water inside is to restore the initial osmotic balance by production of compatible solutes. These are small molecules without a netto charge, which are easily available to the cell and can accumulate to relatively high concentrations in the cytosol to protect the active state of enzymes. A large number of metabolites is known to act as compatible solutes including proline, glycine-betaine, five and six carbon sugars as well as their sugar alcohols. Different sets, of compatible solutes were found to be present during the salt stress response in different plant species.

Polyphosphoinositides and inositidepolyphosphates play a central role in osmotic response signalling [69]. These molecules fulfil multiple roles from precursor molecules for compatible solutes [70,71], to hormone like signalling molecules [69,72-74]. The second very important signalling molecule in the aspect of osmotic stress is the plant hormone ABA. It is produced in roots upon application of salt stress and is then transported to the guard cell where it initializes stomatal closure [4,75,76]. Recent studies suggest that both, ABA and phosphoinositide signalling pathways are connected with each other [69]. However, as interconnection of different signalling pathways in plants is still beginning to be described, more experiments are needed to better understand the interactions of these signalling networks.

The second effect of salt stress on plants is a disturbance in ion homeostasis by the entrance of Na^+ into the cytosol. The organs of the plant which first come into contact with Na^+ are the roots. There Na^+ enters the plant via epidermal cells, passing through the cortex, endodermis, pericycle and finally entering the xylem where it is transported to the leaves [67,77,78]. Shortly after germination and at the root tip it is also possible that Na^+ ions enter the plant directly at the endodermis as there is still no casparian belt established [78]. Na^+ ions passively enter the cytosol along an electrochemical gradient over the plasma membrane [67,77]. The entry sites are most likely different cation channels (cyclic nucleotide gated channels, glutamate receptors) and some members of the HKT potassium transporter family [77,79-81]. Interestingly a Na^+ concentration gradient has been observed from the epidermis to the endodermis [82]. This finding indicates that plants already try to limit Na^+ uptake at the earliest stage possible. It is observed that Na^+ concentrations are highest in the shoot and

there, in older leaves [83]. Although Na^+ was found to be unequally distributed between different cell types in the leaf, the main mechanism of keeping Na^+ out of the cytosol, for the all leaf cells, is to transfer it into the vacuole [77]. For both, root and leaf cells a Na^+/H^+ antiporter family, termed NHX, has been found to be crucial in maintaining proper Na^+ ion homeostasis [105-107]. In *A.thaliana* NHX1 is localized at the tonoplast. NHX1 seems to be the major Na^+/H^+ antiporter in the plant which actively transfers Na^+ into the vacuole [108]. Conveniently, over expresser lines of *AVP1*, a H^+-pyrophosphatase localized at the tonoplast, show a positively correlating phenotype to the respective NHX1 mutants [109]. Another Na^+/H^+ antiporter, NHX7 (SOS1), has also been found to be a crucial element in the salt stress response in plants [85]. It is localized at the plasma membrane where it actively translocates Na^+ ions out of the cytosol to the apoplast. Higher levels of Na^+ in the cytosol were observed in *nhx1* k.o. mutants in root cells as well as in leaf cells [110].

However, exclusion of Na^+ from the cytosol only, is not sufficient for the leaf cell to survive salt stress. Due to osmotic affects, the leaf cell would run out of available water in the cytosol and membranes might rupture due to the pressure difference. Therefore, like in root cells, a rise of compatible solute concentration in leaf cells is observed in plants affected by salt stress as well [77].

The second cation of high importance in NaCl stressed plants is K^+. K^+ fulfils quite diverse functions depending on the cell type in plants. In guard cells K^+ fluxes are the major contributing ion fluxes during stomata opening and closure [87]. Furthermore it has been observed that K^+/Na^+ ratio in the cytosol is crucial for salt tolerance of plants [68]. In the cytosol K^+ has been found to act as important cofactor for proteins [88]. In addition it functions as osmotically active cation under NaCl stress [68,89]. K^+ transport over membranes in plant cells is complex as there are at least seven families of cation transporters known (comprised of aproximately 75 proteins) in *A.thaliana* which are likely to be involved in K^+ translocation via the different membranes [90]. For a recent update on K^+ transport under salt stress the reader is referred to the following extensive review [68].

1.5. Connecting plant Ca^{2+} signalling to salt stress

Studies over the last decades showed that Ca^{2+} signalling is important for plants to sense and properly react to salt stress. One of the first signals observed in plant cells upon salt stress are fluctuations in Ca^{2+} levels, in- and outside the plant cell [161].

1.5.1. Ca^{2+} signals during salt stress

It had been demonstrated that cytosolic Ca^{2+} concentrations are distinct in different tissues in roots upon exposure of plants to salt stress [91]. Only seconds after application of 220 mM NaCl short spikes of Ca^{2+} concentration in the cytosol were observed in cells of the epidermis, endodermis and pericycle [91]. Interestingly a decrease in the amplitude of the Ca^{2+} signal from epidermal cells towards the endodermis was observed [91]. Although this decrease is not as steep as the observed decrease in Na^{+} concentration from epidermal cells towards endodermal cells [82] it still correlates with it. A further study measuring Ca^{2+} levels in cytosol and the apoplast illustrated a still more complex Ca^{2+} signalling pattern in both compartments after repeated salt stress [5]. Ca^{2+} signals were found to differ in cytosol and the apoplast [5]. At the beginning of each salt stress period cytosolic levels of Ca^{2+} reached a maximum as observed before [91]. In parallel apoplastic Ca^{2+} decreased slightly, indicating that a part of the cytosolic calcium peak is a result of the Ca^{2+} influx from the apoplast [5]. The steep rise at the end of the "salt stress phase" is similar to that observed after "osmotic stress treatment" [5] and may therefore account for integration of the osmotic part of the salt stress into the Ca^{2+} signalling response. For the Ca^{2+} peak caused by the change in osmotic potential, no corresponding decrease in apoplastic Ca^{2+} concentration had been observed [5]. Together, these findings may indicate that Ca^{2+} concentration rise in the cytosol, caused by salt stress, originate from the release of Ca^{2+} from intercellular Ca^{2+} stores like the vacuole, and apoplastic Ca^{2+} is rather used to refill intracellular Ca^{2+} stores than to contribute as major Ca^{2+} source for immediate Ca^{2+} signalling. An immediate rise in intracellular Ca^{2+} concentration upon salt stress has also been observed in other species than *A.thaliana* [92,93]. However, one must be careful in generalizing Ca^{2+} concentration patterns upon salt stress over different plant species. It has been shown that differences exist in the cytosolic Ca^{2+} concentrations upon the same stress between different cultivars of rice [92].

1.5.2. Decoding of Ca^{2+} signals during salt stress

Once a cytosolic Ca^{2+} signal emerges it is sensed by a set of Ca^{2+} binding proteins described above. As this thesis addresses Ca^{2+} dependent protein kinase regulation this section will focus on Ca^{2+} regulated protein kinase modules during salt stress only.

The best understood Ca^{2+} dependent signalling pathway during salt stress is the SOS (salt overly sensitive) pathway. Its core consists of three proteins (SOS1-3) of which 2 were identified by forward genetic screens for complementation of a salt sensitive phenotype in

A.thaliana [94,95]. It was shown that *At*CIPK24 (SOS2) and *At*CBL4 (SOS3) physically interact upon salt stress *in vivo* and that they regulate the activity of SOS1, a Na^+/H^+ antiporter, at the plasma membrane via direct phosphorylation of SOS1 [96,97]. Interestingly *At*CIPK24 has also been found to interact with *At*CBL10 and that it is thereby guided to the vacuolar membrane [98,99]. *At*CBL10 has also been shown to contribute to salt stress tolerance in *A.thaliana* [98]. Although it is speculated that *At*CBL10/*At*CIPK24 complex targets the SOS1 homolog NHX1 at the vacuolar membrane [98] no conclusive evidence is available on interaction partners for *At*CIPK24 at the vacuolar membrane so far. In addition CBL1 has also been demonstrated to be part of salt stress signalling in *A.thaliana* [18,100]. There it could act as an integrator for ABA independent Ca^{2+} signalling in the CBL/CIPK module [18]. Furthermore, *At*CIPK23 plays an important role in K^+ homeostasis. *At*CIPK23 has been shown to be activated by *At*CBL1 and *At*CBL9 [20]. The plasma membrane localized K^+ transporter AKT1 in *A.thaliana* was found to be directly activated via phosphorylation by *At*CIPK23 [19,101]. Contributing to the complexity of Ca^{2+} signalling via protein kinases, *At*CBL1/9 *At*CIPK23 have been observed to participate in stomatal regulation [20]. *At*CIPK11 is another Ca^{2+} regulated protein kinase that could play a role in salt stress. It was found that *At*CIPK11 phosphorylates the plasma membrane H^+ ATPase *At*AHA2 at a regulatory site at its C-terminus which led to a decrease in activity of *At*AHA2 [102].

Much less is known about the function of CPKs in the salt stress response. For *At*CPK23 it was shown that k.o. mutants of this kinase were more resistant against salt stress whereas *At*CPK23 over expressing lines were more sensitive towards NaCl compared to the wild-type control [38]. This phenotype can hardly be explained by the observation that *At*CPK23 activates SLAC1 in guard cells [26]. Further work on elucidating additional interaction partners of *At*CPK23 has to be done to explain the salt tolerance phenotype. Two members of the zinc finger like domain containing, *A.thaliana* drought induced 19 (*At*Di19) family were found to be salt induced on a transcriptional basis in an ABA independent way [103]. *In vitro* it has been shown that *At*CPK3 and *At*CPK11 could phosphorylate these two *At*Di19 family members which are believed to play a crucial role in salinity tolerance [103]. In another study over expression of *At*CPK6 was found to confer enhanced resistance towards salt and drought stress to the plant [104]. It was also observed that *At*CPK6 expression levels positively correlated with proline levels in the plant, suggesting a role of *At*CPK6 in the osmotic part of salt stress signalling [104]. CPKs were also found to be involved in the salt stress response of other species than *A.thaliana*. In rice, for example, over expression of *Os*CPK13 leads to an enhanced salt stress tolerance [162]. Remarkably, the strongest effects for CPKs under salt

stress have been observed in CPK over expressing plants which may indicate a functional redundancy of CPKs in signalling.

1.6. Aim of this thesis

There are 34 different CPKs encoded in the *A.thaliana* genome. Although data on their physiological function in the plant accumulates, hardly anything is known about molecular CPK targets within the plant cell. By investigating the role of CPK3 in *A.thaliana*, this thesis should shed more light on how one of the 34 CPKs acts within sub-cellular signalling cascades.

A physiological function should be assigned to CPK3 by screening different *cpk3* k.o. and over expresser lines. For these screens T-DNA insertion lines will be used which first will be characterised on their transcript as well as on their protein level. The physiological function of CPK3 should furthermore be explained on a sub-cellular level by monitoring CPK3 kinase activation and identifying CPK3 interaction partners. Therefore, interaction between the already suggested targets bZIP63, TPK1 and nitrate reductase will be investigated in more detail, which means: Identifying functional phosphorylation sites of CPK3 on these proteins and describing a mechanism of interaction between CPK3 and these three targets. In addition results of "unbiased" protein-protein interaction-screens should be correlated to the known targets of *At*CPK3 and the phenotype of the different *cpk3* mutant plants. Studies on the sub-cellular localization of the endogenous CPK3 are planned to further validate results obtained from CPK3 interaction partner screening.

2. Results

According to genevestigator data *At*CPK3 is the most abundant CPK in vegetative tissue of *A.thaliana* on mRNA levels (Fig 5). Furthermore it had been shown before that activity of transiently over expressed CPK3 in *A.thaliana* protoplasts rises upon application of NaCl stress compared to CPK3 activity in mock treated protoplasts [29]. Last but not least a single N-terminal myristoylation site, as well as a predicted chloroplast localization make CPK3 an interesting target to investigate.

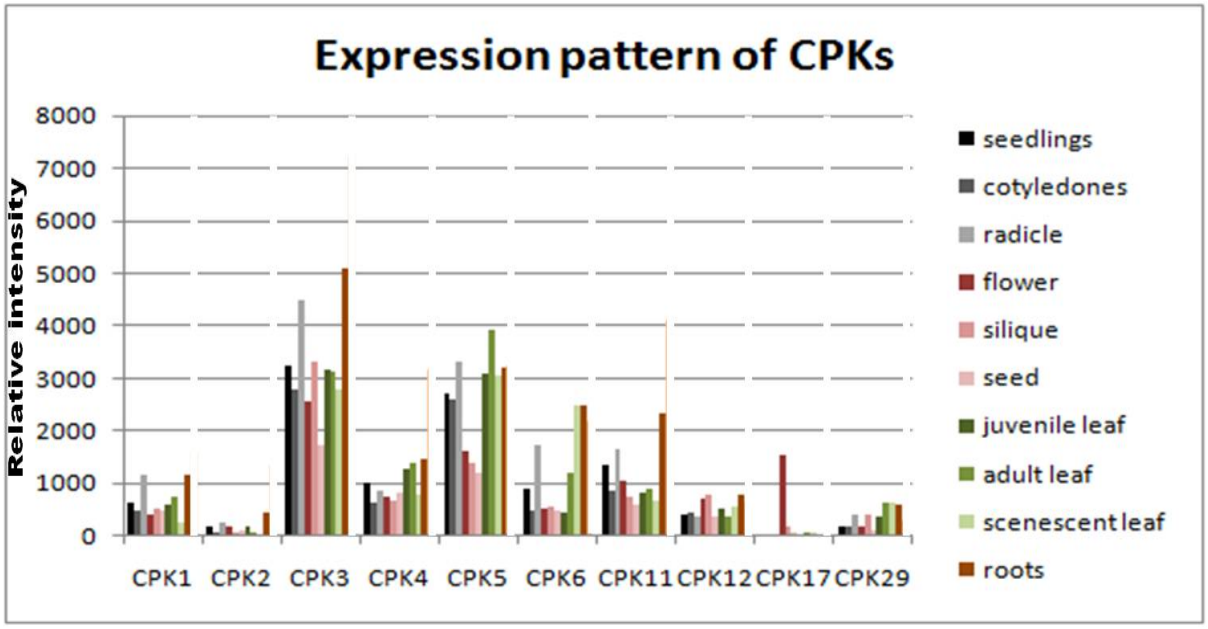

Fig5. Expression pattern of selected *At*CPKs. Relative levels of CPK expression were retrieved from publically available genvestigator data. [163]

2.1. Analysis of *CPK3* T-DNA insertion lines

To obtain insight into the physiological function of CPK3 three different T-DNA insertion lines (*salk_022862*, *salk_107620*, *sail_120_H09*) were obtained from ABRC [111]. T-DNA insertion plants were propagated until homozygous lines could be isolated. The position of the inserted T-DNA was determined by PCR (Fig 6a,b). To control homozygosity, a first set of primers had been selected, which would allow for amplification of a PCR product with defined length, containing a part of the genomic as well as the respective T-DNA insertion sequence, according to the mapped insertion at SIGnAl [112] (Fig 6a). As a complementary control a second set of primers was chosen that would only allow amplification of the wild type locus but not the T-DNA insertion locus with the selected parameters for the PCR reaction (Fig 6a). Homozygosity of the *salk_022862* line was tested by N. Mehlmer before.

The band visible at ~500 bp in the Col0 control for the primer combination "FW-RV" is a result of unspecific primer binding as described at SIGnAl [112]. Still, the line was considered to be homozygous as the specific PCR product obtained from the mutant differs clearly in length and the wild type fragment was not observed in the second control (Fig 6b). For the two other lines, only predicted PCR fragments have been observed in the respective lines, indicating a homozygous genotype concerning the T-DNA insertion locus
(Fig 6b). For further studies only homozygous T-DNA insertion lines were used. Expression levels of CPK3 in each of the aforementioned T-DNA insertion lines were analyzed by RT-

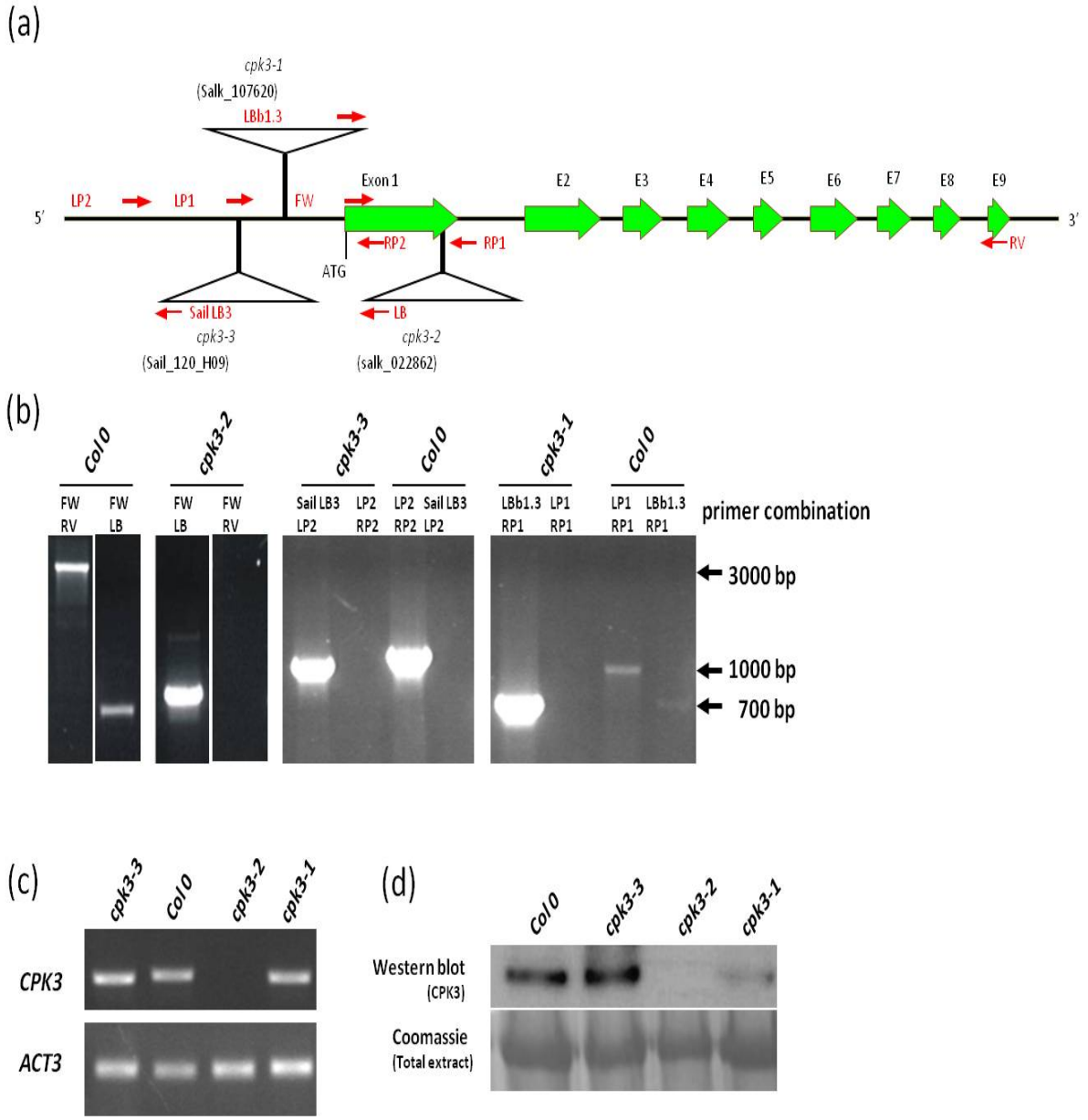

Fig6. Analysis of CPK3 of three different T-DNA insertion lines. (a) A scheme of the genomic CPK3 locus. Exons are coloured in green, primers used for mapping are indicated as red arrows, triangles symbolize the T-DNA insertion sites. (b) PCRs for rough mapping of T-DNA insertion sites and checking homozygosity in the different lines. Primer combinations correspond to the primers depicted in (a). (c) RT-PCRs of CPK3. (d) western blot against CPK3

PCR. The homozygous *salk_022862* line was identified as a true CPK3 knock out line on mRNA level and was termed *cpk3-2* according to literature [36] (Fig 6c). The homozygous *salk_107620* line has been observed to be a knock down mutant of CPK3 on mRNA level and termed *cpk3-1* (Fig 6c). Finally the homozygous *sail_120_H09* line with a T-DNA insertion in the promoter region turned out to be a over expresser of CPK3 on mRNA level and was termed *cpk3-3* (Fig6c). In addition western a blot analysis with a CPK3 specific antibody against a motive at the C-terminus of *At*CPK3 was done. As a result a positive correlation between mRNA levels of CPK3 and protein levels of CPK3 in the tested *A.thaliana* lines was observed. CPK3 protein levels in the *cpk3-3* line are ~2 times higher than in *Col0.* The *cpk3-1* line is a strong knock down of CPK3 compared to Col0 on protein level. The *cpk3-2* line has also been confirmed to be a complete CPK3 knock out on protein level (Fig 6d).

2.2. A physiological function of CPK3

Considdering that CPK3 protein kinase was activated upon salt stress in protoplasts, several screens including all three T-DNA insertion lines described above and *Col0* were performed. Interestingly differences in the germination efficiency upon germination of the four different *A.thaliana* lines on 1/4 Hogland containing 150 mM NaCl have been observed (Fig7). About 30 % of the *Col0* seeds germinated under the conditions described above. More than 40 % of the seeds of the *cpk3-3* line have been observed to germinate under salt stress. Seeds of the *cpk3-2* line displayed germination rates of about 15 % and for the seeds of the *cpk3-2* line germination rates of ~18 % have been observed when seeds germinated on plates containing 150 mM NaCl. On plates without addition

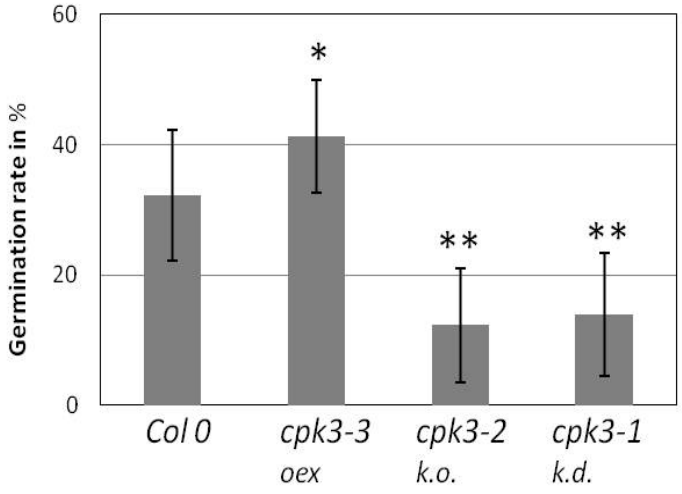

Fig7. Phenotype of different CPK3 mutants during germination under salt stress. The fraction of seeds that germinated on 1/4 Hogland is indicated on the y-axis in per cent. the different lines are indicated at the x-axis; oex, over expresser; k.o., knock out; k.d., knock down. Error bars indicate standard deviation (n=10). Statistical significance values were calculated by a two-tailed Student's t-test and are indicated by asterisks: *P ≤ 0.05; **P ≤ 0.001.

of NaCl all seeds from the four *A.thaliana* lines germinated to 100 %. Together these results show that the amount of CPK3 protein in the plant positively correlates with the germination rates observed in the germination assays. At this point it would be interesting to test if the observed phenotype is due to the osmotic phase of the salt stress or due to the toxicity of NaCl. Therefore the assays above should be repeated with osmotically active compounds like sorbitol instead of NaCl in future experiments.

As the root is the first organ of the plant affected by salt stress further assays for measuring, root growth, root complexity and root bending were done with the previously used four *A.thaliana* lines (data not shown). However, in none of these assays a difference between the knock out, over expresser and *Col0* lines had been observed. Nevertheless, the results obtained from the germination assays strongly suggest a role of CPK3 in acclimation to salt stress.

2.3. Activation of *At*CPK3 under salt stress

To gain further knowledge on the endogenous activity of CPK3 in the plant during initial salt stress immunocomplex kinase assays were done. Therefore CPK3 was pulled down using a CPK3 specific antibody bound to Protein A sepharose beads. Subsequently kinase assays with histone III S as artificial substrate for CPK3 were done. The *cpk3-2* k.o. line was used as a control throughout the whole experiment. In this line no endogenous CPK3 activity has been observed, neither without salt stress nor 10 minutes after application of the salt stress (Fig 8a,b,c). First, CPK3 kinase activity of 12 day old seedlings grown in liquid culture was assayed. Surprisingly, in this setup no induction of CPK3 kinase activity compared to the amount of CPK3 protein could be observed in several independent experiments after application of 150 mM NaCl to the growth medium for 10 and 30 minutes (Fig 8a). However, CPK3, isolated out of leaves of 6 week old hydroponically grown Col0 plants, has been repeatedly observed to have a higher kinase activity 10 minutes after application of 150 mM NaCl than before the salt stress. The results of the corresponding western blot indicate that the observed elevated kinase activity is rather a result of CPK3 activation than of additional CPK3 protein synthesis (Fig 8b). To obtain a more detailed picture of CPK3 activation in the plant CPK3 activity derived from roots of 6 week old hydroponically grown plants has also been assayed. There, a decrease in CPK3 kinase activity by about 50 % compared to the unstressed control has been observed 10 minutes after treatment with 150 mM NaCl. However, the western blot revealed that the amount of CPK3 protein measured in the salt treated samples was more than 50 % lower than that in the non treated plants (Fig 8c). To

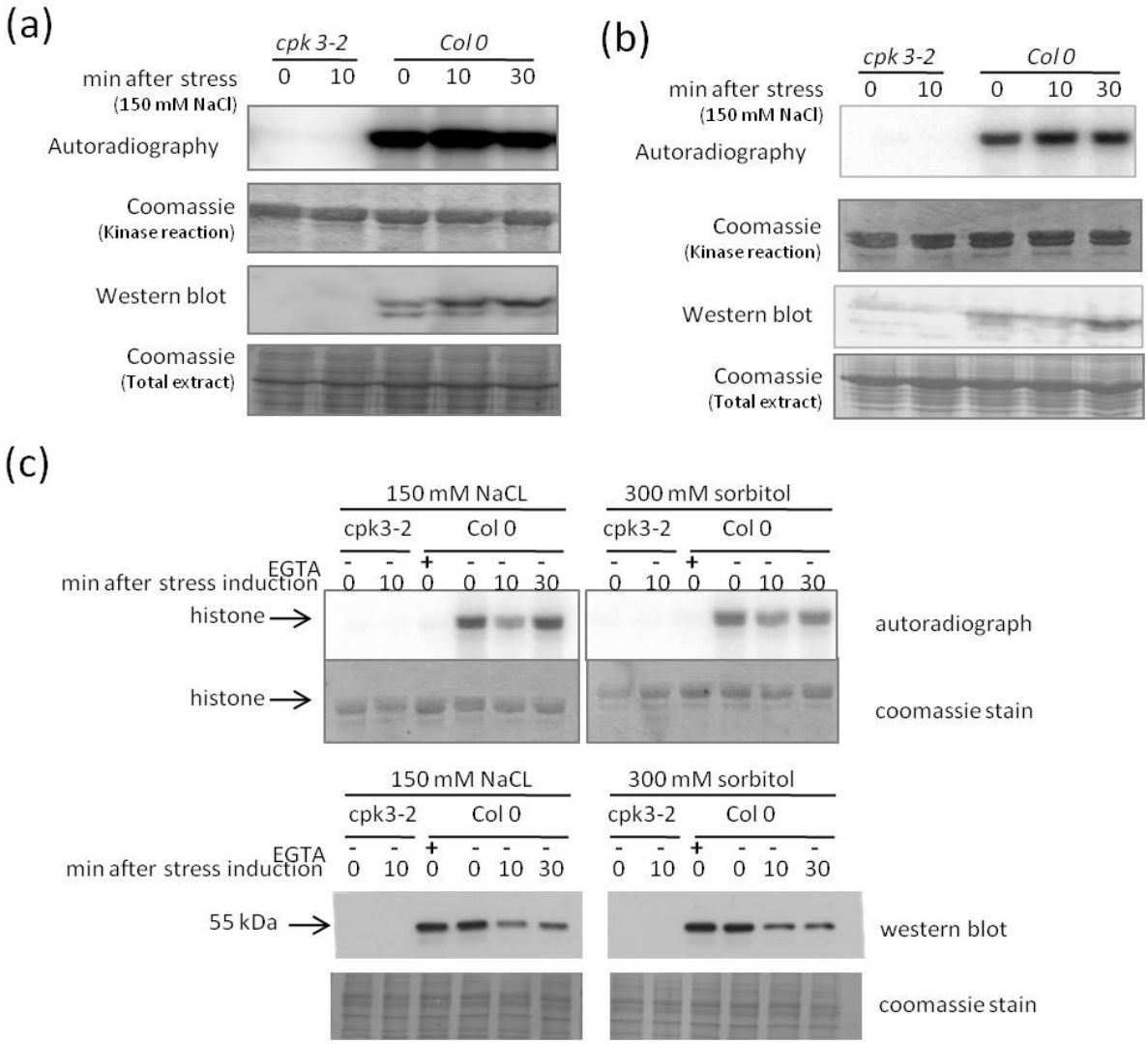

Fig8. Kinase activity of CPK3. (a) Kinase assays with CPK3 obtained from seedlings 0, 10 and 30 min after application of 150 mM NaCl. (b) Kinase assays with CPK3 from leaves of hydroponic cultures 0, 10 and 30 min after application of 150 mM NaCl. (c) Kinase assays with CPK3 obtained from roots of hydroponically grown plants after application of 150 mM NaCl or 300 mM sorbitol. In all kinase assays histone III S was used as artifical CPK3 substrate (a-c). A CPK3 specific antibody was used to extract CPK3 for the kinase assays (a-c) and for detection of CPK3 in the western blots (a-c).

address the question if CPK3 is activated by the ionic component of salt stress or by the osmotic component, CPK3 kinase activity was followed over time in plants exposed to sorbitol. For that CPK3 kinase activity derived from roots of 6 week old, hydroponically grown *Col0* plants treated with 300 mM sorbitol instead of NaCl were measured. Similar to the NaCl treated plants CPK3 kinase activity has been observed to be slightly lower after 10 minutes exposure to sorbitol than before the stress treatment. Also in this case the western blot shows a decrease of more than 50 % in CPK3 protein extracted from the roots of the sorbitol treated plants (Fig 8c). The reduced ammount of protein extracted from NaCl and sorbitol treated roots is likely due to less efficient homogenization of the dehydrated tissue

after the stress treatment. An already high activity of CPK3, before the stress treatment, compared to protoplast data [29] may be explained by the fact that upon homogenization additional Ca^{2+} from the apoplast was set free which might have led to activation of CPK3.
It was also shown that CPK3 is a strictly Ca^{2+} dependent protein kinase. No kinase activity has been observed when the kinase was purified in extraction buffer containing 200 µM of EGTA, although equal amounts of CPK3 protein have been used in the kinase assay reaction as indicated by the western blot analysis (Fig 8c).

2.4. Sub-cellular localization of CPK3

To obtain knowledge on the sub-cellular localization of CPK3 several approaches were followed. In vivo localization studies of CPK3 where done together with N. Mehlmer, B. Pfister and S. Stael [29]. In these studies CPK3 was tagged with a single YFP on its C-terminus and expressed in tobacco epidermal leaf cells. The sub-cellular localization of CPK3 turned out to be complex. In this microscopy study CPK3 has been clearly observed within the nucleus (Fig 9). YFP signals from cytosolic strands in the cell also indicate a cytosolic localization of CPK3 (Fig 9). In addition the images from microscopy provide first evidence that CPK3 is also localized at endomembrane systems (Fig 9).
To complement the data obtained from microscopy and analyze the localization of endogenous CPK3, biochemical fractionation experiments were done. Together with N.Mehlmer, R.Bayer and B. Pfister it was observed that CPK3 can be detected in the microsomal fraction as well as in the supernatant after separation of membranes from the cytosol by centrifugation [29, 113], supporting both membrane and cytosolic localization of CPK3. Further separation of the total membrane preparation was then done by sucrose density gradient centrifugation to analyze the distribution of CPK3 within the different endomembrane systems. After the centrifugation fractions were taken and analyzed by western blotting with antibodies against marker proteins for the different endomembrane systems. In this experiment it could be shown that in leaves, the CPK3 distribution over the gradient largely overlaps with the distribution of V-ATPase (a marker for the tonoplast membrane) and to a lesser extent with H^+-ATPase from the plasma membrane (Fig 9c). The weak overlap of CPK3 signal with that of Porin from mitochondria can be taken as validation for the microscopic data where CPK3 has never been observed to localize at mitochondria nor to any plastids. Almost no overlap of signals has been observed between CPK3 and SAR1 (an ER marker). Together these findings suggest that the major fraction of endogenous membrane localized CPK3 in leaves resides at the vacuolar membrane.

(a)

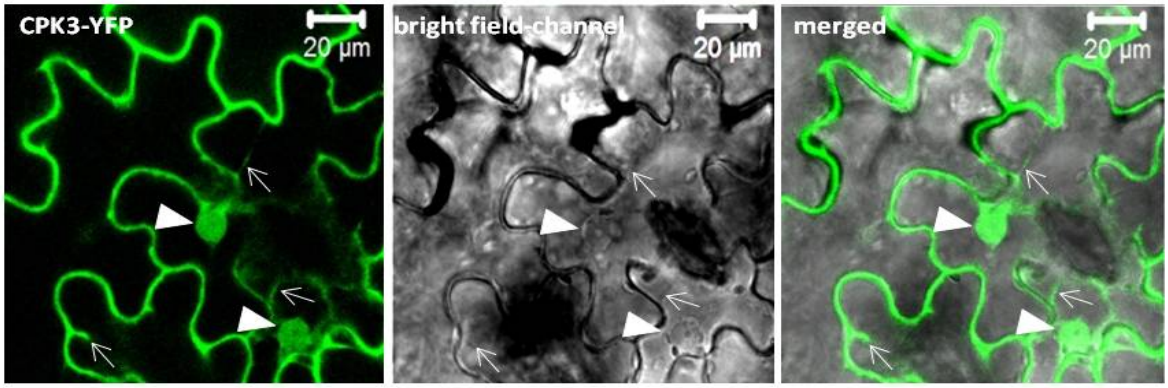
CPK3-YFP
20 µm
bright field-channel
20 µm
merged
20 µm

(b)

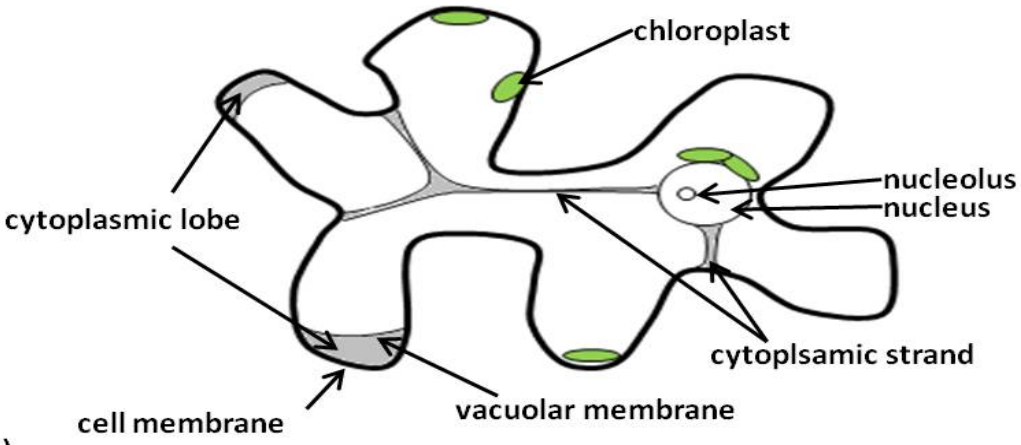
chloroplast
nucleolus
nucleus
cytoplasmic lobe
cytoplsamic strand
cell membrane
vacuolar membrane

(c)

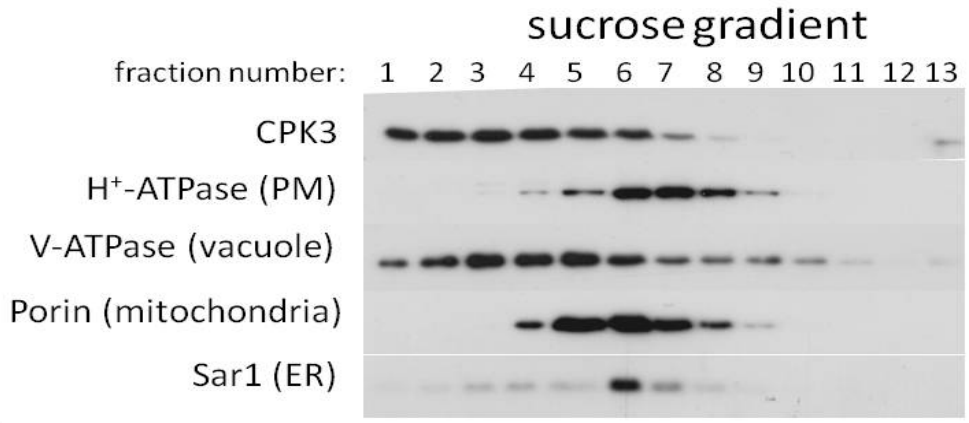
sucrose gradient
fraction number: 1 2 3 4 5 6 7 8 9 10 11 12 13
CPK3
H+-ATPase (PM)
V-ATPase (vacuole)
Porin (mitochondria)
Sar1 (ER)

(d)

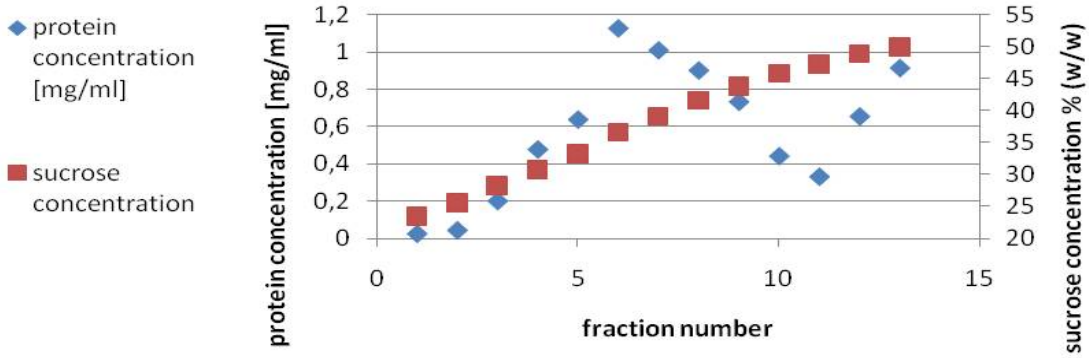
protein concentration [mg/ml]
sucrose concentration
protein concentration [mg/ml]
sucrose concentration % (w/w)
fraction number
0
0,2
0,4
0,6
0,8
1
1,2
20
25
30
35
40
45
50
55
0
5
10
15

Fig9. Sub-cellular localization of CPK3. (a) Sub-cellular localization of CPK3-YFP fusion protein in tobacco epidermal leaf cells. White triangles indicate the position of nuclei, white arrows indicate the position of cytosolic strands. (b) A schematic model of a tobacco epidermal leaf cell and a selection of its compartments indicated. (c) Fractions taken of a linear sucrose gradient after centrifugation. Western blots have been performed with antibodies against marker proteins of different sub-cellular compartments. (d) diagrams showing the total protein as well as the sucrose concentration in each fraction of the gradient which were used for the western blots.

2.5. Unbiased search for targets of CPK3

At the start of this thesis there was compelling evidence for three targets of *At*CPK3. Most *in vitro* data has been collected on the interaction of the *At*CPK3 homolog in spinach with spinach nitrate reductase [49-53)]. M. Teige repeatedly identified *At*bZIP63, a transcription factor, as interaction partner in a yeast two hybrid screen (personal communication by M. Teige). TPK1 a vacuolar K^+ channel has also been demonstrated to be phosphorylated at a 14-3-3 regulatory site by CPK3 (personal communication by D. Becker and M. Teige). More additional data obtained on describing the aforementioned interactions is given later on in the results section. One central question of this thesis was, if there are more, still unknown, substrates regulated through phosphorylation by CPK3. The localization studies strongly suggest the presence of potential CPK3 substrates at membranes. Microsomal membranes were prepared from *Col0* and *cpk3-2* plants, treated once for 30 min with 150 mM NaCl and once only with water, to obtain an overview on global phosphorylation changes. After incubation of the microsomal membranes with radioactively labelled ^{32}P ATP in a kinase assay buffer, the containing proteins were separated via SDS-PAGE and analyzed by autoradiography (Fig 10). However, neither in the mock treated plants nor in the salt treated plants obvious differences between the *Col0* phosphorylation pattern and the *cpk3-2* phosphorylation pattern could be observed (Fig 10a). In parallel recombinantly expressed *At*CPK3 of E.coli has been added to the

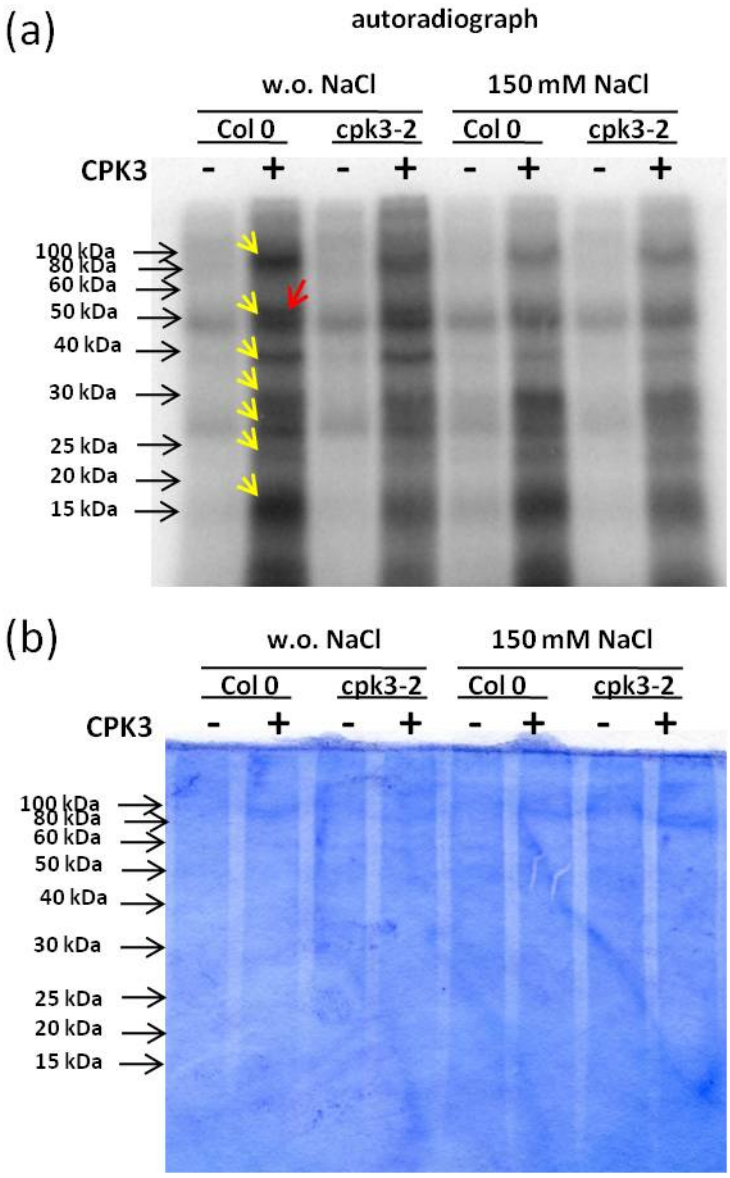

Fig10. Global phosphorylation pattern of *A.thaliana* microsomal membranes from *Col0* and *cpk3-2* roots with and without NaCl treatment. (a) Autoradiograph of Kinase reactions with microsomal membranes after separation via SDS-PAGE. + and - indicate reactions where recombinant CPK3 has been added. Plants were either treated with 150 mM NaCl or water for 30 minutes before the preparation of the microsomal membranes. Yellow arrows indicate distinct bands observed to be specifically phosphorylated by CPK3. The red arrow indicates a signal from autophosphorylated CPK3. (b) Coomassie stained template gel for the autoradiograph

described reaction mixtures and the kinase assays have been repeated. The first difference observed is, that in contrast to the membranes with their endogenous kinases, microsomal membranes treated with recombinant CPK3 give a strong signal in the autoradiograph. The signal is also connected to seven distinct bands in the gel indicated by yellow arrows (Fig 10a) which leads to the conclusion that CPK3 has the potential to specifically phosphorylate at least 7 targets in *A.thaliana* microsomal membranes. The upper band in the autoradiograph at ~ 50 kDa (indicated by a red arrow) is most likely a result of the excess recombinant CPK3 autophosphorylating itself.

This approach of phosphorylating microsomal membrane fractions with recombinant CPK3 has been further refined and explored in more detail by N. Mehlmer by the use of 2-D

	Annotation	*p*-Score
AT2G30870	ERD13, Glutathione S-Transferase 10	32
*AT2G45820	Remorin, putative -binding protein, salt-induced	22
AT1G04690	KAB1 (Potassium Channel SUBUNIT)	18
*AT3G18240	unknown protein, phosphorylated	18
*AT1G53070	legume lectin family protein, cell wall asscociated	15
*AT1G09210	2, Calreticulin 2; calcium ion binding	13
*AT1G56340	1, Calreticulin 1; calcium ion binding	12
*AT5G38480	GRF3, , overexpression confers salt tolerance	9
*AT3G02750	PP2C, Protein phosphatase 2C family, group E;	9
AT5G19440	CAD, Cinnamyl-alcohol dehydrogenase, putative;	9
AT3G18820	RAB71, (Arabidopsis RAB GTPase Homolog G3F); GTP binding	8
AT2G02990	RNS1, (Ribonuclease 1); cell wall/plasma membrane associated	8
*AT1G02090	CSN7, kinase kinase; subunit of 9 signalosome	7
*AT5G16050	GRF5, UPSILON (General Regularory Factor 5)	6
AT2G43940	Thiol methyltransferase, putative, chloroplast envelope	6
AT5G07340	Calnexin, putative, vacuolar	6
AT1G28200	FIP1 (FH interacting Protein 1), VirF-interacting protein FIP1	5
AT1G78300	GRF2, OMEGA, (General Regularory Factor 2)	5
AT3G06300	P4H-2, (Prolyl-4 Hydroxylase, Isoform 2); endomembrane system	5
*AT1G77120	ADH1, (Alcohol Dehdrogenase 1); salt stress-responsive	5
AT5G67500	VDAC2 (Voltage Dependent Anion Channel 2), seedling development	5
AT3G01280	VDAC1 (Voltage Dependent Anion Channel 1)	5
AT1G74020	SS2 (STRICTOSIDINE SYNTHASE 2); strictosidine synthase	5
*AT4G17720	RNA recognition motif (RRM)-containing protein, phosphorylated	5
AT4G18800	RABA1D (Arabidopsis RAB GTPase Homolog A1D);	5
AT3G61990	O-methyltransferase family 3 protein, cytosolic	4
*AT1G22280	PAPP2C, Phytochrome-Associated Protein Phosphatase 2C; group F	4
*AT3G15260	PP2C, Protein phosphatase 2C family, group F	4

Table2. List potential CPK3 targets. The first column contains ATG identifiers for the proteins found. Asterisks in front of the ATG number indicate that a phosphorylated peptide of this protein has been reported to PhosPhAt database. The second column contains an annotation for each protein retrieved from the TAIR database. The third column lists the p-score for each protein.

gelelectrophoresis [29]. Those gels were screened for spots which where exclusively phosphorylated by CPK3. Spots obtained from autoradiography were then traced back on a non-radioactive 2-D gel. The proteins within these spots were subsequently digested with trypsin and analyzed by mass spectrometry to identify potential targets of CPK3. The original list obtained from mass spectrometry was screened for unique proteins containing a canonical CPK3 phosphorylation motive leaving us with a list of ~ 700 proteins. After sorting out all identified proteins of which the molecular weight differed by more than 10 % from the observed position of the spot, the list could be reduced to 72 proteins. These proteins where then ranked for their presence of CPK consensus sites. Therefore a p-score was defined, summarizing the presence and distribution of five known CPK3 consensus sequences over the peptide sequence, thus reflecting the likelihood of a protein to be phosphorylated by CPK3.

The higher the score the more likely is a phosphorylation event by CPK3. The 28 highest ranked proteins -with a p-score >4- where then considered as potential targets of CPK3 and are summarized in Table 2. 20 out of the 28 selected proteins are at least predicted to be localized at a membrane. Thirteen out of the 28 proteins have already been observed to be phosphorylated according to PhosPhAt database [114,115]. Further screening for *in vivo* interaction between seven of the proteins retrieved from the list and CPK3 has been performed by B. Pfister [113].

In addition to the 2-D gel approach, *in vivo* cross-linking was done to see if CPK3 could be coupled to specific targets in the plant. This was chosen because in Co-IPs done with an antibody against CPK3, only bands for CPK3 and the antibody but not for a potential substrate were observed after separation via SDS-PAGE. For crosslinking roots from 6 week old hydroponically grown *A.thaliana* plants, which had been treated with 150 mM of NaCl for 15 min, were infiltrated with 1 % formaldehyde solution to stably link CPK3 substrates to the kinase. This in vivo approach should account for more specificity, as cross-linking of a protein extract would certainly be more susceptible to false positive results due to miss-localization of the kinase and its substrates. The cross-linked root tissue was homogenized and protein extracts were analyzed by western blotting using a CPK3 specific antibody to recognize all cross-linked complexes containing CPK3. In plants which have not been treated with a protein cross-linker only a signal at the predicted mw of ~50 kDa for single CPK3 molecules has been observed in western blots done with a CPK3 specific antibody. This experiment has been repeated 3 times with biological independent samples and indeed four distinct bands with molecular weights larger than that of CPK3 were observed each time (Fig 12). The strongest signal on the western blot still derives from non cross-linked CPK3 monomers (Fig 11a). Nevertheless, the obtained results suggest that CPK3 is present in a complex with a molecular weight (mw) of ~70 kDa, a second one with a mw of ~80 kDa, a third one with a mw of ~90 kDa and a fourth one with a mw of ~150 kDa

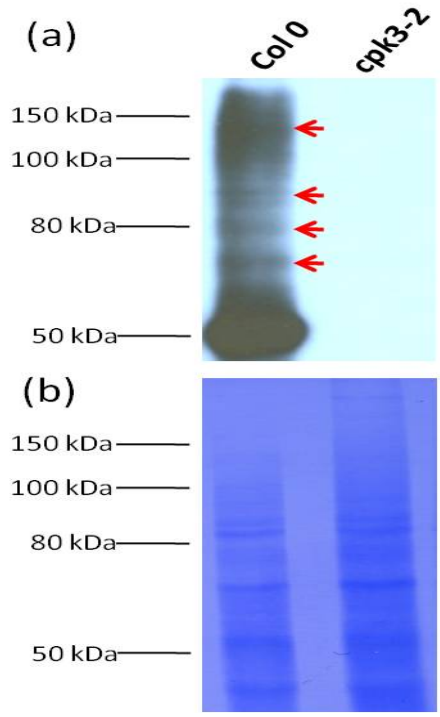

Fig11. In vivo crosslinking of CPK3. (a) Western blot with CPK3 specific antibody, once in Col0 plants and once in cpk3-2 plants. Red arrows indicate distinct complexes of CPK3 and possible subastrates. (b) coomassie stained membrane used for the western blot.

(compelxes are indicated by red arrows in Fig 11a). Similar to the results of the microsomal protein phosphorylation assay (Fig 10), these data indicates existence of CPK3 specific targets, as distinct bands were observed (Fig 11). However, it is difficult to make reliable predictions of CPK3 interaction partners by just looking at the molecular weight of complexes in this cross link assay. Considering the fact that targets of CPK3 might interact with other proteins as well one would expect that these proteins get cross-linked too. The result will rather be a complex of CPK3 and several different proteins than just CPK3 and its target alone, which could be an explanation of the fuzzy band at ~ 150 kDa. In conclusion, it seems that cross linking indeed leads to an accumulation of CPK3-substarte complexes which have not been observed in CoIPs due to the transient interaction between CPK3 and its substrates. Still, to use the full potential of the cross-link assay it should be combined with a CoIP and subsequent identification of CPK3 interaction partners by identifying the proteins present in a CPK3-complex-band via mass spectrometry in future experiments.

2.6. The transcription factor bZIP63, a target of CPK3?

Apart of finding new substrates for CPK3, more detailed data on the interaction of the kinase with already known substrates should be gathered during this thesis. The *A.thaliana* transcription factor bZIP63 is one of them. It belongs to the 75 member spanning leucine zipper transcription factor family in *A.thaliana* and is one of four members of the C-subgroup within this family [116]. Data from genevestigator showed a rhythmic change of bZIP63 transcript between night and day. This could be confirmed by semi quantitative RT-PCRs, with primers recognizing all three splicing forms of bZIP63, on RNA extracted from Col0 plants grown under a 12 hour light/ 12 hour dark cycle and samples taken over a period of 24 hours (Fig 12). It can be clearly observed that bZIP63 transcript accumulates to the highest levels at the end of the dark period (Fig 12). In the literature first evidence appeared

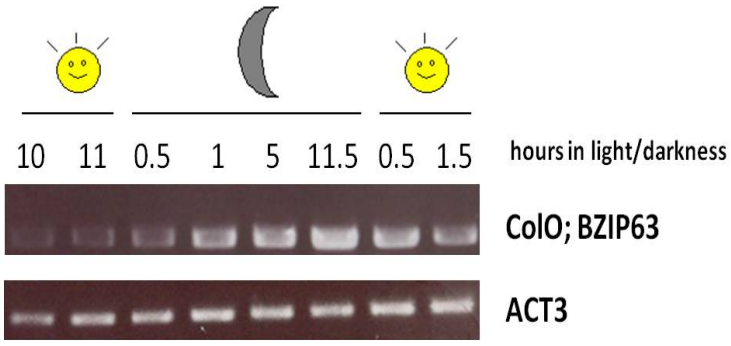

Fig12. Change of *At*bZIP63 mRNA levels. The suns indicate light period, the moon indicates dark period, the numbers above the bands indicate the time of sampling. The bZIP63 lane shows transcript levels of bZIP63. ACT3 was used as a control. Samples were taken over a period of 24 hours.

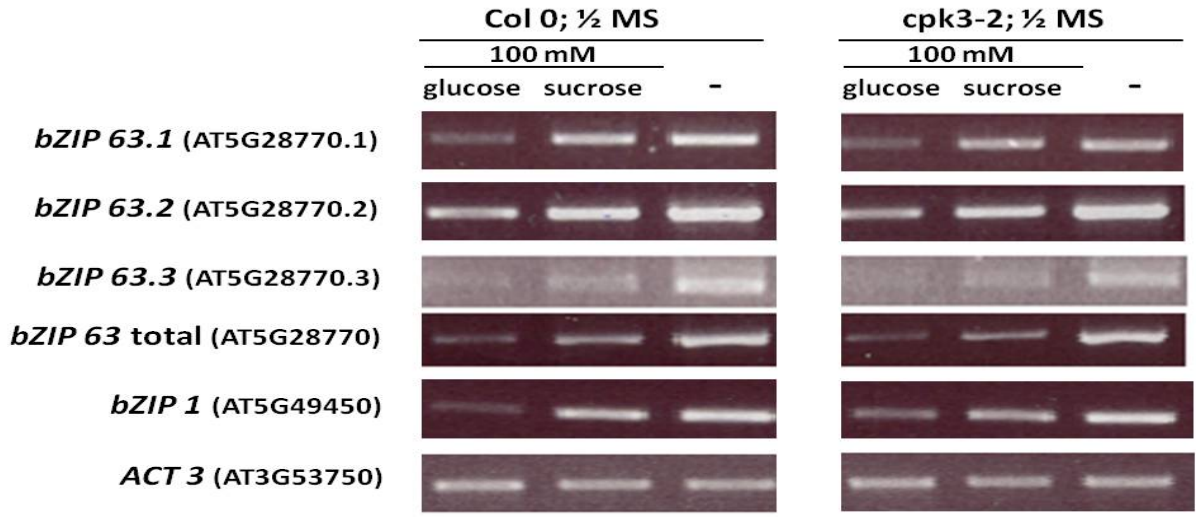

Fig13. Energy dependent change of *At*bZIP63 expression levels. *Col0* and *cpk3-2* termed columns contain the RT-PCR results for the respective genotype. bZIP63.1, bZIP63.2, bZIP63.3 refer to the respective splicing form of bZIP63 observed in this experiment. In the bZIP63 total line primers were used that recognise all three bZIP63 splicing forms. AtbZIP1 has been used as control if sugar sensing works properly in the tested plants. ACT3 was used as a control for quality of the reverse transcription reaction.

that *At*bZIP63 might be involved in energy signalling as it has been observed to synergistically activate a DIN6/luciferase reporter construct when expressed together with the kinase AKIN10 in protoplasts [117]. Therefore it was checked by semi-quantitative RT-PCRs if transcriptional regulation of bZIP63 is rather energy dependent than light dependent. It was also tested if the three splicing forms of bZIP63 are differentially expressed and if there are differences in bZIP63 transcription in the CPK3 knock out mutant compared to Col0 (Fig 13, 6.1.1. FigureS1). At the end of the dark period (see Fig 12) RNA was isolated from 14 day-old seedlings grown on 1/2 MS agar-plates supplemented with either 100 mM glucose, 100 mM sucrose or water as a control. In the control group bZIP63 mRNA levels were found to be high at the end of the dark period as observed before. However, if plants were grown on medium containing glucose or sucrose transcription levels of bZIP63 were significantly lower than compared to the control (Fig 13). Interestingly, plants grown on glucose supplemented medium show a higher decrease in bZIP63 transcript levels than it is the case for plants grown on sucrose supplemented medium. Transcripts from the bZIP63.2 splicing form are most abundant in the seedlings and bZIP63.3 transcripts were found to be least abundant. No differences between the three different bZIP63 splicing forms can be observed in terms of response to the tested sugars. Also, no difference between the expression levels of bZIP63s in *Col0* and *cpk3-2* could be observed. *At*bZIP1 has been monitored in this study to see if sugar sensing in the tested plants works properly as it has previously been reported that its mRNA levels are down regulated in response to sugar exposure of the plant [128].

As the yeast two hybrid screen in which bZIP63 was found to be an interaction partner of CPK3 was done with a C-terminally truncated version of CPK3, consisting only of its kinase domain, we wanted to know if bZIP63 is indeed a substrate for CPK3 in planta. Therefore in-gel kinase assays were done together with A. Mair. *At*bZIP63.2 protein, expressed in *E.coli* was used as a substrate. For the unbiassed assay root protein extract has been loaded onto the gel and as a control recombinant CPK3 expressed in *E.coli* has been used in a separate lane (Fig 14). When the kinase assay was done with Ca^{2+} in the buffer three major bands could be observed at molecular weights of ~40 kDa, ~50 kDa, and ~60 kDa. This indicates that bZIP63 is most likely a substrate for at least three different protein kinases in the plant. The control with recombinant CPK3 gave a signal at ~60 kDa corresponding to the highest of the three bands observed in the lane with root protein extract, suggesting that CPK3 can indeed be one of the kinases phosphorylating bZIP63. To gain a more detailed picture, EGTA was added to the kinase assay buffer for the in-gel kinase assay. Surprisingly the band at ~50 kDa disappeared completely and the intensity of the ~60 kDa band decreased substantially. The lowest band more or less remained at the same intensity. In a third kinase assay GTP was used instead of ATP. Under these conditions only the lowest of the three bands remained visible. This is an indication that the kinase responsible for phosphorylating bZIP63 at ~40 kDa is a casein kinase as these kinases are one of the few protein kinases known to be capable of using GTP as phosphate donor instead of ATP. It should be mentioned here that if protein extract from roots of *cpk3-2* plants was used for the in-gel kinase assay the same three band pattern was observed as for the *Col0* protein extract (data not shown).

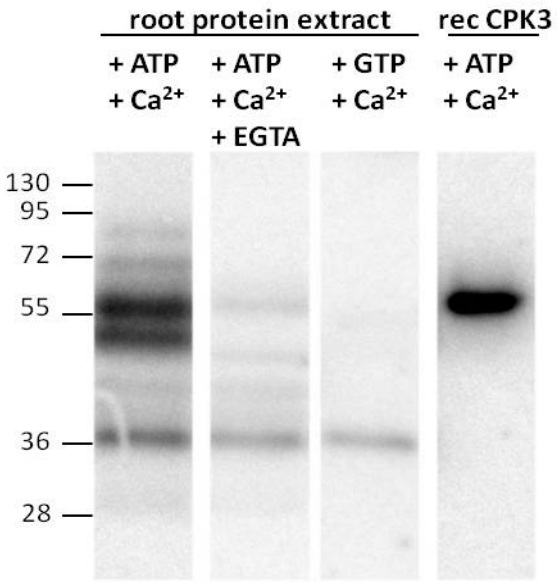

Fig14. In-gel kinase assays with bZIP63 as substrate. In all lanes recombinantly expressed bZIP63 protein was present. In the first three lanes Col0 root extract was separated. In the last lane recombinant CPK3 was separated.

Next, GST tagged bZIP63 protein was loaded on a GST-trap column. Total plant protein extract was subsequently loaded onto the column followed by elution of proteins with rising concentration of NaCl, indicated in Fig 15. With the obtained protein fractions another in-gel kinase assay was done (Fig 15a). It can be observed, that after washing with 75 mM NaCl all

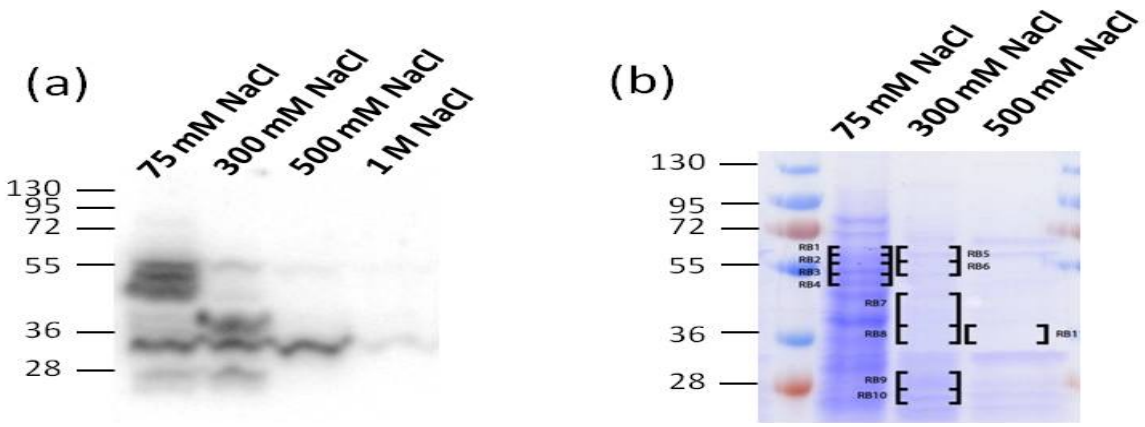

Fig15. Affinity purified fractions from bZIP63 bound column. (a) In-gel kinase assay with fractions obtained after affinity purification of total protein extracts against bZIP63. (b) A part of the fractions separated on a conventional SDS-PAGE gel for analysis via MS. Protein bands cut out for MS analysis are indicated in parenthesis.

three bands still appeared in the assay indicating that all kinases responsible for the signal are still bound to the column. Already after washing with 300 mM NaCl the upper two bands in the in-gel assay disappeared. This suggests a dissociation of the kinases responsible for the signal at ~50 and ~60 kDa from the column. Interestingly a new band was observed between the height of the lowest band and the lower signal of the upper two bands. The lowest mw activity was only eluted from the column after washing with 1 M NaCl. In parallel fractions obtained from the affinity purification were separated via a conventional SDS-PAGE gel (Fig 15b). Bands at corresponding heights to the ones observed in the in-gel assays were then cut out. Proteins therein were digested with trypsin and the resulting peptides subsequently analyzed by mass spectrometry. The results obtained were screened for kinases or kinase regulatory proteins. At the positions of the ~60 kDa band and the ~50 kDa band AKIN10, AKIN11, CKA1, CKA2, CKαcp and SNF4 could be identified. At the position of the ~40 kDa band CKB1 could be identified (Table 3). AKIN10, AKIN11, CKA1 and CKA2 are all proteins which contain a S/T kinase domain within their poly peptide chain. SNF4 does not harbour a kinase domain on its polypeptide chain and is thought to be a regulatory subunit of the AKINs. Similarly CKB, also lacking a kinase domain on its poly peptide chain, is a regulatory subunit of CKAs. CKαcp is the chloroplast localized casein kinase iso-form. For all kinases and subunits at least 4 unique peptides were found with mascot peptide scores above 70. A complete list of peptides identified for the kinases together with a sequence coverage table can be found in the supplementary data section (6.1.5 Lost S1). It should be mentioned here that for most of the kinases and the subunits found, more than one splicing form is predicted to be expressed. Only for the casein kinases splicing forms that interact with bZIP63 could be unambiguously determined in this experiment.

ATG number	Name	Function	Molecular weight	Size of excised band
At3g50000	CKA2 (casein kinase II subunit alpha-2)	protein kinase	~47 kDa	~40,50 kDa
At5g67380	CKA1 (casein kinase II subunit alpha-1)	protein kinase	~48 kDa	~40,50 kDa
At2g23070	CKαcp (casein kinase II subunit alpha cp)	protein kinase	~50 kDa	~50 kDa
At5g47080	CKB1 (casein kinase subunit beta-1)	regulatory subunit	~32 kDa	~40 kDa
At3g01090	SnRK1.1 (AKIN10)	protein kinase	~58 kDa	~50, 60 kDa
At3g29160	SnRK1.2 (AKIN11)	protein kinase	~59 kDa	~50, 60 kDa
At1g09020	SNF4	regulatory subunit	~53 kDa	~50, 60 kDa

Table3. protein kinases interacting with bZIP63. ATG number, gene identifier according to TAIR; Name, short description of the gene; Function, predicted molecular funktion; Molecular weight, predicted molecular weight according to peptide sequence; Fraction #, the approx. mol weight of the bands where peptides were detected.

To further validate the results obtained by the in-gel kinase assays, AKIN10 and AKIN11 were expressed as GST-fusions in *E.coli* and the purified kinases were then used in an *in vitro* kinase assay with bZIP63 as a substrate (Fig16a,b). Indeed the results of this assay show that bZIP63 is specifically phosphorylated by AKIN11 and AKIN10 and that this phosphorylation is reversible by λ-phosphatase if added to the reaction after 15 minutes (Fig16a,b). It is interesting to observe that the signal obtained from phosphorylated bZIP63 is stronger in the kinase reaction combination bZIP63 + CPK3 than bZIP63 + AKIN10 or AKIN11 (Fig 16a. Furthermore it seems that Akin10 phosphorylates bZIP63 more efficiently than AKIN11 (Fig16a,b).

In vivo interaction between the kinases and their regulatory subunits was studied in a series of BIFC experiments (Fig 18). As bZIP63.2 is the most abundant splicing form of bZIP63 according to RT-PCR studies it was chosen as interaction partner in all BIFC studies. C-terminal and N-terminal moiety of CFP were fused to the respective proteins which were

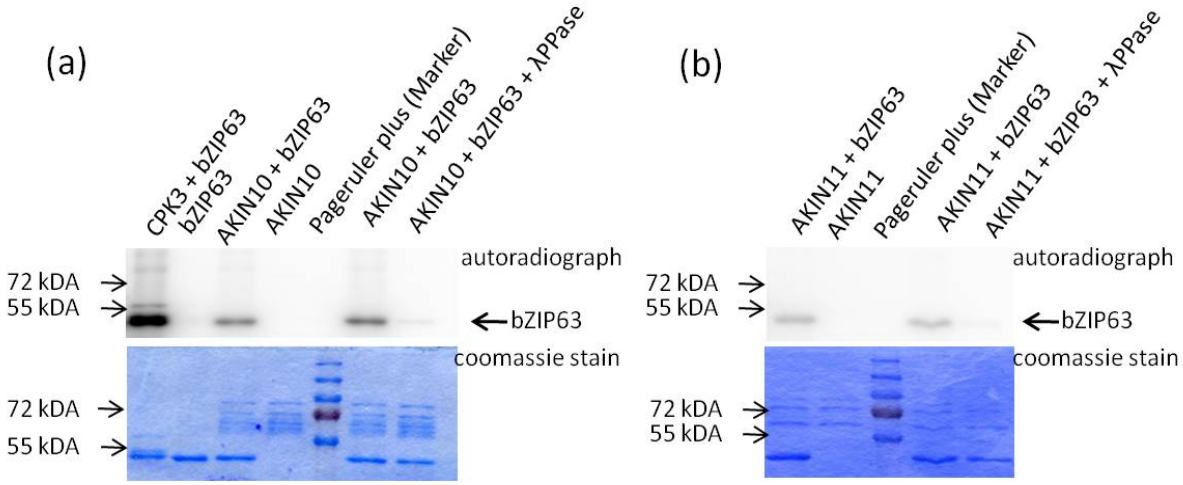

Fig16. Kinase assays with AKIN10 and AKIN11. (a) Kinase assays with AKIN10 and bZIP63 as substrate. (b) Kinase assays with AKIN11 and bZIP63. (a,b) coomassie stains are templates of the autoradiographs, bZIP63 is indicated by a arrow in the autoradiograph.

tested in this study. The setup at the microscope was kept the same throughout the whole experiment. CFP signals were obtained from AKIN10, SNF4, CKB1 and CKA1 if co expressed together with bZIP63.2. Interaction signals were only obtained from nuclei (Fig17). It is interesting to note that the signal intensity was strongly dependent on the position of the fluorophore moieties if they were fused either downstream or upstream of the tested proteins. In case of CKA1 - bZIP63.2 the interaction signal was observed to be strongest if both interaction partners were tagged at their respective C-termini (Fig17d). Combinations of CKA1 and bZIP63.2 tagged at different positions than mentioned before led to a considerably weaker signal. In case of AKIN10 - bZIP63.2 interaction a signal was only observed if AKIN10 was tagged at its C-terminus and bZIP63.2 at its N-terminus. For any other orientation no signal was observed. It is remarkable that for AKIN11 together with bZIP63.2 no signal could be observed regardless of all possible different orientations used in the experiment. Almost equally intense and speckled signals within the nucleus have been observed for the interactions between bZIP63.2 and SNF4, CKB1 and CKA1. However, some differences in localization of the CFP signal were observed between these interaction partners. SNF4 - bZIP63.2 interaction signal seemed to be excluded from the nucleolus (Fig 17b), whereas signals from interaction between CKA1 and bZIP63.2 originated to a major part from the nucleolus (Fig 17d). CPK3 has also been tested for interaction with bZIP63.2 however, under the conditions used no CFP signal was obtained.

In summary it can be said that the mRNA levels of transcription factor bZIP63 are regulated in an energy dependent manner. Furthermore, bZIP63 was found to be a substrate of the protein kinases AKIN10/11 and CK2 in the plant. However the functional consequences of bZIP63 phosphorylation by one of these kinases has still to be elucidated. Taking into account the results of the in-gel kinase assays it remains questionable if CPK3 phosphorylates bZIP63 *in vivo* and if this phosphorylation would have any functional significance to the plant.

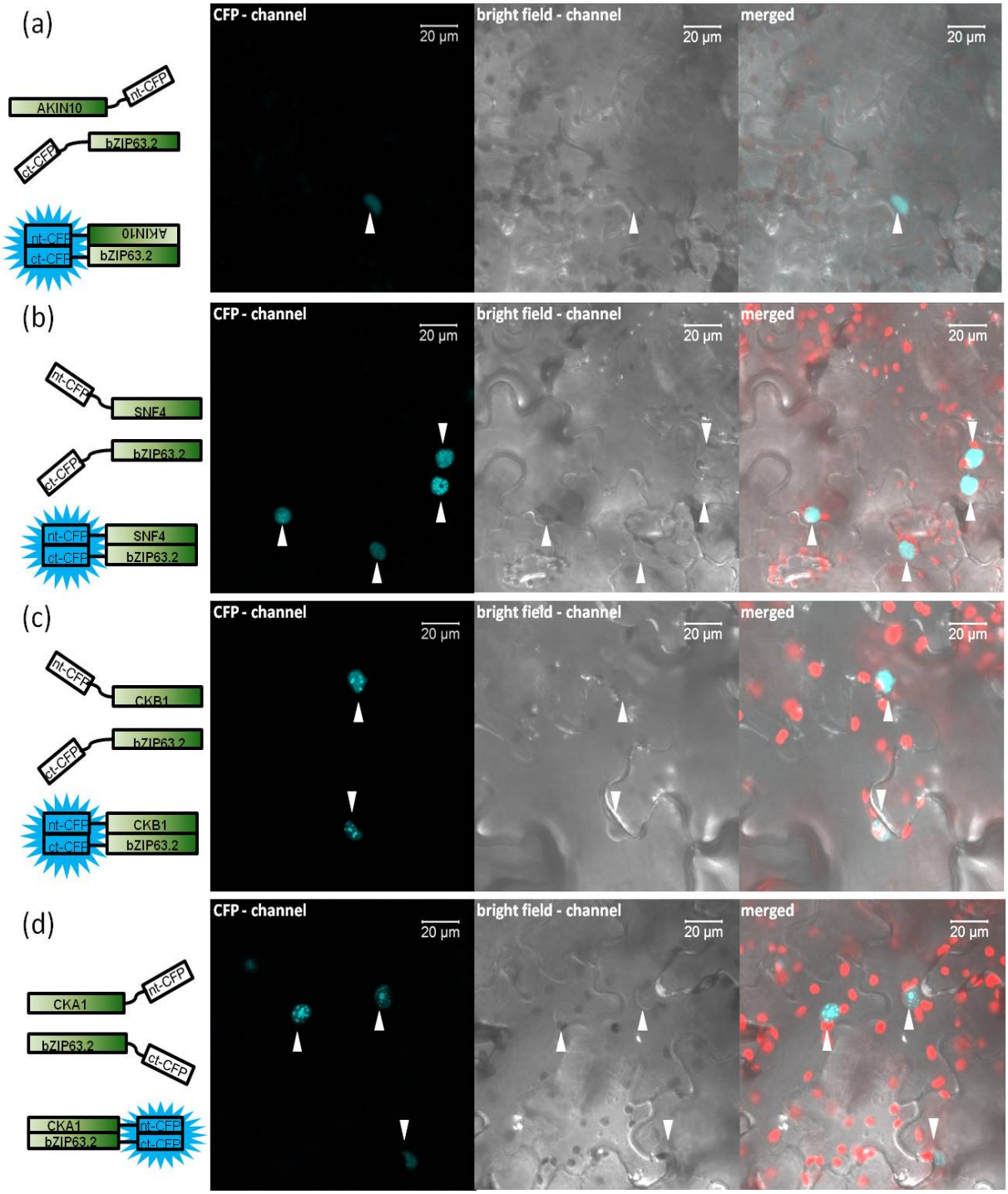

Fig17. BIFC studies with bZIP63.2 interaction partners. (a) Interaction of bZIP63.2 with AKIN10. (b) Interaction of bZIP63.2 with SNF4. (c) Interaction of bZIP63.2 with CKB1. (d) Interaction of bZIP63.2 with CKA1. In the first column drawings illustrate the position of the fluorophore moieties within the fusion protein. Attachment on the left symbolizes a N-terminal fusion and attachment on the right symbolizes a C-terminal fusion of the fluorophore moieties to the respective interaction partner. ct-CFP symbolizes the C-terminal moiety of CFP; nt-CFP symbolizes the N-terminal moiety of CFP. Signals in the CFP channel result from reconstituted CFP molecules. Nuclei in all pictures are marked by white triangles. The last column shows a merged picture of the chloroplast-, CFP- and the bright field-channel. Red coloured signals in the merged picture result from chlorophyll auto fluorescence in chloroplasts.

2.7. The vacuolar two-pore K+ channel TPK1 interacts with CPK3

TPK1 is a K^+ channel that enables K^+ currents from the vacuole into the cytosol [118]. It functions as dimer and it is Ca^{2+} activated [118]. In the TPK1 sequence a C-terminal pair of EF-hands is predicted as well as a 14-3-3 regulatory site at its N-terminus [118]. Furthermore it has been shown that binding of GRF6 (GF14λ) increases TPK1 activation in a dose dependent manner [118]. For binding of GRF6 the phosphorylation of S42 in TPK1 is necessary. In kinase assays with ^{32}P labelled ATP it has been shown that CPK3 can phosphorylate S42 in the N-terminus of TPK1 and therefore allow binding of GRF6 (personal communication M. Teige).

To connect TPK1 and CPK3 on a physiological level germination assays were done, together with B. Pfister. Seeds of Col0, the previously described *cpk3* lines, *tpk1-3* (a *tpk1* knock out line) and *tpk1 ox3* (a *tpk1* over expresser line) were germinated on agar plates under three conditions. First on the control plates seeds of all lines except *Col0* germinated with 100 % efficiency (Fig 18). This indicates that the *Col0* seeds used in this experiment were for unknown reason of less quality than the seeds from the other lines used. To correlate any data of the mutant lines to Col0 the experiment must be repeated. Under conditions where the medium was supplemented with 150 mM NaCl, the *cpk3-2* line germinated less efficient than

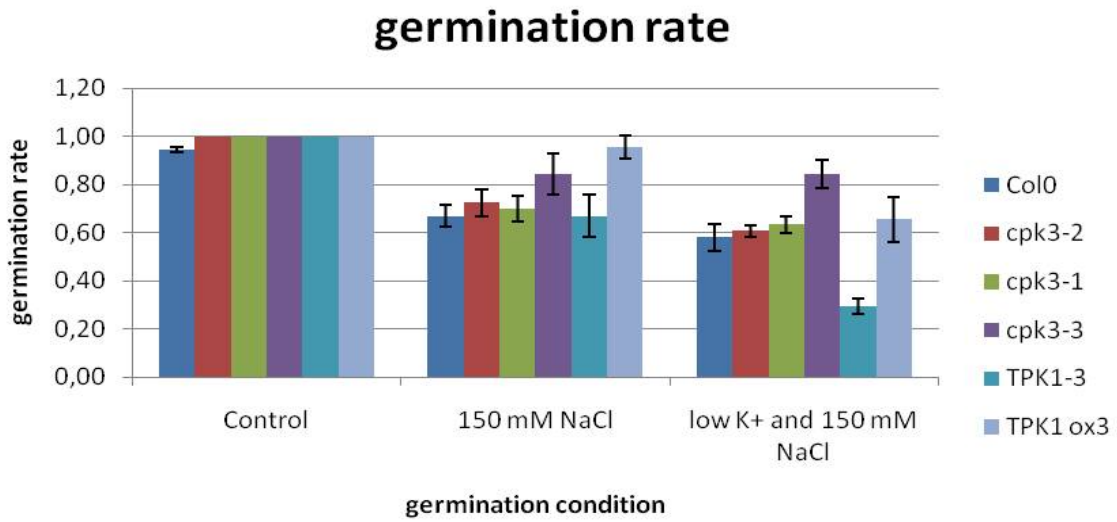

Fig18. Germination assays under salt stress and K^+ limiting conditions. Control: mineral medium containing 2 mM K^+; 150 mM NaCl: mineral medium containing additional 150 mM NaCL; low K^+ and 150 mM NaCl: mineral medium containing 50 µM K^+ and additional 150 mM NaCl. Col0, wild type; *cpk3-2*, cpk3 knock out; *cpk3-1*, cpk3 knock down; *cpk3-3*, cpk3 over expresser; *TPK1-3*, tpk1 knock out; *TPK1 ox3*, tpk1 over expresser. ~100 seeds were distributed per plate. for each line and condition four plates were analyzed. error bars indicate standard deviation. Germination rate is the fraction of seeds that germinated from all seeds put on the plate.

the *cpk3-3* line resembling the results from the initial experiments. Similar to that, the *tpk1-3* line germinated less efficient than the *tpk1 ox3* line(Fig18). If, in addition to the 150 mM NaCl, the medium was adjusted to a final concentration of 50 µM of K^+ (indicated as low K^+) the *cpk3-2* line germinated less efficient than under salt stress only (Fig19). The germination rate of the *cpk3-3* line, however, stayed the same as under high salt conditions. For the seeds of the *tpk1-3* line a drop of the germination rate by ~50 % compared to the "high salt only germination rate" could be observed under K^+ limiting conditions (Fig19). The germination rate of the *tpk1 ox3* line also dropped under salt stress and K^+ limiting conditions by ~20 % compared to salt stress only (Fig 18). This decrease in germination rate is less pronounced than in the *tpk1-3* line (Fig 18). The results clearly assign an important physiological function to TPK1 under salt stress and K^+ limiting conditions. Furthermore they also suggest that CPK3 is indeed involved in the regulation of ion homeostasis under salt stress. Therefore it was decided to further investigate the interaction between CPK3 and TPK1.

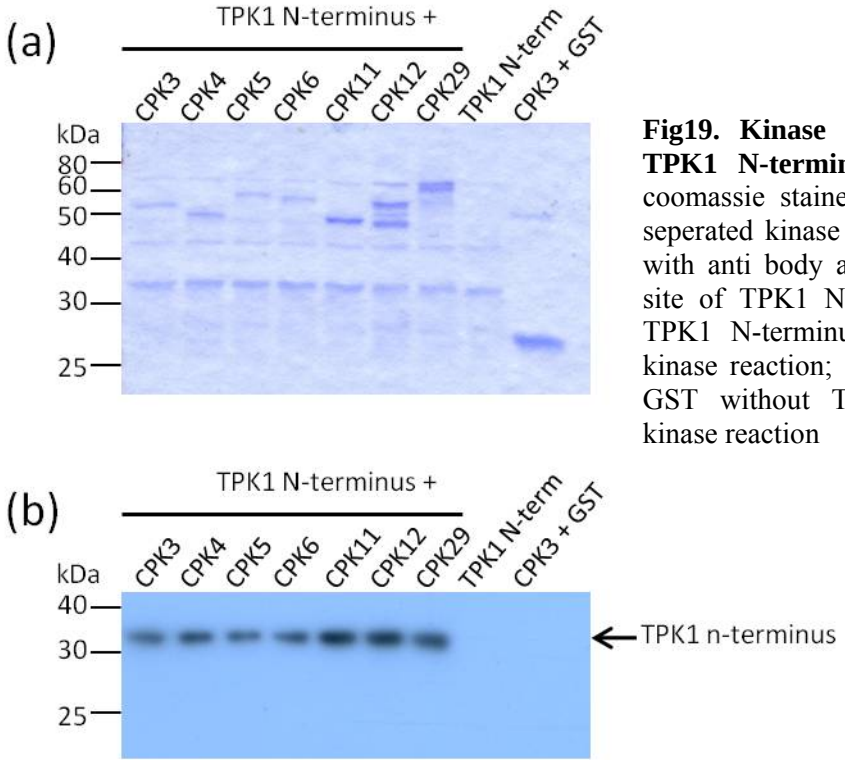

Fig19. Kinase assays with CPKs and TPK1 N-terminus as a substrate. (a) coomassie stained gel of the SDS-PAGE seperated kinase reaction. (b) western blot with anti body against (P)S in the 14-3-3 site of TPK1 N-terminus. TPK1 N-term: TPK1 N-terminus without kinase in the kinase reaction; CPK3 + GST: CPK3 and GST without TPK1 N-terminus in the kinase reaction

The N-terminal part of TPK1 was expressed and purified from *E.coli* as a GST fusion protein. This was subsequently used as a substrate for selected full length CPKs in a series of kinase assays. By using an antibody that specifically recognises a 14-3-3 motive [(R/K)XXSXP] in which the indicated serine is phosphorylated, it was tested which CPKs can specifically phosphorylate TPK1 at the serine critical for GRF6 binding (Fig 20). Surprisingly all tested CPKs were able to phosphorylate TPK1 at S42 (Fig 20b). Furthermore it seems that this

phosphorylation takes place in a dose dependent manner as the signals from assays where more kinase has been used are stronger (Fig 20a,b).

In a BIFC study where CPK3 and TPK1 were tagged with moieties of CFP at their N-termini a signal from the vacuolar membrane was observed (Fig 20b). This supports the results of the previous experiments. Furthermore T. Müller (university of Würzburg) modelled the interaction between TPK1 and CPK3 at an atomic level (Fig 21a). This model predicts that the amino acids R35, R36, R38 R39 in the N-terminus of TPK1 and E163, D166 in the kinase domain of CPK3 are important for interaction between the two proteins (Fig 21a). To test if this holds true *in vivo*, proteins with point mutations of the respective amino acids were created.

As we had already established the BIFC system for testing interactions *in vivo* and *in planta,* we tried to assess how well it is suited for quantification of protein-protein interactions. One major obstacle was an unequal signal intensity observed between different tobacco leaves infiltrated with the same agrobacteria strain carrying the same expression vector. To overcome this problem, a tobacco leaf was divided into 4 quadrants (Fig 20c) and each quadrant was co-infiltrated with an equal amount of agrobacteria carrying CPK3 or TPK1 tagged with CFP moieties at their N-termini (Fig 20a,b) (for a detailed description of the procedure see material and methods section). Afterwards leaf discs of each of the quadrants were analyzed with an LSM with a fixed laser, optic and detector setup for one leaf. At eight randomly selected positions on the leaf disc, pictures were taken of the vacuolar membranes (e.g. Fig 20b) and analyzed for their CFP fluorescence intensity originating from the vacuolar membrane. From these 8 pictures a mean signal intensity was then calculated per pixel of the selected area. In all four quadrants this mean signal intensity was found to be almost equal. According to student's t test all samples are > 95 % likely to be from the same group (Fig 21c). The same experiment was repeated on 2 more leaves with similar results. These findings suggest that the BIFC system is also suitable for relative quantification of protein-protein interaction. For all following quantitative BIFC experiments, relative intensities of one tobacco leaf were measured and afterwards normalized to a standard control on the same leaf, which in this case was the signal intensity obtained from interaction between wild type CPK3 and TPK1. The resulting value is then a fraction referred to as normalized intensity.

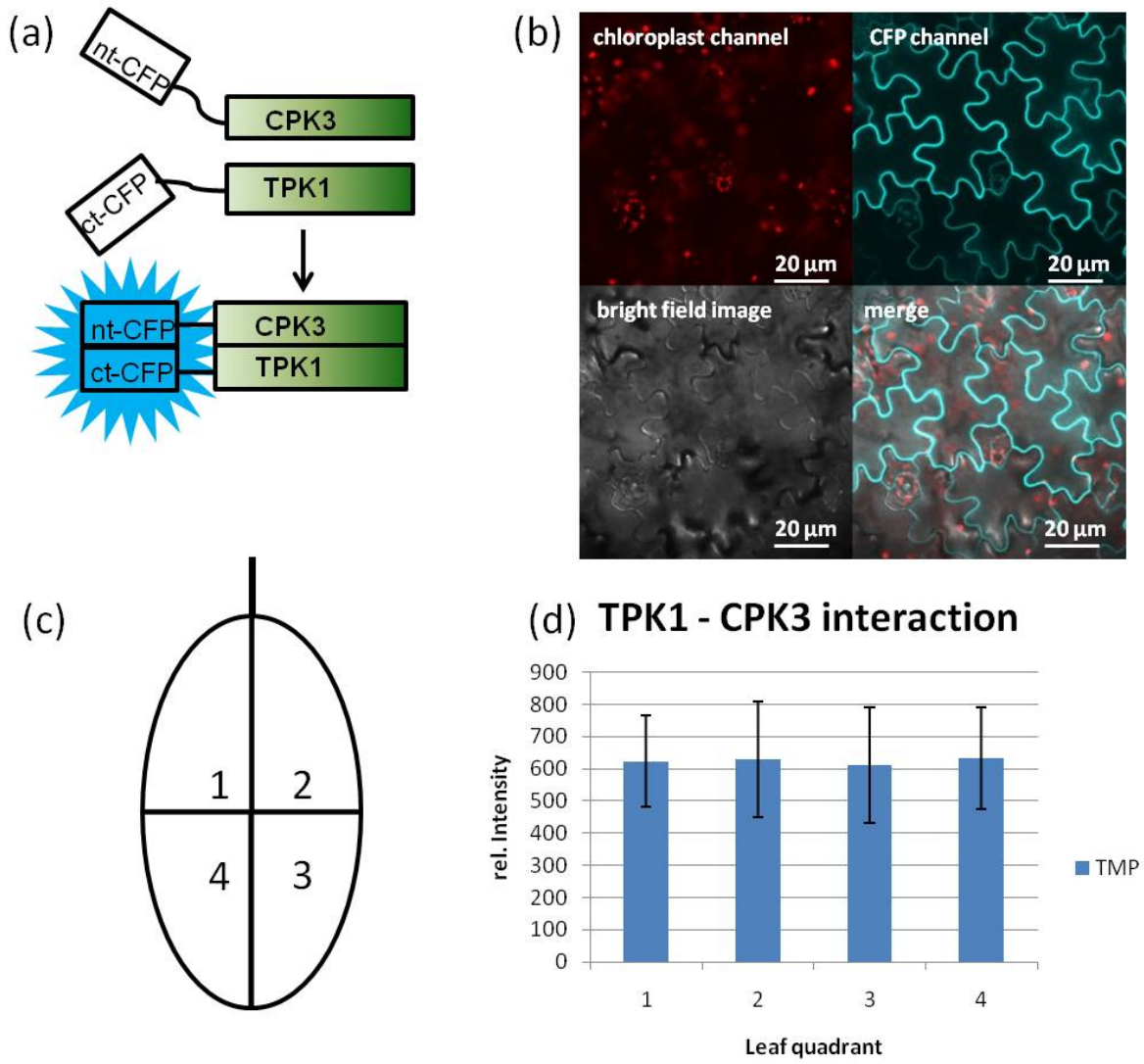

Fig20. Assesment of BIFC for quantification of protein-protein interaction. (a) A drawing of the interacting proteins used in this study with their respective tags. (b) BIFC Micorscopy pictures: Chloroplast channel, chlorophyll auto fluorescence from chloroplasts; CFP channel, signal obtained from complemented CFP; merge, chloroplast channel, CFP channel, bright field image merged into one picture. (c) A scheme of a tobacco leaf, depicting how leaf quadrants were selected. The quadrant number corresponds to quadrants in the diagram. (d) Diagram of relative fluorescence intensities measured at the LSM. Values are depicted in mean pixel intensities (TMP). Error bars indicate the standard deviation, n = 8.

When the interaction between TPK1 wild type and a CPK3 E163A D166A double mutant was tested, no fluorescence signal of the reconstituted CFP could be observed. In contrast, the wild type versions of both proteins interacted perfectly on the leaves tested. A western blot with an antibody against the FLAG epitope, fused to the CPK3 BIFC peptide, revealed that the mutated CPK3 variant was not expressed at all, explaining, the absence of a fluorescence signal (data not shown). Why the mutated CPK3 version was not expressed or rapidly degraded after synthesis is not clear. If a TPK1 R35, R39 to alanine double mutant (Fig 21b) was tested for interaction with wild type CPK3 a reduction of the fluorescence signal by

~ 40 % was observed (Fig 21d). Here the western blot with specific antibodies for each of the both interaction partner constructs showed that the protein amounts of the wild type version of the proteins and the mutants were equal (Fig 21e). Taken together these results suggest that R35 and R39 are indeed involved in stabilizing the interaction between CPK3 and TPK1. Testing of the interaction between CPK3 wild type and a TPK1 version with R36 and R38 mutated to alanine brought similar results as the other TPK1 double mutant (data not shown). This indicates that most likely both pairs of arginines are involved in the interaction between TPK1 and CPK3.

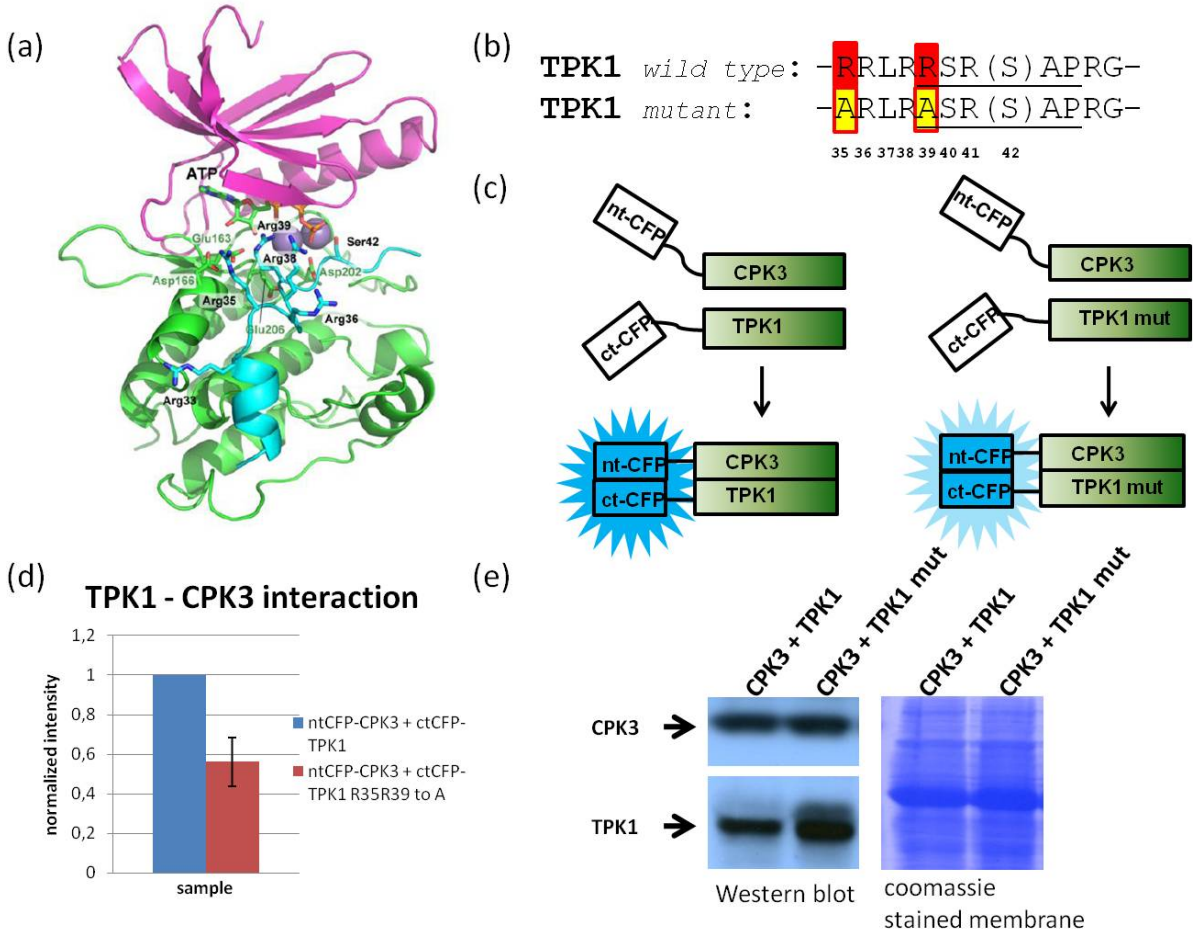

Fig21. Important aa residues for interaction between TPK1 and CPK3. (a) A model of the interaction between the TPK1 N-terminus and CPK3. Amino acids predicted to be important for the interactions are numbered. The model is kindly provided by Thomas Müller (university of Würzburg) (b) Comparison of the wild type sequence of TPK1 and the R35, R39 to A mutant (marked red and yellow). Underlined amino acids represent the 14-3-3 sequence. S in parenthesis is phosphorylated by CPK3. Numbers of the amino acids are below the sequence. (c) a simple graphical summary of the results obtained in this experiment, faint blue indicates a weak interaction signal. (d) diagram depicting the difference between interaction of wild type CPK3 and TPK1 and CPK3 and TPK1 R35R39 to A (TPK1 mut). The error bar indicates standard deviation n = 4. (e) western blot and coomassie stained membrane for testing protein amounts of CPK3 and TPK1 wild type and mutant.

With this BIFC system we also tried to observe differences between interactions of TPK1 and other CPKs than CPK3. Unfortunately the differences observed in signal intensity of reconstituted CFP positively correlated with the different amounts of protein of the expressed kinases, observed in a western blot. Thus it was not possible to determine any differences in *in vivo* interactions between TPK1 and different CPKs with this assay.

2.8. Interaction between *A.thaliana* nitrate reductase and CPK3

Plants take up the majority of the needed nitrogen in form of nitrate. Nitrate is reduced by nitrate reductase to nitrite in the cytosol and nitrite is further reduced to ammonium by nitrite reductase in the choloroplast. There, the ammonium is transferred to glutamate, forming glutamine via GS/GOGAT cycle. In this chain, nitrate reductase is thought to be the rate limiting enzyme [124]. In *A.thaliana* it consists of a molybdenum binding oxidoreductase domain where the reduction of nitrate takes place, followed by the dimerisation domain. A 14-3-3 regulatory site is immediately downstream of the cytochrome b_5 binding domain. At the nitrate reductase C-terminus a FAD and NADH binding site are present (Fig 22c). More than 10 years ago it was found that nitrate reductase from spinach was phosphorylated at serine 543 by a calcium dependent protein kinase which was a homolog to *At*CPK3 [50]. Similar to TPK1, this phosphorylation event subsequently leads to binding of a 14-3-3 protein to the nitrate reductase thereby inactivating it [53]. However, in that particular study [53] *At*CPK17 was found to be the kinase most efficiently phorsphorylating *At*NIA2 (assimilatory nitrate reductase in *A.thaliana*). Considering the expression data of *At*CPK17, which suggest that *At*CPK17 is only present in pollen, it seems unlikely that *At*CPK17 is really the CPK regulating the assimilatory *At*NIA2 in vegetative tissue of *A.thaliana*. As nitrate reductase was found to be located in the cytosol [119] CPKs which are known or at least predicted to be localized in the cytosol were tested if they are able to phosphorylate regulatory S534 in *A.thaliana* NIA2. Therefore *At*NIA2 expressed in *P.pastoris* (kindly provided by G. Schwarz, University of Cologne) was used as a substrate in kinase assays with different CPKs recombinantly expressed and purified from *E.coli*. Phosphorylation of S534 was detected by western blot analysis with a 14-3-3 antibody recognising the phosphorylated 14-3-3 consensus sequence. It could be shown that *At*CPK3, *At*CPK4, *At*CPK11, *At*CPK12 and *At*CPK29 phosphorylate S534 in a Ca^{2+} dependant manner (Fig 22). This confirms the in vitro results where *At*CPK3 was found to phosphorylate spinach nitrate reductase at its regulatory serine 543 [50]. Most interesting is the observation that *At*CPK5 and *At*CPK6 do not phosphorylate

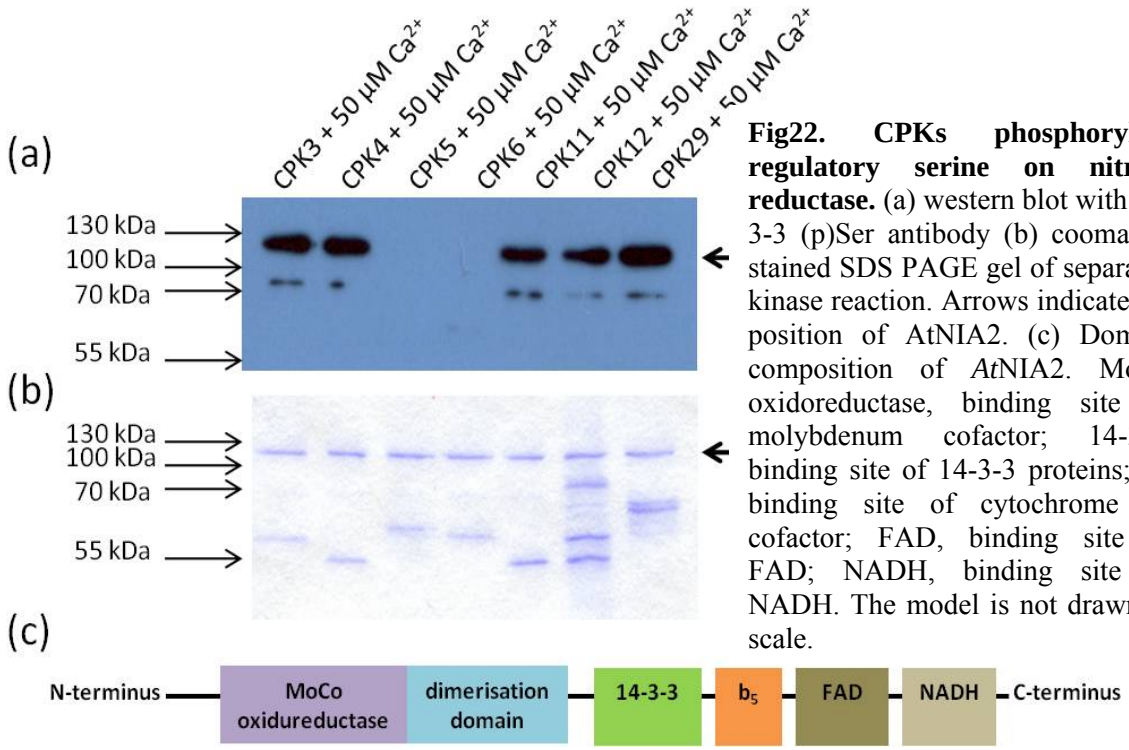

Fig22. CPKs phosphorylate regulatory serine on nitrate reductase. (a) western blot with 14-3-3 (p)Ser antibody (b) coomassie stained SDS PAGE gel of separated kinase reaction. Arrows indicate the position of AtNIA2. (c) Domain composition of *At*NIA2. MoCo oxidoreductase, binding site of molybdenum cofactor; 14-3-3, binding site of 14-3-3 proteins; b_5, binding site of cytochrome b5 cofactor; FAD, binding site of FAD; NADH, binding site of NADH. The model is not drawn to scale.

AtNIA2 at S534. This indicates that there exists a difference in target specificity between the soluble CPKs in *A.thaliana*. As *At*CPK3 is the most abundant CPK in *A.thaliana* according to gene expression studies, and the second most efficient CPK in inhibiting nitrate reductase after *At*CPK17 (personal communication by G. Schwarz), further experiments on the regulation of nitrate reductase focused on CPK3.

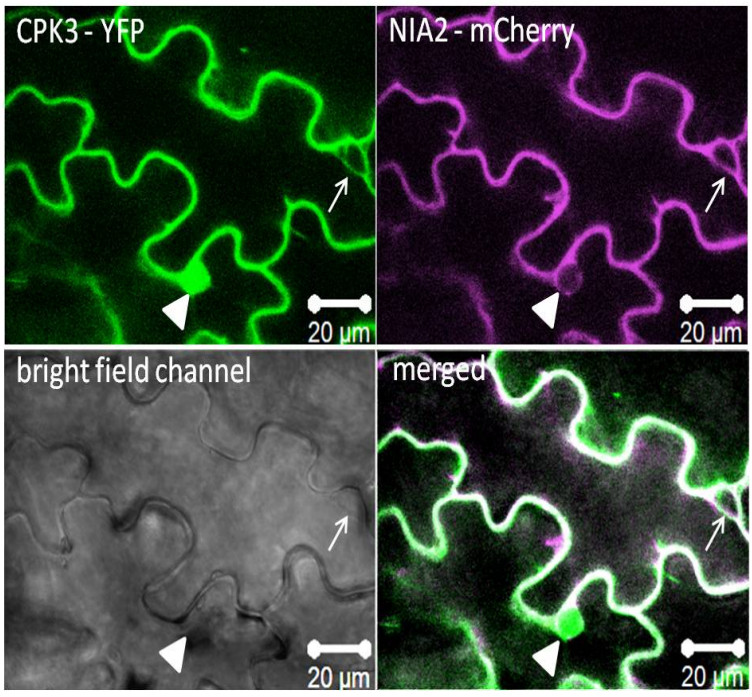

Fig23. Co localization of CPK3 and nitrate reductase. CPK3-YFP, fluorescence signal from YFP; NIA2-mcherry, fluorescence signal from mcherry; merged, an overlay of the YFP, mcherry and bright field channels. White triangle indicates position of a nucleus. White arrow indicates a cytosolic strand. White coloured signal from the cytosol indicates co localization of CPK3 and nitrate reductase.

So far only in vitro data exist concerning the interaction between CPKs and nitrate reductase. Therefore a set of experiments was done to verify in vivo interaction between both *At*CPK3

and *At*NIA2. To test if interaction between *At*NIA2 and *At*CPK3 is theoretically possible *in vivo,* a co-localization study was done in infiltrated tobacco epidermal leaf cells. There, nitrate reductase C-terminally tagged with mCherry only gave a signal in the cytosol and not in the nucleus (Fig 23). In contrast a signal from *At*CPK3 C-terminally tagged with YFP can also be observed from the nucleus as well as the cytosol (Fig 23). A merge of both channels clearly shows co-localization of nitrate reductase and *At*CPK3 in the cytosol (Fig 23, white colour in merged image). The presence of both proteins at the same sub-cellular compartment indicates that interaction between *At*CPK3 and *At*NIA2 can be possible. Next a further BIFC study was done with *At*CPK3 and *At*NIA2 tagged with the corresponding moieties of CFP at their N-termini. A CFP signal was observed from cytosolic lobes and cytosolic strands but not from the nucleus or chloroplasts (Fig 24). The signal intensity was similar to the signal intensity obtained on the interaction of AtCPK3 and *At*TPK1 in the same BIFC system. These findings strongly suggest that *At*CPK3 and *At*NIA2, *in vivo*, indeed interact exclusively in the cytosol. To gain more insight into the mode of interaction between *At*CPK3 and *At*NIA2 the sequence around the 14-3-3 consensus site of both proteins were compared. Both R38 and R39 from TPK1 are replaced by two lysine residues at the corresponding position in nitrate reductase

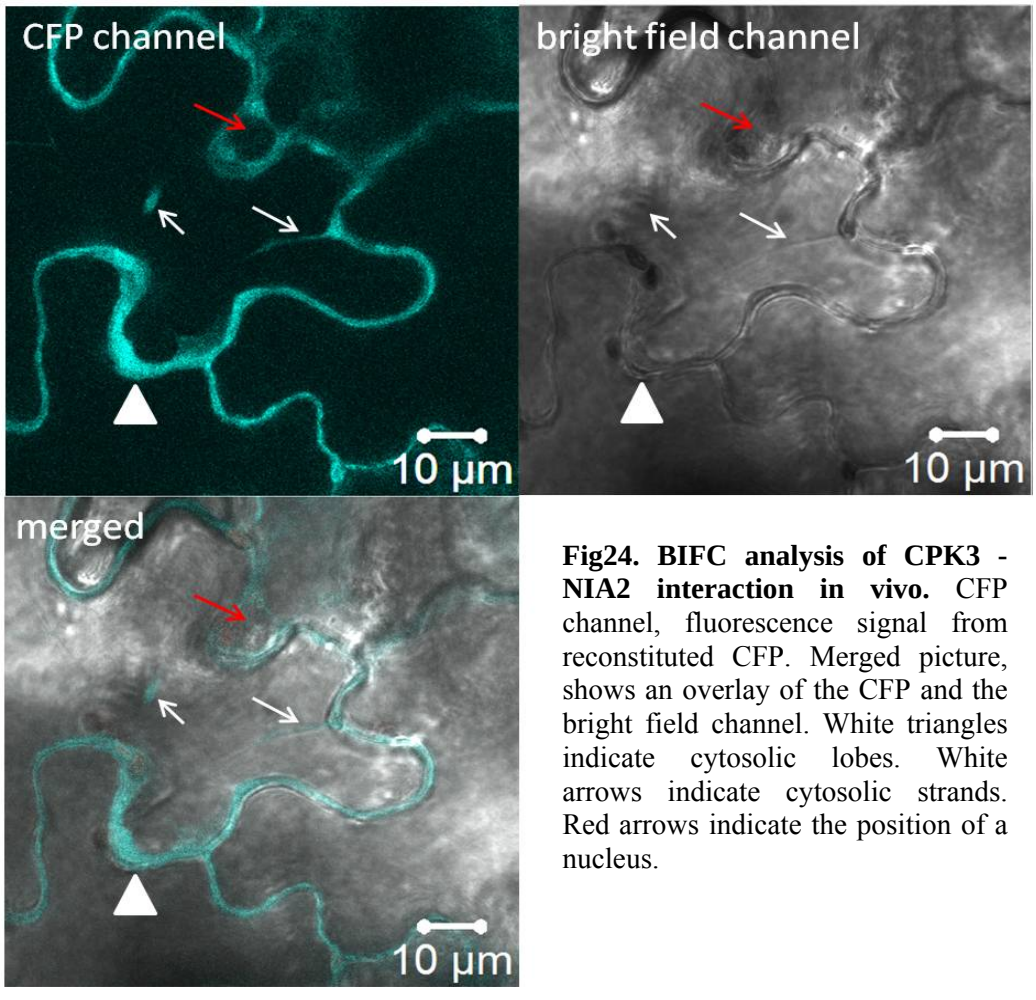

Fig24. BIFC analysis of CPK3 - NIA2 interaction in vivo. CFP channel, fluorescence signal from reconstituted CFP. Merged picture, shows an overlay of the CFP and the bright field channel. White triangles indicate cytosolic lobes. White arrows indicate cytosolic strands. Red arrows indicate the position of a nucleus.

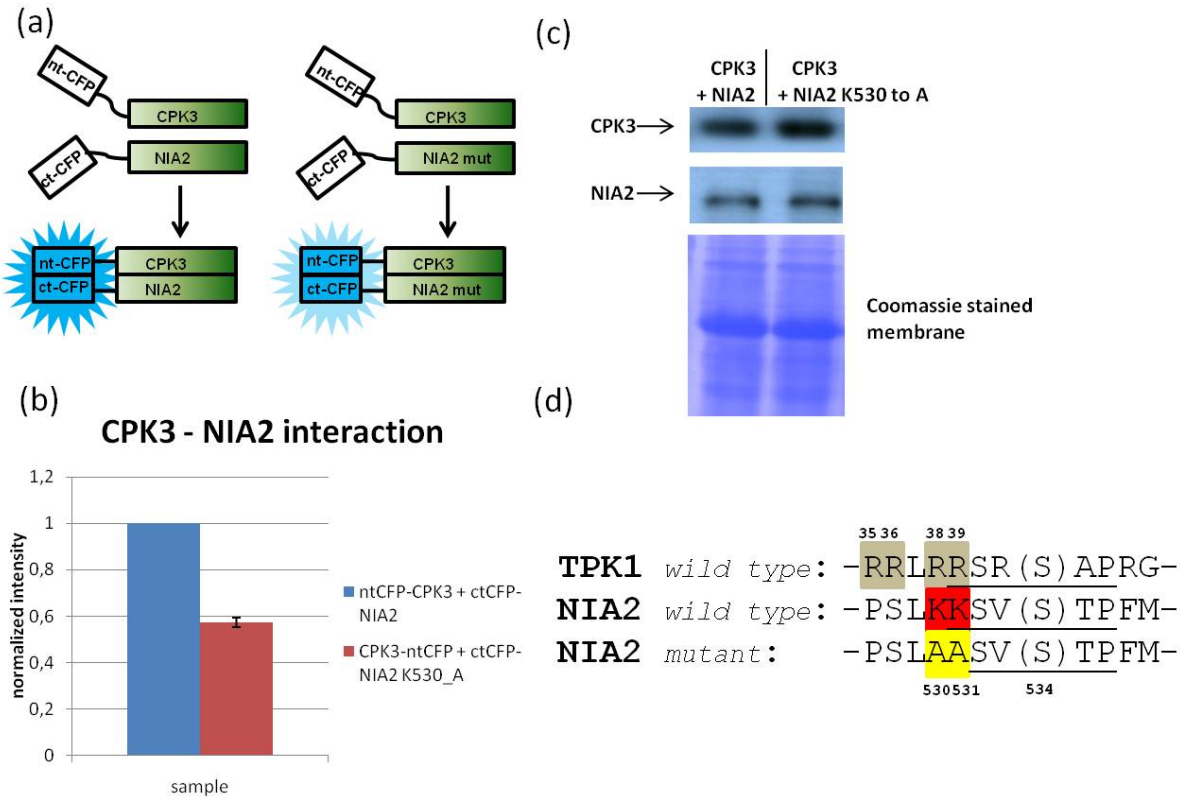

Fig25. Interaction between nitrate reductase and CPK3. (a) A drawing of the experimental setup used for the BIFC experiments. (b) A diagram summarising the BIFC experiments between CPK3 and NIA2 wild type and NIA2 K530 to A. The error bar indicates standard deviation n = 4. (c) Western blots with antibodies against CPK3 and NIA2 constructs used in BIFC experiments and the coosmassie stained membrane of the western blots. (d) Alignment of neighbouring sequences of the 14-3-3 consensus sequence in TPK1 and NIA2. 14-3-3 consensus sequence is underlined. S in parenthesis is phosphorylated by CPK3. Numbers above and below the amino acid sequence indicate the position of the amino acids in the respective proteins.

(Fig 25d). The other two positively charged amino acids R35 and R36 downstream of the 14-3-3 site in TPK1 are absent in the nitrate reductase sequence, instead there are the non-charged amino acids proline and serine on the corresponding positions of *At*NIA2(Fig 25d). Obviously, mutation of the positively charged residues downstream the 14-3-3 consensus site in TPK1 has an effect on the binding efficiency of CPK3 to its substrate.

Therefore the nitrate reductase sequence was analyzed with two publicly available structure prediction programs NetSurfP1.1 [120] and JPred3 [121]. Both programs predicted K530 and K531 of *At*NIA2 to be exposed to the surface of the protein which makes them potential interaction sites for CPK3. To test if this holds true *in vivo*, K530 and K531 were independently mutated to alanine (Fig 25d). Subsequently the mutants were tested for interaction with CPK3 in a quantitative BIFC assay. Similar to the tested TPK1 mutants, a decrease in fluorescence intensity of ~50 % could be detected when CPK3 was co infiltrated with the point mutants of nitrate reductase compared to the interaction between wild type

nitrate reductase and CPK3 (Fig 25a,b). In a western blot it was confirmed that both, the mutated and the wild type version of nitrate reductase as well as CPK3 were equally expressed in the tobacco leaf (Fig 25c). Together these findings suggest that the positively charged residues immediately downstream of the 14-3-3 site are essential for interaction with the CPK at this site.

2.9. An evolutionary view on posttranslational nitrate reductase regulation

To obtain a global overview on the regulation of nitrate reductase by 14-3-3 proteins in plants all nitrate reductase sequences of 22 different plant genomes were compared by multiple sequence alignments. The nitrate reductase sequences were retrieved from the total sequences of the 22 plant genomes which are provided at the Phytozome v6.0 [122]. Using the publicly available "3of5" software [123], all nitrate reductase sequences were screened for 14-3-3 consensus sequences. Although all 22 genomes contained at least one nitrate reductase sequence that was similar in structure and sequence to that of *At*NIA2, only species from the clade of tracheophytes contained nitrate reductase sequences containing 14-3-3 consensus sites (Fig 26, FigS4). In *M.truncatula* it is uncertain if the nitrate reductase not carrying a 14-3-3 site is functional. Rather than encoding all functional domains on one polypeptide chain this gene has an operon like structure where the MoCo domain, the dimerisation domain and the cytb5 binding, FAD and NADH domain are encoded on three separate genes immediately downstream of each other. In *M.esculenta* two nitrate reductase sequences are predicted to be present. However, it seems that both genes account for only one functional protein as one gene lacks the FAD and NADH binding domain and the other one lacks the MoCo oxidoreductase domain. Still a 14-3-3 consensus sequence is present at the same position within the polypeptide chain of *M.esculenta* nitrate reductase like in nitrate reductases sequences, harbouring this regulatory domain, from other plant species. Therefore it is highly likely that the nitrate reductase activity in *M.esculenta* is also regulated by 14-3-3 proteins. The nitrate reductase sequence not harbouring a 14-3-3 site from *C.sativus* is least related to all other nitrate reductase sequences in angiosperms contained in the data set, according to sequence alignments (FigS4). Also the nitrate reductase sequences of *S.italica* and *S.bicolor* without 14-3-3 site branch separately from all other analyzed nitrate reductase sequences within the group of grasses (FigS4). Together these data likely reflect an adaptation of nitrate reductase to new signalling pathways during evolution of vascular plants. In a multiple sequence alignment of all nitrate reductase sequences containing a 14-3-3 consensus motive a conserved stretch of ~18 amino acids around the 14-3-3 motive was identified (FigS3). The

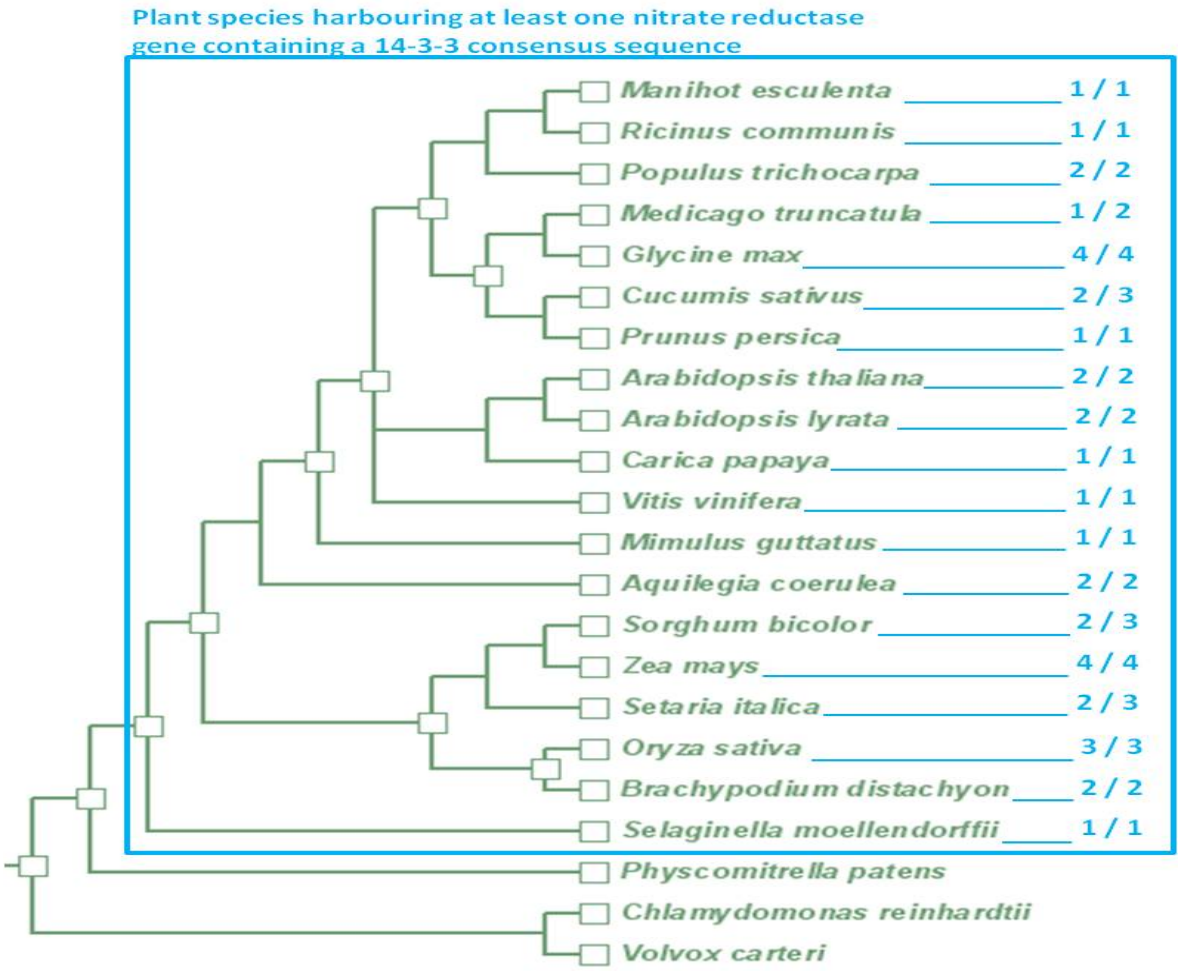

Fig26. Evolutionary tree of 22 sequenced plant species (adapted from phytozome v6.0). The blue rectangle highlights all sequenced species containing at least one nitrate reductase sequence with a 14-3-3 consensus motive. The number on the left side of the slash indicates the number of nitrate reductase sequences containing a 14-3-3 motive in the respective species. The number after the slash indicates the number of total nitrate reductase sequences in the genome of the respective species.

nitrate reductase sequence of *S.moellendorffii* is the only one observed in the set with a non-charged isoleucine on position -4 relative to the phosphorylted serine in the 14-3-3 motive (FigS3). The other nitrate reductase sequences contain a lysine at this position. In *B.distachyon* and *O.sativa* an argenine at position -3 is present in all nitrate reductase sequences. In *Z.mays*, *S.bicolor*, *S.italica* and *G.max* at least one nitrate reductase sequence contains an argenine at position -3. All other nitrate reductase sequences have a lysine at this position (Fig 26, FigS3,4). If this exchange of lysine to argenine at position -3 observed in all grasses has any functional relevance has still to be tested.

2.10. Testing the impact of CPK3 on metabolite levels

To assess the physiological impact of nitrate reductase regulation by CPK3, *in situ*, nitrate reductase activity of *cpk3* k.o. plants was compared to nitrate reductase activity of wild type

plants under various conditions (data not shown). Unfortunately the results varied strongly so that no conclusive picture of nitrate reductase activity regulation by CPK3 can be drawn from those experiments.

In parallel an analysis of polar metabolites from roots via GC-MS has been done. Metabolites were extracted from 6 week old, hydroponically grown Col0 and *cpk3* k.o. plants which were treated either with 100 mM NaCl, 200 mM sorbitol or standard growth medium (as a reference) for 3 hours immediately before harvesting the roots. To obtain confidence on the results the experiment was repeated twice with four biological replicates for each condition tested. More than 100 seperated peaks could be detected after gas chromatography. Most obvious were the changes of hexose and pentose levels between stressed plants and the control group (FigS2). Unfortunately hexose and pentose levels in stressed plants were so high that they could not be measured quantitatively nor could the single sugars species be unambiguously separated from each other on the GC column. By using a reference metabolite library in total 64 different compounds were identified within the dynamic range of the system. Data of both experiments were compared and analysed by two way ANOVA (analysis of variance). Metabolites which were found to have at least one outlier value in one factor (growth condition or plant line), in one of the two experiments, were excluded from further analysis. The 22 metabolites which were showing similar changes in both experiments are summarized in table 4. Basically they can be divided into four groups, metabolites which levels do not change significantly under all conditions tested, metabolites which change under both salt stress and osmotic stress, metabolites which predominantly change under NaCl treatment and metabolites which predominantly change under osmotic stress. Sucrose, malic acid, and citric acid levels were found to be elevated under both salt and osmotic stress in roots. Glutamic acid levels dropped under both stress conditions. 2-oxoglutaric acid and succinic acid are the only two metabolites in this study which have been found to exhibit increased levels predominantly under NaCl stress only. The highest increase of all metabolites towards the control was observed for arbutin under osmotic stress. Although arbutin can be detected in non stressed *A.thaliana*, the high levels of it detected in sorbitol treated plants may be the result of a contamination of the sorbitol used with arbutin. The higher levels of hexoses observed under sorbitol stress compared to NaCl stress may also be explained by contamination of sorbitol with hexoses. Both assumptions could be tested by analyzing a fraction of the sorbitol used for the assays alone. Under the same treatment leucine, glycine, myoinositol and aspartic acid levels were found to be significantly decreased under osmotic stress. For amino acids changing significantly under all stress conditions tested, only

decreasing levels compared to the control were observed. No statistically significant differences in metabolite levels were observed between Col0 and *cpk3-2* plants. Glutamine levels, which would have been an indicator for nitrate reductase activity in this assay, were not determined quantitatively as glutamine was only identified in 30 % of all samples.

Summarizing the data, it can be said that the response of Col0 and *cpk3-2* knock out plants between NaCl treatment and sorbitol treatment are similar, indicating that salt stressed plants were still in the osmotic phase of salt stress [67].

	growth condition dependent changes				plant line dependent changes		
	Col0		cpk3-2		control	NaCl	sorbitol
metabolite	NaCl / control	sorbitol / control	NaCl / control	sorbitol / control	cpk3-2 / Col0	cpk3-2 / Col0	cpk3-2 / Col0
sucrose	1.749	2.108	1.571	1.817	1.200	1.077	1.034
malic acid	1.846	1.841	1.893	2.278	0.980	1.005	1.213
citric acid	1.168	1.171	1.222	1.317	0.902	0.944	1.014
glutamic acid	0.709	0.143	0.540	0.126	1.144	0.871	1.006
2-oxoglutaric acid	2.554	1.804	2.338	1.668	1.242	1.137	1.149
succinic acid	2.238	1.249	1.882	1.502	1.088	0.915	1.309
arbutin	1.254	200.489	1.070	201.581	1.410	1.203	1.418
erythrose	0.948	6.847	0.985	8.439	0.776	0.806	0.956
glutaric acid	1.343	2.871	1.651	3.057	0.823	1.012	1.216
aspartic acid	0.936	0.731	0.644	0.440	1.355	0.932	0.815
myoinositol	0.873	0.698	0.657	0.500	1.217	0.917	0.872
glycine	0.489	0.204	0.493	0.173	1.129	1.137	0.956
leucine	0.768	0.057	0.092	0.002	0.835	0.100	0.034
alanine	0.870	0.819	1.233	1.132	1.091	1.546	1.508
fumaric acid	1.714	1.285	1.377	1.533	1.043	0.838	1.244
serine	1.436	1.159	0.332	0.784	0.995	0.230	0.673
glyceric acid	0.807	1.254	1.093	1.614	0.734	0.994	0.944
threonine	1.376	1.083	0.581	0.785	1.035	0.437	0.750
shicimic acid	1.363	1.142	1.105	1.232	1.106	0.897	1.194
lyxonic acid	1.085	1.158	1.059	1.016	1.122	1.095	0.984
dehydroascorbic acid	0.968	0.897	0.418	0.599	1.229	0.530	0.820
galactonic acid	1.006	0.795	1.066	0.786	1.049	1.111	1.038

Table4. Metabolic changes in *A.thaliana* roots upon salt or osmotic stress. Metabolic changes are depicted as fractions using the stress or mutant metabolite levels as numerator and the control or wild type metabolite levels as denominator. For comparison of means the Bonferroni test was used. Changes of metabolite levels were termed to be significant at the 0.05 level. Cyan background indicates a statistically significant decrease in metabolite levels. Yellow background indicates a statistically significant rise in metabolite levels.

3. Discussion

3.1. Sub-cellular localization of CPK3

In previous studies CPK3 has been observed to localize in the cytosol and in the nucleus as well as at membranes [29, 66] which could be confirmed by microscopy studies (Fig 9, Fig 23, Fig S2). Mehlmer and colleagues also demonstrated that myristic acid can be attached to the glycine on position two of the CPK3 protein sequence and that this myristoylation is requiered for the membrane localization in *A.thaliana* [29]. 14 of 18 studied CPKs in *A.thaliana* were observed to localize at least partly at the membrane which may account for a more efficient perception of the spatially restricted Ca^{2+} signals by CPKs. By applying linear density gradients for membrane fractionation it was shown that in leaves of *A.thaliana* endogenous CPK3 is primarily localized at the vacuolar membrane (Fig 9). B. Pfister could furthermore demonstrate in a similar experiment that in membranes isolated from *A.thaliana* roots CPK3 localizes preferentially at the plasma membrane [113]. This suggests that CPK3 may have different targets in roots and in leaves. However, myristoylation alone is not sufficient for stable membrane localization of a protein. [125-127]. Therefore it is not surprising that B. Pfister found at least 50 % of the endogenous CPK3 protein to be present as soluble form rather than as membrane associated form [113], which therefore opens the possibility that CPK3 also targets cytosolic or nuclear targets in vivo. If Ca^{2+} binding and the resulting change in conformation of CPK3 has an effect on the sub-cellular localization of the kinase is so far unknown. However, considering the different, predicted and described, targets of CPK3 so far, one would expect that Ca^{2+} activated CPK3 is active as membrane attached- and as soluble form.

3.2. Transcription factor *At*bZIP63 - interaction with protein kinases

At the beginning of this thesis we were confronted with slightly puzzling data. On one hand no evidence for transcriptional reprogramming of described pathways under salt stress was observed in *cpk3* k.o. mutants [29]. On the other hand, bZIP63, a transcription factor, was the only protein repeatedly identified as interaction partner of CPK3 in a yeast two hybrid screen. However, as yeast two hybrid screens are prone to give false positive results, it was decided to do an in-gel kinase assay as an unbiased attempt to identify bZIP63 kinases in total plant

protein extracts. There, direct phosphorylation of bZIP63 by CPK3 could only be confirmed for recombinantly expressed CPK3 (Fig 14). Testing of a protein extract from *cpk3* k.o. plants (data not shown) did not reveal a change in the band pattern compared to wild type protein extracts. In addition, protein kinases from two different groups, casein kinase 2 (CK2) and SNF1 (termed after its yeast homolog "sucrose non fermenting 1"), were clearly identified to phosphorylate bZIP63. Due to the constant unfolding and refolding of the proteins occurring during the in-gel kinase assay, it might discriminate for protein kinases of high abundance or/and of low molecular weight. Nevertheless, the affinity purification step prior to the kinase assay and subsequent MS analysis should have served as an enrichment for specific protein kinases of bZIP63 and circumvent loss of detection due to low abundance of the kinase. Therefore, it remains questionable if direct phosphorylation of bZIP63 by CPK3 happens in vivo and leads to physiological changes in the plant.

Different catalytic and regulatory subunits of CK2 were identified after the in-gel kinase assay. In BIFC assays, *in vivo* interaction between these subunits and bZIP63 was observed (Fig 17c,d). CK2 belongs to the best studied protein kinases to date. It functions as a heterotetrameric enzyme consisting of two catalytic subunits (CKA) and two regulatory subunits (CKB) and is highly conserved in all eukaryotes analyzed so far, indicating a critical function [129]. However, already a decade ago more than 160 known hypothetical *in vitro* protein targets were identified for CK2, which makes it also one of the most unspecific protein kinases [130]. The lack of specificity might also explain why the chloroplast casein kinase was identified after affinity chromatography as bZIP63 interacting kinase together with the cytosolic and nuclear localized CK2. Genetic evidence indicates that CK2 plays an important role in the circadian clock [131-133].

Similar to CK2, catalytic and regulatory subunits of an SNF1 complex have been identified after the in-gel kinase assay. In contrast to the catalytic subunit of CK2, AKIN10 has less affinity to bZIP63 according to the BIFC studies (Fig 17a). However, BIFC fluorescence signals of SNF4, a regulatory subunit of AKIN10, and bZIP63 where approximately as intense as the ones of the CK2 subunits and bZIP63 (Fig 17b). From literature it is known that SNF1 functions as a heterotrimer consisting of a catalytic subunit alpha (in *A.thaliana* termed AKNI10 and AKIN11), one regulatory subunit beta and one regulatory subunit gamma [134]. In *A.thaliana* SNF4 was found to be a fusion of the beta and gamma regulatory subunits of the SNF1 complex. SNF1 is a kinase that gets activated on high AMP levels by the gamma subunit, which binds AMP [134]. Interaction of SNF1 kinase with its gamma subunit increases its activity by ~ 1000 fold [134]. Beta subunits of the SNF1 complex were observed

to guide the catalytic subunit to its targets [135]. In case of bZIP63 the results from the BIFC studies suggest that SNF4 might target AKIN10 to the transcription factor. Furthermore the observation that AKIN10 and AKIN11 phosphorylate bZIP63 less efficient than CPK3 in an in vitro kinase assay could be explained by the absence of the activating gamma subunit in the reaction. This should be tested by adding recombinantly expressed SNF4 to the kinase reaction to better understand the molecular interaction between bZIP63 and AKIN10. A model where bZIP63 acts as an integrating platform of circadian- and energy signalling can be imagined, however, especially further functional data on the role of phosphorylation of bZIP63 has to be gathered to support this.

3.3. CPK3 - a regulator of TPK1

Initial studies showed that TPK1 is a functional K^+ channel located at the vacuolar membrane which gets activated by Ca^{2+} and by binding of 14-3-3 proteins [118]. As mentioned before, binding of a 14-3-3 protein to its target requires phosphorylation of a serine in the binding site. It has been demonstrated that CPK3 can phosphorylate the serine within the 14-3-3 binding site in the N-terminus of TPK1 (Fig 19b), which has been independently confirmed by N. Mehlmer. From physiological studies it is known that K^+ currents from the vacuole to the cytosol occur upon NaCl stress [68]. The germination assays done with *tpk1* mutant lines, indicate that TPK1 is an important channel for these K^+ currents, which correlates well with electrophysiological data on TPK1 [118]. Considering the presence of CPK3 at vacuolar membranes in leaves, it seems likely that CPK3 indeed regulates TPK1. After in vivo cross linking, a band at ~ 90 kDa was detected to contain CPK3, which might be a further hint for TPK1-CPK3 interaction as the molecular weight of CPK3 (50 kDa) and TPK1 (40 kDa) would sum up to 90 kDa. Further evidence that CPK3 in vivo interacts with TPK1 was gathered using BIFC assays. In these assays an in silico predicted model of the TPK1 - CPK3 interaction could be confirmed experimentally by testing different point mutants of TPK1 (Fig 21). Even though the data from the BIFC assays cannot be interpreted absolutely quantitative [136], it is the first evidence for an interaction mechanism between CPK3 and one of its targets. From these data it can be concluded that the two arginines at -4 and -3 position relative to the phosphorylated serine in the 14-3-3 site may be important for stabilizing the interaction between the kinase domain of CPK3 and its target TPK1. Different *cpk3* mutant lines tested in germination assays did not fully resemble the phenotype of the respective *tpk1* mutant lines. Still, the results do not contradict the hypothesis that CPK3 regulates TPK1 in

vivo. Considering that no changes in known salt regulated transcripts were observed in *cpk3* k.o. lines [29], the post translational regulation of TPK1 by CPK3 might partially explain the salt sensitive phenotype observed for *cpk3* knock out mutants. Furthermore the direct activation of TPK1 by Ca^{2+} and the additional activation by binding of 14-3-3 proteins, which is mediated by Ca^{2+} activated kinase, presents an excellent example how a plant cell responds immediately to the initial Ca^{2+} stimulus of NaCl stress.

To directly observe regulatory effects of CPK3 on the cellular ion homeostasis, measuring ion concentration in the cytosol of different *cpk3* mutant lines would be valuable in future. It also remains unknown to what extent other CPKs are involved in regulating TPK1. Apparently all 7 CPKs tested can in vitro phosphorylate TPK1 at its regulatory 14-3-3 site (Fig 19). Indicators like expression levels, tissue and subcellular localization of the other CPKs may help to obtain an idea on how likely it is that TPK1 would get into contact with the kinases. However, ultimately only analysis of respective *cpk* k.o. and over expresser lines, like it has been done for *cpk3* mutant lines, would allow to answer this question.

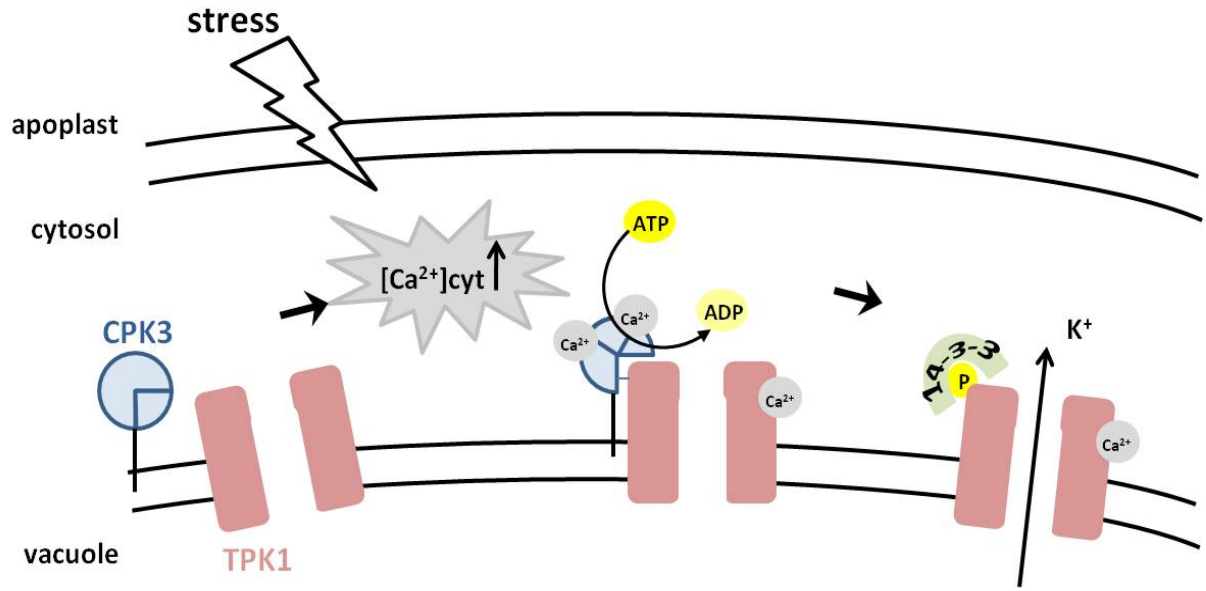

Fig27. A simplified model depicting the regulation of TPK1 by CPK3 under salt stress.

3.4. Post translational regulation of nitrate reductase

The enzyme nitrate reductase is essential for use of nitrate as a nitorgen source in plants by reducing nitrate to nitrite. The reduction cost for the conversion of one molecule nitrate to ammonium via nitrate- and nitrite reductase was calculated to be one NADH and six reduced ferredoxins [137]. Furthermore nitrite becomes toxic to the plant at higher concentrations. Therefore nitrate reductase is tightly regulated in plants on transcriptional as well as on post

transcriptional level [138]. It had been shown that post translational modification of nitrate reductase is capable of compensating for deregulated nitrate reductase transcript levels in tobacco [139,144]. Post translational regulation of nitrate reductase involves binding of 14-3-3 proteins which leads to a down regulation of nitrate reductase activity [53]. In vitro it was demonstrated that a CPK phosphorylates S543 in tobacco nitrate reductase which is crucial for 14-3-3 binding [140,141]. Further in vitro studies also suggest that a homolog of *A.thaliana* AKIN10 is able to phosphorylate nitrate reductase of wheat and spinach at the same serine within the 14-3-3 binding site [142,143].

During this thesis interaction between the *A.thaliana* nitrate reductase (*At*NIA2) and CPK3 could be demonstrated in vitro (Fig 22a) and in vivo (Fig 23,24). This finding is in accordance with the observation that CPK3 together with CPK4, 6 and 29, inhibits nitrate reductase most efficiently in a dose dependent manner (personal communication by G. Schwarz). Interaction of CPK3 with nitrate reductase was found to be partly dependent on the two positively charged lysines at the -3 and -4 position relative to the phosphorylated serine in the 14-3-3 site (Fig 25). In combination with the observation that the two positively charged arginines at the similar sites in the TPK1 N-terminus are required for proper interaction with CPK3, these data provide first evidence on the mechanism how CPKs target proteins with 14-3-3 sites. However, as there is still an interaction signal observed in studies with mutated versions of TPK1 and NIA2 it is likely that other amino acids contribute in stabilizing the interaction with CPK3 as well. Interestingly out of seven soluble CPKs tested CPK5 and CPK6 were not able to phosphorylate NIA2 at its 14-3-3 site. If this difference in specificity of the CPKs between TPK1 and NIA2 is only due to the different sequence surrounding the 14-3-3 site, remains open. Recently it had been demonstrated that the N-terminal part of *Nt*CPK1 was essential for recognition of its substrate [32]. This can be the case for the investigated *A.thaliana* CPKs as well. In case of CPK3, mutation of its N-terminal variable domain would therefore be the next experiment to do, to further understand interaction between CPK3 and its substrates.

It was also tried to assess the physiological impact of nitrate reductase regulation by CPK3. The hypothesis is that under conditions where CPK3 is active nitrate reductase activities should be down regulated due to binding of 14-3-3 proteins to phosphorylated nitrate reductase. Therefore it was chosen to test nitrate reductase activities in salt stressed plants. Unfortunately under the conditions tested no statistically significant changes in nitrate reductase activities between *cpk3* k.o. and *wild type* plants could be measured. That observation could be the result of various effects. It was reported that nitrate reductase transcript levels in tobacco were down regulated at high malate levels [145]. Interestingly

malate levels in roots were found to be increased by approx. two fold upon salt and osmotic stress treatment in *A.thaliana* (Table 4). Considering the incubation times chosen, it could be possible that any regulation of nitrate reductase by CPK3 could have been "abolished" by the fact that less total protein of nitrate reductase was present at the time of the assay. The activities of AKIN10/11 are not known under the conditions tested. Therefore CPK3 activity on nitrate reductase might by masked by the activity of AKIN10/11. Also functional redundancy of other CPKs cannot be ruled out at this point. As shown in (Fig 22) the CPKs 4, 11, 12 and 29 are all capable of phosphorylating the serine in the nitrate reductase 14-3-3 site. The use of an inducible constantly active CPK3 lines may be a chance to circumvent the above mentioned problems in future experiments studying the impact of CPK3 on nitrate reductase regulation.

In *A.thaliana* nitrate reductase is so far the only enzyme for which the catalysis of the reduction of nitrite to nitric oxide (NO) was shown [150]. NO has been demonstrated to be an versatile signalling molecule involved in various processes like, seed germination, stomatal closure and lateral root formation [152-154]. Recently it has been shown that nitric oxide production in A.thaliana roots positively correlates with the nitrate reductase activity [151]. Furthermore the authors of this manuscript present data which suggests that nitrate reductase activity and NO production are enhanced by phosphorylation of serine 627 in *At*NIA2 through oxidative stress activated *At*MPK6 [151]. However, as a complex phenotype was observed under *At*MPK6 activating conditions using over expressing lines of NIA2 S627 mutated either to alanine or aspartate, the physiological function of *At*NIA2 regulation by *At*MPK6 remains under discussion. Considering that phosphorylation dependent binding of 14-3-3 proteins to nitrate reductase leads to a blockade in nitrate reductase internal electron transport [53], one assumption would be that in this 14-3-3 bound state also NO production of *A.thaliana* must be lower than in the unbound state. In first assays including *cpk3* knock out plants no significant differences in root architecture compared to the *wild type* was observed under standard growth conditions indicating that CPK3 is not involved in stress independent developmental processes. Still, as it is well described that rising NO levels lead to higher cytosolic free Ca^{2+} levels in plants [153,155] it is possible that a CPK is involved in a feedback mechanism reducing NO production by inactivating nitrate reductase after stress preception. Indeed, it had been shown that also a calcium dependent protein kinase gets activated after NO treatment in cucumber [153].

Comparison of the nitrate reductase sequences of 22 different plant species revealed that regulatory 14-3-3 sites in nitrate reductase proteins are exclusive to vascular plants contained

in the data set (Figure 26). Conservation of this regulatory site over ~420 million years in plants suggests that it is of functional importance to the plant. In an evolutionary context efficient water transport through vascular tissue permitted plants to grow bigger. In parallel the site of nitrate uptake (roots) and the site of nitrate reduction (leaves and roots) got more distant to each other which automatically leads to fluctuations in the nitrate supply of different tissues throughout the plant. Although nitrate uptake, transport, storage and reduction within the plant are tightly regulated on a transcriptional level [138, 146, 147], posttranscriptional regulation of nitrate reductase via 14-3-3 proteins may be beneficial for the plant as it allows for still faster adaptation to a wider variety of environmental factors. For example, it has been shown that a *N.plumbaginifolia* nitrate reductase mutant in which the regulatory 14-3-3 site was rendered dysfunctional, accumulated higher nitrite levels than did *wild type* plants during the night [141]. A long term effect of that was an enhanced likelihood for formation of chlorotic young leaves in the mutant [141].

3.5. Metabolic changes in roots upon salt stress

In roots, the metabolites malate, citrate, 2-oxogluterate and succinate were found to be present at higher concentrations in salt stressed plants as in non stressed plants (Table 4). This might be an indication for a higher activity of enzymes in the citric acid cycle. Considering that maintaining a proper ion homeostasis in the cytosol is achieved through an active translocation of ions over membranes [67], it makes sense that under salt stress translocation of excess Na^+ ions to the vacuole requires additional energy which in roots is provided by respiration via the citric acid cycle. In this aspect it is important to note that changes observed for these four citric acid cycle intermediates seem to be exactly the opposite of the changes observed in *A.thaliana* leaves after salt stress treatment for more than 10 days [149].

In contrast to the citric acid cycle intermediates, amino acid levels were found to be lower under osmotic stress than under control conditions (Table 4). An explanation for this could provide the fact that six carbon sugars seem to be the major compatible solutes during the initial phase of salt/osmotic stress in *A.thaliana* roots. As a result, less carbon skeletons are available for amino acid synthesis leading to an overall decrease in amino acid levels observed especially under osmotic stress. This is in accordance with reports which show a tight connection between carbon and nitrogen metabolism in plants [137]. It should be mentioned though, that much more data have been created on understanding connections between carbon and nitrogen metabolism on a long term, transcriptional regulatory basis, than

on a post transcriptional regulatory basis which would account for immediate response regulation to a stress.

Interestingly, under long term salt stress conditions (more than 6 days) in leaves of several species, including *A.thaliana*, a decrease in succinate, malate, citrate and 2-oxogluterate upon salt stress has been observed [149]. Also for the amino acids glycine and leucine, which were found to decrease in roots under short term osmotic stress (Table 4), the opposite was observed in leaves after long term salt stress [149]. The differences of citric acid cycle intermediates between the two data sets are likely explained by the differences in energy generation in roots and leaves. This assumption is supported by the observation that maize plants exposed to salt stress for 6 days exhibited decreased levels of succinate and malate in leaves but increased levels of these two metabolites in roots [156]. However, due to the experimental setup in that study only amino acid levels of alanine and aspartate were quantified and both were not found to be decreased after salt stress [156]. In a series of experiments with *A.thaliana* T87 cells over a time period of 72 hours also no decrease in amino acid levels had been observed during the short term salt stress response [157]. Therefore it may be concluded that the observed decrease of amino acid levels is specific to the short term salt/osmotic stress response in *A.thaliana* roots.

3.6. The role of CPK3 in *A.thaliana* salt stress acclimation

From a sensor protein that functions as a first relay in a signalling cascade it should be assumed that it is present already before a cell is exposed to a signal such as harmful concentrations of NaCl. Only this allows it to elicit immediate changes of metabolism and developmental processes either through posttranslational modification of metabolic enzymes or other signalling modules such as transcription factors, which subsequently would lead to an adaptation of the cell to the initial signal. CPK3 fulfils this prerequisite as it was observed to be constantly present throughout all vegetative tissues of *A.thaliana* [29]. A role in salt stress acclimation of CPK3 is suggested by the observation that germination rates of *A.thaliana* seeds correlate positively with the amount of CPK3 protein (Fig 7). CPK3 has also been shown to be activated upon salt stress in a strictly Ca^{2+} dependent manner (Fig 8, [29]). This is in accordance with the documented rise in cytosolic free Ca^{2+} levels upon salt stress [5, 91]. The observed cytosolic- and membrane localization of CPK3 in roots and in leaves (Fig 9) would allow for activation of CPK3 by NaCl elicited Ca^{2+} changes. TPK1 a vacuolar two pore potassium channel has been shown to be responsible for major K^+ currents from the vacuole to the cytosol [118]. It has been shown that it can be activated by a Ca^{2+} and in addition by

CPK mediated binding of 14-3-3 protein ([118], personal communication by Teige). As mentioned before, it is likely that CPK3 mediated activation of TPK1 leads to K^+ currents from the vacuole into the cytosol as initial response to salt stress. Indeed, a rise in cytosolic K^+ concentration is reported to be one of the first physiological adaptations of the plant cells to NaCl stress [68, 158].

However, CPK3 has only been found to be located at the vacuolar membrane in leaves and not in roots (Fig 9, [113]). Together, these data indicate that CPK3 transmits acclimation to salt stress by regulating the ion homeostasis in leaves but may have a different function in the root. One assumption for a physiological function of CPK3 in the root could be the inactivation of nitrate reductase upon salt stress. It was demonstrated that CPK3 specifically interacts with nitrate reductase *in vivo* and that it can transmit inactivation of *A.thaliana* nitrate reductase *in vitro*. Low levels of glutamate under short term salt and osmotic stress probably evoked by the lack of available carbon back bones for amino acid synthesis (Table 4) would likely not allow for efficient nitrogen integration via the GS/GOGAT cycle [159, 137]. Under these conditions it might be beneficial for the plant to inactivate NR and therefore avoid accumulation of nitrite during a phase of metabolic reprogramming in the initial salt stress. To test this hypothesis the nitrite levels between *wild type* and different *cpk3* mutant lines in roots could be compared during the initial phase of NaCl phase. It would be expected to observe a negative correlation between nitrite levels and CPK3 protein.

3.7. Further aspects on CPK3

If CPK3 also acts in transcriptional reprogramming upon salt stress cannot be said at the moment. In the single *cpk3* k.o. mutant no transcriptional change on known salt stress regulated genes has been observed. However, previous reports [42] and results of this thesis (Fig 20) suggest that due to their close homology CPKs function at least partly redundant in the cell which might abolish effects caused by a single *cpk3* loss of function mutation. For the aforementioned reason it cannot be ruled out either, that CPK3 might be involved in other signalling pathways than the salt and osmotic stress response. Complementation of multiple CPK knock-out lines with a single CPK might be the only way to get insight into the exact physiological function of the CPK and determine the signalling networks it is involved in. From experiments aiming at the unbiased identification of CPK3 targets, data is still not complete and data obtained so far from the 2-D gel approach (Table 2) still needs validation by independent methods testing for kinase substrate interactions. Although it has been demonstrated that the N-terminal myristoylation is important for membrane association, other

factors might be as well, since it was observed that N-terminally tagged versions, in which the N-myristoylation of CPK3 is blocked, can interact with TPK1 at the vacuolar membrane. Other kinases like AKIN10/11 and CKA are known to be targeted to their substrates via non catalytic subunits [129, 134]. For CPKs no similar multimeric kinase complex has been identified yet. However, the N-terminus of *Nt*CPK1 was shown to be important for non catalytic substrate interaction [32]. Maybe this holds also true for CPK3. Mutations of the N-terminal part of CPK3 and testing for interaction with its known substrates is likely to be helpful in understanding the interaction mechanism between CPK3 and its substrates. This could subsequently lead to a more accurate bioinformatic model on CPK3 - substrate interaction based on more sequence data than a consensus site for the catalytic site alone would allow for.

3.8. Conclusions

During this thesis it was found out that CPK3 plays a role in salt stress acclimation in *A.thaliana*. The presented model of CPK3-TPK1 interaction suggests a role of CPK3 in intracellular ion homeostasis regulation and could account, in parts, for the salt sensitive phenotype observed in *cpk3* mutants. Based on data describing *in vivo* and *in vitro* interaction between CPK3 and nitrate reductase as well as root metabolite analysis during salt stress it is assumed that CPK3 is involved in nitrate reductase inactivation during initial salt stress. The observations that CPK3, *in vivo*, specifically interacts with proteins harbouring a 14-3-3 consensus site and that other CPKs can interact with 14-3-3 consensus sites *in vitro* suggest that CPKs are an essential part of the 14-3-3 regulatory network. A role of transcriptional reprogramming due to action of CPK3 has not been observed so far. However, it cannot be ruled out at this point as comprehensive analysis of transcript levels, for example in form of a microarray, of *cpk3* mutants has not been done yet.

4. Materials and Methods

If not indicated differently in the text, H_2O always refers to sterile Milli Q standard water.

4.1. Molecular cloning

4.1.1. RNA isolation from *A.thaliana*

Plant material was frozen and homogenized in a QIAGEN TissueLyser II (frequency: 30/second; duration: 1 min; glass beads were used as impactors). To ~200 mg tissue powder 500 µl RNA extraction buffer (1% SDS, 10mM Na_2EDTA in H_2O) and 500 µl phenole pH4.0 were added. The mixture was vortexed for 1 min and afterwards centrifuged for 10 min at 16100g at 4°C. The aqueous phase was subjected to PCI (25:24:1) extraction twice and once to chloroform using equal volumes of aqueous phase and organic phase for each extraction step. The aqueous supernatant was then mixed with 1/3 of its volume of 10M LiCl and incubated for 4 hours at 4°C. RNA was precipitated by centrifugation at 16100 g at 4°C for 30 min. The pellet was washed once with 2.5 M LiCl and once with 80 % ethanol in H_2O. The RNA was finally dissolved in 40 µl H_2O. RNA concentration was determined by measuring extinction at 260/280 nm.

4.1.2. Reverse transcription

Prior to reverse transcription RNA was subjected to DNAse treatment for removing residual DNA co purified with RNA. RQ1 DNase (M198A) was used for DNAse treatment according to manufacturer's instructions. For reverse transcription Promega M-MLV reverse transcriptase (M531A) was used according to manufacturer's instructions. Oligo $(dT)_{15}$ were used as primers. cDNA obtained from this procedure was then used as template for semi-quentitative RT PCR as well as for molecular cloning.

4.1.3. Semiquantitative RT PCR

For PCR, PROMEGA goTAQ polymerase (M3178) was used according to manufacturer's instructions. Primers and PCR program for RT PCR were selected according to guidelines of [164] and goTAQ polymerase manual. RoboCycler 96 gradient from Stratagene was used for the RT PCR reaction.

4.1.4. PCR for cloning

For all PCRs done to obtain DNA fragments for molecular cloning including site directed mutagenesis NEB Phusion™ High-Fidelity DNA Polymerase (F530-L) was used according to manufacturer's instructions. All DNA fragments used in functional assays were subsequently checked by DNA sequencing at Microsynth [http://www.microsynth.ch/]. RoboCycler 96 gradient from Stratagene was used for the PCR reaction.

4.1.5. DNA Ligation

All PCR products were cloned into pCR-Blunt vector with the Zero Blunt PCR Cloning Kit (Prt. no. 44-0302) from invitrogen according to the manufacturer's instructions. Sub cloning of restriction fragments after restriction digests were done with T4 DNA Ligase from NEB (M0202S) according to the manufacturer's instructions.

4.1.6. DNA Restriction

All DNA restriction reactions were performed with restriction enzymes from NEB according to the manufacturer's instructions.

4.1.7. Agarose gel electrophoresis

0.5% - 2.0% agarose in TAE (40 mM Tris acetate, 1 mM Na2EDTA, pH8.0) gels were poured according to the DNA fragment sizes to be separated. DNA were stained with ethidium bromide (0.25 µl/ml). DNA ladders according to the separated fragment sizes from Fermentas were used as markers.

4.1.8. DNA extraction from agarose gels

DNA was excised from the agarose gels with a razor blade and extracted with the Promega SV gel and PCR Cleanup system according to the manufacturer's instructions.

4.1.9. Genomic DNA Isolation of *A.thaliana*

~100 mg of plant material were frozen and homogenized in a QIAGEN TissueLyser II (frequency: 30/second; duration: 1 min; glass beads were used as impactors). 400 µl of CTAB buffer (2% CTAB (hexadecyltrimethylammonium bromide), 100 mM TrisCl pH8.0, 20 mM EDTA, 1.4 M NaCl, 1% polyvinylpyrrolidone) were added and vortexed for 1 min. After centrifugation (16100 g, for 10 min at 4°C) the supernatant was mixed with 0.7 volumes of 2-propanol and centrifuged for 30 min at 16100g and 4°C to precipitate the DNA. The pellet was washed with 70 % EtOH and the DNA was then dissolved in 50 µl of H_2O.

4.1.10. DNA mini-preps from *E.coli*

4 ml over-night culture were pelleted by centrifugation at 16100 g for 1 min at RT. The pellet was resuspended in 300 µl TE + RNAse (50 mM TrisCl pH 8.0, 10 mM Na_2EDTA, 100 µg/ml RNAse A). 300 µl P2 (200 mM NaOH, 1%SDS) were added after resuspension of the pellet and gently shaken for 2 min. 300 µl P3 (3 M potassium acetate pH 5.5) were added to neutralize the reaction. Cell debris was pelleted by centrifugation at 16100 g for 10 min at 4°C. DNA was precipitated by adding one volume of 2-propanol to the supernatant and centrifugation at 16100 g for 30 min at 4°C. The DNA was then washed with 70% EtOH and finally dissolved in 40 µl of H_2O.

4.1.11. Preparation of chemically competent *E.coli*

A pre-culture of LB (5 g yeast extract, 10 g peptone, 10 g NaCl in H_2O) supplemented with 20 mM $MgSO_4$ was inoculated with an E.coli single cell culture grown on an LB agar plate, over night at 20°C. 600 ml LB supplemented with 20 mM $MgSO_4$ were adjusted to an OD_{600} of 0.2 using the pre-culture. The culture was then incubated at 20°C until it reached an OD_{600} of 0.5. Cells were then immediately cooled down to 4°C and pelleted by centrifugation at 1000g for 10 min at 4°C. The cells were resuspended in 50 ml of ice cooled TB (10 mM $CaCl_2$, 10 mM PIPES-NaOH pH 6.7, 15 mM KCl, 55 mM $MnCl_2$) buffer and incubated for 30 min on ice. The cells were then pelleted by centrifugation at 1000g for 10 min at 4°C and gently resuspended in 5ml ice cooled TB supplemented with 7% DMSO. 300 µl aliquotes of this suspension were then frozen in liquid N_2 and stored at -80°C.

4.1.12. Transformation of chemically competent *E.coli*

~1 µl of DNA [0.5 µg/µl] was added to 50 µl of chemically competent E.coli and incubated on ice for 15 minutes. Then the mixture was exposed to a heat shock at 42 °C for 1 min. Immediately afterwards the mixture was put on ice and supplemented with 1 ml of LB. The transformed cells were then incubated for 1 h at 37 °C and vigorous shaking. Cells were then pelleted by centrifugation at 16100 g for 1 min at RT (room temperature) and resuspended in 200 µl of LB. Afterwards cells were transferred to LB agarplates supplemented with an antibiotic of choice.

4.1.13. Preparation of electro competent Agrobacteria

An overnight culture of Agrobacteria was used to adjust 300 ml of LB to an OD_{600} of 0.2. Cells were then incubated at 30°C under virgorous shaking until an OD_{600} of 0.7 was reached. The suspension was then cooled down in ice and cells were harvested by centrifugation at 6000g for 15 min at 4 °C. Cells were then washed with 50 ml of ice coold 1 mM HEPES pH7.0 twice. Finally the cells were resuspended in 2 ml 10 % glycerol and aliquoted into portions of 300 µl which were frozen in liquid N_2 and stored at -80 °C.

4.1.14. Transformation of electro competent Agrobacteria

1 µl of DNA [1µg/µl] was mixed with 50 µl of electro competent Agrobacteria in a clean and sterile electroporation cuvete on ice. Electroporation was done with a BioRad Gene Pulser™ under following conditions: 200 Ohm resistance, 1.4 kV voltage and 25 µF capacitance. Immediately after the electric pulse cells were incubated in 1 ml LB and incubated at 30 °C and vigorous shaking for 1 hour. Cells were then transferred onto appropriate selective LB agar plates and incubated at 30 °C.

4.2. Protein extraction, separation and western blotting

4.2.1. Protein extraction

If not indicated differently 100 mg of plant material was frozen in liquid N_2 and homogenized in a QIAGEN TissueLyser II (frequency: 30/second; duration: 1 min; glass beads were used as impactors). 200 µl of 1x SDS-Loading buffer (4x SDS Loading buffer: 0.25 M TrisCl pH 6.8, 8% SDS, 40 % glycerine, 20% 2-mercapthoethanol, 0.016% bromophenol blue) were added to the obtained powder. The mixture was vortexed for 30 sec and centrifuged at 16100 g for 5 min at 4°C. The supernatant was then transferred into a new reaction tube and incubated at 95 °C for 5 min. Then proteins were loaded onto an SDS-polyacrylamide gel for separation.

4.2.2. SDS-PAGE

To determine protein molecular weight, discontinuous SDS-PAGE was used [165]. For running and casting of gels Mini Protean 3 devices from BIORAD were used according to manufacturer's indications. Polyacrylamide concentrations in the gel were adjusted to the molecular weight of proteins of interest to obtain optimal resolution if no polyacrylamid linear gradient gels were used. Runningbuffer composition (25 mM Tris, 250 mM glycine and 0.1 % SDS). Appropriate protein ladders from Fermentas and NEB were used as molecular weight references. To make the proteins visible on the gel coomassie staining or silver staining was used.

4.2.3. Western blotting

All western blots were performed on PVDF membranes with a Tran-Blot semidry system from BIORAD. The blotting procedure was done according to PVDF membrane manufacturers' instructions. Blotting was controlled with Ponceau staining (0.1% Ponceau S in 5% acetic acid; subsequent removal by washing with H_2O). The blocking procedure was done according to the antibody manufacturers' instructions. For detection an HRP coupled secondary antibodies from GE Healthcare were used in combination with the ECL PLUS Western Blotting Detection System also from GE Healthcare. The signal was captured on photosensitive film. Afterwards the membranes were coomassie stained; maembrane was incubated in coomassie staining solution (2.5 g Coomasie R250/G250 (4:1), 10 % 2-propanol, 10 % acetic acid) for 5 min at RT and subsequently washed two times for 10 min with destain solution (10 % 2-propanol, 10 % acetic acid).

4.2.4. Antibodies used

CPK3	Affinity purified antibody from rabbit against the last 15 amino acids of the CPK3 C-terminus (MKKGNPELVPNRRRM) produced from rabbit by (Davids Biotechnologie, Germany)
Phospho-(Ser) 14-3-3 binding motif	Commercial antibody from Cell Signaling Technology (#9601) from rabbit against Phospho-(Ser) 14-3-3 binding motif (R/K)XX(S*)XP X = any amino acid S* is the phosphorylated serine.
H+-ATPase	Commercial antibody from Agrisera (AS07 260) against plasma membrane H+-ATPase from *A.thaliana* (At2g18960)
V-ATPase	Commercial antibody from Agrisera (AS07 213) against *A.thaliana* (At4g11150) epsilon subunit of tonoplast H+-ATPase
Sar1	Commercial antibody from Agrisera (AS08 326) against *A.thaliana* Sar1 protein on ER-Golgi transport vesicles.
Porin	Monoclonal antibodies against the mouse porin kindly provided by Harvey Millar (University of western Australia)

4.2.5. Coomassie staining of SDS-PAGE gels

Gels were incubated in coomassie staining solution (2.5 g Coomasie R250/G250 (4:1), 10 % 2-propanol, 10 % acetic acid) for 30 min at RT and then destained twice for one hour with destain solution (10 % 2-propanol, 10 % acetic acid). Afterwards stained gels were scanned for documentation.

4.2.6. Silver staining of SDS-PAGE gels

All incubation steps were done under gentle shaking conditions at RT if not indicated differently. Gels were incubated in solution 1 (50 % methanol and 5 % acedic acid for 20 min. Then gels were incubated in solution 2 (50 % methanol) for 10 min. Next, the gel was incubated in H_2O for 2 hours. Then the gel was incubated in sensitizing solution (0.03 % $Na_2S_2O_3$) for one min and rinsed 2 times with water afterwards. Next it was incubated in 0.1 % $AgNO_3$ for 20 min at 4°C. The gel was then incubated in H_2O twice for 2 min. Developing was started by incubating the gel in solution 3 (2 % Na_2CO_3 and 0.00014 % Formaldehyde. When bands turned dark the reaction was stopped by incubating the gel in 5 % acetic acid.

4.3. Cultivation of plants

4.3.1. Vapor sterilization of *A.thaliana* seeds

Seeds were surface sterilized by using Cl-gas [166]. Seeds were transferred in 1.5 ml reaction tubes which were put open into a ~10 litre plastic box. Cl-gas was produced by mixing 100 ml of 2.8% NaClO with 50 ml 10 M HCl. The box was sealed tightly and the seeds were then incubated for 2 hours. Afterwards seeds were directly spread on soil or appropriate agar plates.

4.3.2. Cultivation *of A.thaliana* on soil

Seeds were directly spread on soil (10 part spezialblumenerde, Diwoky; 3 part sand (rasenquarz Quarzwerke Österreich Melk; 1 part perlite (Granuperl S3-6, KNAUF Perlite GmbH, Austria)) and grown under 200 µmol $m^{-2}sec^{-1}$ light intensity at 20 °C. under a short day (8 hours light/16 hours dark), long day (16 hours light/ 8 hours dark) or a 12 hour light 12 hour dark cycle. Seeds were obtained from plants grown first for 4 weeks under short day conditions and were then shifted to long day conditions.

4.3.3. Cultivation *of A.thaliana* as a hydroponic culture

Hydroponic A.thaliana cultures were done according to [167]. Single seeds were put onto 1/2 Hoagland agar filled 0.5 ml PCR tubes, which were placed in a foil coverd 1 ml Gilson tip box (Gilson Middleton, WI, USA) filled with 1/2 Hoagland medium (1 time Hoagland medium: 4 mM $Ca(NO_3)_2$, 0.5 mM K_3PO_4, 6 mM KNO_3, 2 mM $MgSO_2$, 90 µM $NaFe_{III}$ EDTA, 10 µM H_3BO_3, 2 µM $MnCl_2$, 0.3 µM $ZnSO_4$, 0.2 µM $CuSO_4$, 14 nM MoO_3, 9 nM $Co(NO_3)$ pH was adjusted to pH6.0 with either NaOH or KOH to allow solidification of the agar). The bottom of the PCR tubes were de capped so that the root can grow into the nutrient solution. For the first 2 weeks the box was covered with transparent plastic foil to prevent early evaporation of the water in the agar. Plants were than grown under 200 µmol $m^{-2}sec^{-1}$ light intensity at 20 °C. under a short day (8 hours light/16 hours dark), long day (16 hours light/ 8 hours dark) or a 12 hour light 12 hour dark cycle.

4.3.4. Cultivation of *Nicotiana tabacum* on soil

Seeds were directly spread on soil (10 part spezialblumenerde, Diwoky; 3 part sand (rasenquarz Quarzwerke Österreich Melk; 1 part perlite (Granuperl S3-6, KNAUF Perlite GmbH, Austria)) and grown under 200 µmol $m^{-2}sec^{-1}$ light intensity at 20 °C. under a short day cycle (8 hours light/16 hours dark). Seeds were obtained from plants grown first for 4 weeks under short day conditions and were then shifted to long day conditions.

4.4. Germination assays

Only seeds from plants grown in parallel were used for germination assays. For all germination assays the same basal salt medium was used (2.5 mM $NaNO_3$, 2.5 mM $Ca(NO_3)_2$, 2 mM $MgSO_4$, 2 mM $NH_4H_2PO_4$, 1mM KCl, 0.1 mM $NaFe_{III}$EDTA, $CaCl_2$, H_3BO_3, $ZnSO_4$, $MnSO_4$, $CuSO_4$, Na_2MoO_4, $CoCl_2$, 2.5 mM MES adjusted to pH5.6 with NaOH). For low K^+ conditions 50µM KCl instead of 1 mM KCl were used. For salt stress conditions the medium was supplemented with 150 mM NaCl. The medium was autoclaved with 0.5 % plant agar (Duchef Biochemie) and poured into petri dishes. Seeds were then spread onto the agar plates and stratified for 2 days at 4°C in the dark. For germination the plates were shifted to long day conditions and 200 µmol $m^{-2}sec^{-1}$ light intensity at 20 °C. Germination rates were than evaluated after two, three and 4 and 6 days after transfer to the light.

4.5. Immuno complex assays

~ 200 mg of fresh (not frozen in liquid N_2) plant material was homogenized with a drill in an 1.5 ml reaction tube also containing 50 µl of sea sand and 600 µl of LACUS buffer (25 mM TrisCl pH 7.8, 10 mM $MgCl_2$, 75 mM NaCl, 1 mM DTT, 1 mM NaF, 0.5 mM Na_3VO_4, 15 mM beta-glycerophosphate, 0.1 % Tween 20, 1 EDTA free complete protease inhibitor tablet (Roche)/25 ml). The homogenate was centrifuged at 16100g for 10 min at 4°C. Protein concentration in the supernatant was then determined by Bradford assay (BIORAD) according to the manufacturers' manual. Protein concentrations were then adjusted in the different samples to an OD_{595} of 0.2. To 400 µl of protein solution 25 µl of LACUS buffer equilibrated Protein A Sepharose CL-4B beads (GE Healthcare) and 5 µl of CPK3 antibody were added. The mixture was then incubated at 4 °C for 1 h under steady gentle mixing. The mixture was then centrifugated at 500 g for 1 min at 4 °C and washed once with LACUS buffer and 2 times with SUC buffer (50 mM TrisCl pH7.4, 250 mM NaCl, 0.1% Tween 20, 5 mM NaF, 0.1 % Nonidet P40, 0.5 mM PMSF) and once with appropriate kinase buffer. Afterwards the beads with the bound kinase were subjected to kinase assays.

4.6. Kinase assays (with/without radio labelled γ^{32}P-ATP)

For immuno complex assays:

The beads were incubated in kinase buffer (20 mM HEPES pH 7.5, 20 mM MgCl2, 1 mM DTT, 0.05 % Tween 20. Histone IIIS was added to the reaction as a substrate [5 mg/25µl reaction]. The reaction was started by the addition of ATP (50µM "cold" ATP + 20 nM active ATP-[γ-32P]: 6000Ci/mMol (PerkinElmer, Waltham, MA, USA) per 25 µl reaction. The reaction was incubated at 20 °C for 20 min and then stopped by adding SDS Loading buffer and heating of the mix for 5 min at 95 °C. The proteins were then separated via SDS-PAGE. Proteins were coomassie stained. After subsequent drying of the gel it was exposed to a Storage Phosphoscreen (GE Healthcare) which was then read out by a Typhoon Trio Imager (GE Healthcare, Chalfont St. Giles, England).

For assays analyzing the calcium dependent kinase activity of CPK3 0.5 mM EGTA were added to the kinase buffer.

For in vitro kinase assays with recombinantly expressed proteins the same kinase buffer and conditions described above were used in a 25 µl kinase reaction containing 0.05 mg/25 µl recombinantly expressed kinases and 5 mg/25 µl substrate. The kinase reaction was stopped and analyzed like described above.

For kinase assays on microsomal fractions of A.thaliana the same 25 µl reaction setup was used as described above for recombinantly expressed proteins. instead of a single substrate, 8 µl of microsomal fraction were used.

For kinase assays which were subsequently analyzed by westernblotting and a phospho S 14-3-3 specifc antibody, the kinase reaction was done under the same conditions described above. Instead of radioactive ATP only "cold" ATP was used for the kinase reaction. The reaction was then analyzed by SDS-PAGE and subsequent western blot analysis.

4.7. Recombinant expression of proteins in E.coli

4.7.1. Expression and purification of GST tagged proteins

Desired proteins were cloned into pGEX4T-3 derivatives allowing the fusion of a GST (glutathion S-transferase) at the N-terminaus or C-terminus of the desired protein. Constructs were transferred into E.coli strain BL21. Overnight liquid cultures were used to adjust 300 ml of LB to an OD_{600} of 0.1. The cells were then incubated at

37°C until they reached an OD_{600} of 0.7. Expression was induced by adding IPTG to a final concentration of 1mM and the culture was incubated at 30°C for 4 h. The cells were then harvested by centrifugation and washed once with GST buffer (50mM Tris, 20mM $MgSO_4$, 5mM EDTA, pH to 8 with HCl, 1 mM DTT). Afterwards cells were resuspended in 10 ml of GST buffer and sonicated (4 times 30 s with 10 s cooling intervals on ice). After sonication Triton X-100 was added to a final concentration of 1% and the suspension was mixed by gentle inverting. Cell debris was pelleted by centrifugation at 16000 g for 30 min at 4 °C. The supernatant was filtered through Miracloth (#475855 Calbiochem) and incubated with 100 µl of GSTbuffer equilibrated Gluthathion sepharose 4B (GE Healthcare, Chalfont St. Giles, England) slurry for 1 h at 4°C under constant shaking. The sepharose beads were then pelleted by centrifugation (500 g for 1 min at 4°C) and washed twice with GST buffer. Afterwards proteins were eluted by applying 300 µl of GE buffer (10mM reduced glutathione, 50mM Tris-HCl (pH 8)) for 30 min twice. If necessary the obtained protein was further concentrated using by using Amicon Ultra centrifugal filters (Millipore), with molecular weight cut offs appropriate for the expressed proteins, according to manufacturers' instructions.

4.7.2. Expression and purification of Intein tagged proteins

Desired proteins were cloned into pTWIN vector system (NEB) derivatives allowing the fusion of a intein-tag at the N-terminaus of the desired protein. Constructs were transferred into E.coli strain ER2566. Overnight liquid cultures were used to adjust 300 ml of LB to an OD_{600} of 0.2. The cells were then incubated at 37°C until they reached an OD_{600} of 0.7. Expression was induced by adding IPTG to a final concentration of 1mM and the culture was incubated at 16°C for 8-12 h. The cells were then harvested by centrifugation and resuspended in pre cooled buffer B1 (20 mM HEPES pH 7.0, 1 M NaCl, 1 mM EDTA, 0.2 mM 2-mercapthoethanol). The cells were then sonicated (4 times 30 s with 10 s cooling intervals on ice) and cell debris was after wards removed by centrifugation at 16000g for 20 min at 4°C. The supernatant was then filtered through Miracloth and subsequently applied to a column packed with 2 ml of chitin beads (NEB # S6651S) equilibrated in cold buffer B1. The column was subsequently washed with 20 ml of cold buffer B1 and then flushed with 4 ml of cold buffer B2 (20 mM HEPES pH 7.0, 500 mM NaCl, 1 mM EDTA, 0.2 mM 2-mercapthoethanol). To induce cleavage of the intein tag the columns were incubated at 22 °C for 12 hours. Proteins were then eluted in 4 ml of buffer B2. If necessary the obtained protein was further concentrated using by using Amicon Ultra centrifugal filters (Millipore), with molecular weight cut offs appropriate for the expressed proteins, according to manufacturer's instructions.

4.7.3. Expression and purification of HIS tagged proteins

Desired proteins were cloned into pCool derivatives allowing the fusion of a 6xHis tag at the N-terminaus or C-terminus of the desired protein. Constructs were transferred into E.coli strain BL21. Overnight liquid cultures were used to adjust 300 ml of LB to an OD_{600} of 0.1. The cells were then incubated at 37°C until they reached an OD_{600} of 0.7. Expression was induced by adding IPTG to a final concentration of 1mM and the culture was incubated at 30°C for 4 h. The cells were then harvested by centrifugation and resuspended in binding buffer (0.5 M NaCl, 5 mM imidazole, 1 mM 2-mercapthoethanol, 6 M guanidine hydrochloride 20 mM Na_3PO_4 pH8.0). Afterwards cells were sonicated (4 times 30 s with 10 s cooling intervals on ice). After sonication, cell debris was pelleted by centrifugation at 16000 g for 30 min at 4 °C. The supernatant was filtered through Miracloth (#475855 Calbiochem) HiTRAP™ chelating columns (Amersham) were prepared as indicated by the manufacturers' instructions and the protein extract was loaded onto the column by using a peristaltic pump.

Columns were washed with 5 ml of binding buffer and 5 ml of wash buffer. Then His tagged proteins were subsequently eluted by using a linear imidazol gradient from 20 to 150 mM in wash buffer (0.5 M NaCl, 1 mM 2-mercapthoethanol, 8 M urea, pH8.0) The fraction containing the desired protein were then further used. If necessary the obtained protein was further concentrated using by using Amicon Ultra centrifugal filters (Millipore), with molecular weight cut offs appropriate for the expressed proteins, according to manufacturers' instructions.

4.8. Microsomal membrane preparation

If not indicated differently all steps were carried out on 4 °C. For preparation of microsomal membranes either 10 g (fresh weight) of leafs or 10 g (fresh weight) of root material, from 6 week old hydroponically grown plants, was homogenized in pre cooled 100 ml homgenization buffer (400 mM sorbitol, 50 mM TrisCl, pH7.8, 1 mM DTT, 1 EDTA free complete tablet (Roche) according to manufacturer's instructions.) by using a waren blender six times for 3 seconds at maximum speed. The homogenate was filtered through miracloth and was centrifuged at 10.000g for 15 min. To obtain the microsomal fractions the supernatant was centrifuged at 100000 g for 1 hour. The obtained pellet was considered the microsomal fraction and used for further experiments.

4.9. Sucrose gradients

If not indicated differently all steps were carried out on 4 °C. The microsomal pellet was rinsed once with microsom resuspension buffer (10 mM TrisCl pH 7.5, 55 % (w/w) sucrose) and then transferred to a 1.5 ml reaction tube and homogenized in 200 µl microsom resuspension buffer with a glass drill (3 intervals of 30 seconds at 8.000 rpm with 30 s cooling intervals in between) and 50 µl of sea sand. The resuspended microsomes were then transferred to the bottom of a 14 ml polyallomer tube (Beckman Coulter). A linear sucrose gradient 20 - 50 % (w/w) in centrifugation buffer (10 mM TrisCl pH7.5, 2 mM EDTA, 15 mM MgCl2) was applied on top of the sample using a mixing chamber connected to a peristaltic pump. The gradient was centrifuged at 100000 g for 18 h. Afterwards 1 ml fractions were taken and analyzed by western blotting. (sucrose gradient concentrations were controlled with a Pal-1 refractometer (Atago) in each fraction).

4.10. *In vivo* FA (formaldehyde) cross-linking

For *in vivo* cross-linking either ~200 mg of intact leaf or root material was cut from 6 week old hydroponically grown *A.thaliana* plants. The plant material was then vacuum infiltrated with 1 % FA solution in H_2O using a syringe to apply the vacuum. Cross linking reaction was carried out at RT for 15 min. The reaction was quenched by infiltrating 200 mM Glycine in to the plant material and incubation at RT for 15 min. The plant material was subsequently rinsed with H_2O and homogenized in a 1.5 ml reaction tube with 50 µl of sea sand and 400 µl of 1x SDS-Loading buffer. Care was taken not to heat the sample over 40 °C to avoid breaking up the FA mediated cross links. The homogenate was centrifuged 16000 g for 10 min at 4°C and the supernatant was directly subjected to further analysis by SDS-PAGE and western blotting.

4.11. In-gel kinase assays

4.11.1. Purification of bZIP63 interacting proteins for in-gel kinase assay

GST-tagged bZIP63 protein was recombinantly expressed in E.coli as indicated in (4.7.1.) and subsequently coupled to GSTrap^{TM} columns (GE healthcare) according to the manufacturers instructions. The bZIP63 loaded column was then equilibrated with 4 bed volumes of LACUS buffer. Then 3 bed volumes of concentrated plant

protein extract in LACUS buffer were loaded onto the column. The column was then washed with 2 bed volumes of LACUS buffer. Subsequently proteins were eluted in 1 ml fractions using a step NaCl gardient (75, 100, 300, 500 mM NaCl) in LACUS buffer. The obtained proteins were further concentrated using by using Amicon Ultra centrifugal filters (Millipore), with molecular weight cut offs of 3 kDa, according to manufacturers' instructions.

4.11.2 In-gel kinase assay

In general in-gel kinase assays were performed as described in [168]. For in-gel kinase assays protein extracts obtained directly from homogenizing root or plant material of 6 week old hydroponically grown *A.thaliana* plants in LACUS buffer or bZIP 63 affinity purified proteins were used. Protein extracts were loaded onto a gel containing bZIP63.2-6xHis as a substrate (gel recipe, separating gel: 1 mg/ml substrate, 2 ml separating gel buffer (1.5 M TrisCl pH8.85, 0.1 % SDS, 1.6 ml (30 % acrylamide 0.8 % bisacrylamide) mixture, H_2O to a final volume of 4 ml, 8 µl TEMED, 37.5 µl of 10 % APS; stacking gel: 0.5 ml H_2O, 0.75 ml stacking gel buffer (0.5 M TrisCl pH 6.8, 0.1 % SDS), 0.2 ml (30 % acrylamide 0.8 % bisacrylamide) 3 µl TEMED, 10 µl 10% APS). Proteins were separated at 4 °C by subsequent SDS-PAGE.

the gel was then incubated 3x for 20 min in wash buffer I (50 mM TrisCl pH8.0, 20 % 2-propanol) under moderate shaking at RT. To remove the isopropanol the gel was incubated at RT 3x for 20 min in washbuffer II (50 mM TrisCl pH 8.0, 1 mM DTT). For denaturation the gel was incubated at RT 3x 20 min in denaturation buffer (50 mM TrisCl pH8.0, 1 mM DTT, 6 M guanidinium hydrochloride). For renaturing the proteins the gel was incubated at 4 °C in renaturation buffer (50 mM TrisCl pH8.0, 0.05 % Tween 20) over a period of 10-18 hours changing the buffer 10x in periods of at least 30 min.

Then the gel was incubated at RT 2x 30 min in kinase buffer without ATP (20 mM HEPES pH 7.5, 20 mM $MgCl_2$, 50 µM $CaCl_2$, 1 mM DTT, 0.05 % Tween-20). Then the gel was incubated for 20 min in kinase buffer containing ATP (for 20 ml kinase buffer: 50 µM "cold" ATP + 100 µCi γ^{32}P-ATP (20 nM)). The kinase reaction was stopped by incubating the gel 2x for 15 min with wash buffer III (5 % TCA). Subsequently the gel was washed with wash buffer IV (5 % TCA, 1 % sodium pyrophosphate) until no radiation was detected in the wash fraction (3x-5x incubation for 15 min). After subsequent drying of the gel it was exposed to a Storage Phosphoscreen (GE Healthcare) which was then read out by a Typhoon Trio Imager (GE Healthcare, Chalfont St. Giles, England).

4.12. Protein identification by MS

4.12.1. In-gel digest of proteins with trypsin

Prior to identification of proteins by MS (mass spectrometry), proteins were digested with trypsin to obtain fragments suitable for MS analysis. All of the following steps were performed under clean conditions on a sterile work place with chemicals suitable for MS analysis.

Protein bands/spots were excised from the gel with a scalpel and subsequently cut into pieces (2mm x 2mm). 4-6 gel pieces (2mm x 2mm) were put into a 0.6 ml reaction tube together with 150µl H_2O. The gel pieces were washed 3x 10 min with 200 µl H_2O at RT under steady mixing on a thermomixer. Coomassie stained proteins were then destained by removing the H_2O and adding 200 µl 50 mM NH_4HCO_3 solution together with 160 µl acetonitrile. The mixture was incubated 15 min at RT under steady shaking. This procedure was repeated once if gel pieces were not destained after 15 min. Afterwards gels were dehydrated by removing the previous buffer and adding 160 µl of acetonitrile (ACN) instead. The mixture was then steadily shaken at RT for 5 min. the

acetonitrile was then removed and the gel pieces were dried in a speed vac for 5 min at RT. For reduction of the proteins 200 µl of reduction mix (10 mM DTT in 50 mM NH_4HCO_3 solution) were added to the dry gel pieces. The mix was incubated at 56 °C for 30 min. Then, the reduction mix was removed and 200 µl of ACN were added. The mix was again steadily shaken for 5 min at RT and the ACN removed. A freshly prepared (5 min before use) iodoacetamide solution (0,010 g/ml iodoacetamide in 50 mM NH_4HCO_3) was added to the gel pieces. The mixture was then incubated 20 min in the dark. Subsequently the iodoacetamide solution was removed and the gel pieces were washed 3x 10 min with 50 mM NH_4HCO_3. Finally the aqueous solution was removed and replaced by 200 µl of ACN. The mixture was again incubated for 5 min at RT and gel pieces were dried afterwards in a speed vac. Trypsin solution (10 ng/µl Trypsin in 50 mM NH_4HCO_3) was then added in an appropriate volume (exactly the gel volume) and gels were incubated 10 min on 4 °C. The proteins in the gel were then digested over night by incubating the mixture at 37 °C. The digest was stopped by adding formic acid to a final concentration of 1 %. Samples were then incubated under sonication for 10 min in a water bath at 4 °C. Peptides were then extracted from the gel by washing it 2x with 5 % formic acid (exactly the gel volume), and collecting the wash fractions in a separate reaction tube. Peptides were subsequently used for sequence identification by MS.

4.12.2. Peptide identification via MS

For HPLC an UltiMate™ system (Dionex Corporation, Sunnyvale, CA, USA) equipped with a PepMap C18 purification column (300µm x 5mm) and a 75µm x 150mm analytical column of the same material was used. 0.1% TFA (Thermo Scientific, Waltham, MA, USA) was used on the Switchos module for the binding of the peptides and a linear gradient of ACN.(Chromasolv®; Sigma-Aldrich, St. Louis, MO, USA) and 0.1% formic acid in water was used for the elution. LC-MS/MS analysis was carried out with the UltiMate™ system interfaced to an LTQ (Thermo Scientific, Waltham, MA, USA) linear ion trap mass spectrometer. The nanospray source of Proxeon (Odense, Denmark) was used with the distal coated silica capillaries of New Objective (Woburn, MA, USA). The electrospray voltage was set to 1500V. Peptide spectra were recorded over the mass range of m/z 450 to 1600, MS/MS spectra were recorded in information dependent data acquisition and the default charge state was set to 3. The mass range for MS/MS measurements was calculated according to the masses of the parent ions. One full spectrum was recorded followed by four MS/MS spectra for the most intense ions, automatic gain control was applied and the collision energy was set to the arbitrary value of 35. Helium was used as collision gas. The instrument was operated in data dependent modus. Fragmented ions were set onto an exclusion list for 20 seconds. Raw spectra were interpreted by Mascot 2.2.04 (Matrix Science Ltd., London, England) using Mascot Daemon 2.2.2. Peptide tolerance was set to +/- 2Da, MS/MS tolerance was set to +/- 0.8Da. Carbamidomethylcysteine was set as static modification, oxidation of methionine residues was set as variable modification. Trypsin was selected as protease and 2 missed cleavages were allowed.

Mascot results were loaded into Scaffold (Ver. 2.01.01.1; Proteome Software Inc., Portland, OR, USA) for a X! Tandem Search. Peptide identifications were accepted if they could be established at greater than 95% probability as specified by the Peptide Prophet algorithm [169]. Protein identifications were accepted if they could be established at greater than 99% probability as assigned by the Protein Prophet algorithm [170]. Additionally at least two identified peptides were required. As a reference library the TAIR9 (a reformated version to suite the search algorithm's requirements) non redundant protein database was used.

Subsequent data processing for proteins was done using the Scaffold viewer version 2.0 (Proteome Software Inc., Portland, OR, USA).

4.13. In vivo Fluorescence microscopy

Transformed agrobacteria (AGL1) carrying the construct of interest (for all microscopy studies different variants of the pBIN19 vectors were used) were incubated over night at 30°C in 5 ml LB , with appropriate selection medium, under vigorous shaking. Next morning the culture complete culture was transferred into 50 ml LB with appropriate selection medium and incubated under vigorous shaking at 30°C for 4 h. Cells were then harvested by centrifugation (4000 g, RT, 15 min). The pellet was resuspended in 30 ml of LB containing 150 µM acetosyringone. Cells were then again incubated for 2 h at 30°C under vigorous shaking. Then OD_{600} was determined and after centrifugation (4000 g, RT, 15 min) OD_{600} was adjusted to two by resuspending the cells in the appropriate volume of 5 % sucrose solution in H_2O. If co-infiltrations were done, same volumes of respective agrobacteria cultures were mixed at this stage. The agrobacteria suspension was then infiltrated with a syringe into young leafs of 6 week old *nicotiana tabacum* plants. The leafs were pinched with a needle to facilitate the infiltration process. The infiltrated tobacco plants were then incubated at 26 °C for 40-48 hours. After 40- 48 hours Fluroescence signals were detected with confocal laser scanning microscopes (LSM 510, LSM 510 meta and LSM 710 from Zeiss). Before microscopy leaf discs were vacuum infiltrated with H_2O. Image analysis and extraction of relative fluorescence intensities for quantitative BIFC was done with the ZEN software from Zeiss. Processing and statistical analysis of data for quantitative BIFC was done in microsoft EXCEL.
The leaf discs used for microscopy were frozen in liquid N_2 and then subjected to protein extraction and western blot analysis.

4.14. Metabolite profiling

4.14.1. Metabolite extraction

Metabolite extraction was basically done as described in [173]. ~ 150 mg of root material from 6 week old hydroponically grown plants subjected to the different stress conditions indicated in the text was frozen in liquid N_2 and homogenized in a QIAGEN TissueLyser II (frequency: 30/second; duration: 1 min; glass beads were used as impactors). The resulting homogenized material was then weighed, to normalize metabolite levels to the fresh weight. Subsequently 1 ml of extraction mix (methanol/chloroform/H_2O in the ratio 2.5/1/0.5 [v/v/v]) was added to the frozen plant material and vortexed for 1 min at 4 °C. the cell debris was then pelleted by centrifugation (4 min, 16000g, 4°C). The supernatant was then transferred into a new 2 ml reaction tube and mixed with additional 500 µl H_2O (vortexed 1 min on 4 °C). Rapid phase separation was achieved by centrifugation at 16000 g for 2 min at 4°C. The polar (upper) phase was transferred into a new reaction tube and subsequently split into two aliquots of equal volume (1 aliquot was used as backup). To all aliquotes ribitol was added as internal standard to a final concentration of 5 mg/litre. The solvent was then evaporated in a speed vac. The dried pellet could then be stored at -80 °C until further analysis. Samples chosen for analysis were equilibrated at 20 °C for 20 min before start of derivatisation. Subsequently metabolites were dissolved in 20 µl of methoxymation cocktail (40 mg methoxyaminhydrochloride (CH_3ONH_2*HCl) in 1 ml pyridine and incubated at 30°C for 90 min. Then 80 µl of silylation cocktail (MSTFA (N-methyl-N-trimethylsilyl-trifluoroacetamide) + alkane standard) were added and mixed and incubated at 37 °C for 30 min. Subsequently samples were centrifuged (2 min, 16000 g, 20 °C) and the supernatant was transferred to GC vials.

Samples were automatically injected to a GC-MS coupled system (Gas Chromatograph: TRACE GC Ultra and TriPlus Autosampler (Thermo Fisher Scientific) Mass spectrometer: Thermo Scientific TSQ Quantum GC (Thermo Fisher Scientific, Austin, TX USA); The following instrumental setup was chosen: injection temperature 230°C, constant temperature (CT) split less mode; carrier gas: Helium with constant flow at 1 ml*min^{-1}; separation column: HP-5MS capillary column (30 m x 0.25 mm x 0.25 µm) (Agilent Technologies, Santa Clara, CA); The temperature gradient was modified according to [171]; oven program: initial temp 70°C, 1min 70°C isotherm, 1 °C min^{-1} ramp to 76°C followed by a 6 °C min^{-1} ramp to 350 °C, hold for 5 min. postrun condition: 10 min at 325 °C; Transferline temperature: 340 °C; Ion Source temperature was 250 °C; Electron impact ionisation was used (at 70 eV, emission current: 50 µA); The mass spectrometer operated in full scan mode: *m/z* 40-600, scan time 250 ms;

4.14.2. Data evaluation

Identification of compounds: retention index calibration and mass spectral deconvolution were performed using AMDIS (Automated Mass Spectral Deconvolution and Identification System; National Institute of Standards and Technology, Gaithersburg, MD, USA) [172]. Metabolites were identified by comparison of the EI fragmentation pattern with an in-house mass spectral library as well as using the retention time index based on even alkanes C10-C40. Relative quantification was conducted by LC Quan Version 2.5.6 (Thermo Fisher Scientific) for relative quantification, the peak area of characteristic fragment masses for each metabolite was used.
For metabolite data validation the statistics package including the TWO-WAY ANOVA implemented in the Origin v 8.0724 software was used. For data formatting microsoft EXCEL was used.

4.15. Strains and plant lines

***E.coli* strains**	
DH5α (cloning)	F-, ø80dlacZDM15, D(lacZYA-argF)U169, deoR, recA1, endA1, sdR17(rk,mk+), phoA, supE44, l-, thi-1, gyrA96, relA1
BL 21(DE3)pLysS	F-, ompT, hsdSB (rB- mB-) gal dcm (DE3) pLysS (CamR)
ER2566 (protein expression)	fhuA2, lacZ::T7, gene1, [lon] ompT, gal, sulA11, R(mcr-73::miniTn10--TetS)2 [dcm], R(zgb-210::TN10--TetS), endA1, Δ(mcrC-mrr)114::IS10
Agrobacteria strain	
AGL1	AGL0 (C58 pTiBo542) recA::bla, T-region deleted Mop(+) Cb(R)
Plant lines	
Col0 *(A.thaliana)*	wild type A.thaliana ecotype Col0
cpk3-1 (A.thaliana)	promoter T-DNA insertion line cpk3-1 (Salk_107620)
cpk3-2 (A.thaliana)	exon1 T-DNA insertion line cpk3-2 (Salk_107620)
cpk3-3 (A.thaliana)	promoter T-DNA insertion line cpk3-3 (Sail_120_H09)
tpk1-3 (A.thaliana)	T-DNA insertion line (
tpk1 ox3 (A.thaliana)	35S:TPK1 over-expresser line in Col0 background
Nicotiana tabacum	cv. Petite Havana SR1

4.16. Primer list

primer name	primer sequence
	primers for analyzing T-DNAinsertions
Salk_LB	5'-CGC TGG ACC GCT TGC TGC AAC T-3'
Salk_LBb1.3	5'-ATT TTG CCG ATT TCG GAA C-3'
Sail-LB3	5'-TAG CAT CTG AAT TTC ATA ACC AAT CTC GAT ACA C-3'
CPK 3-2 FW	5'-AAA AGG ATC CGG GCC CAT GGG CCA CAG ACA CAG CAA GTC CAA ATC CTC CG-3'
CPK 3-2 RV	5'-TTT TGT CGA CCT AGC GGC CGC ACA TTC TGC GTC GGT TTG GCA CCA ATT CTG GAT TTC CC-3'
CPK 3-1 RP1	5'-ACG AGG TAC GTG ACA CCA AAC-3'
CPK 3-1 LP1	5'-TTG TGT CGA ACA AGT GGT TTG-3'
Sail 120 H09 RP2	5'-GTA GGC TCC CTT CAA GTC CAC-3'
Sail 120 H09 LP2	5'-CAT TGC CAG AAA AGC TGA AAC-3'
	primers for molecular cloning
TPK1_fw	5'-GGG CCC ATG TCG AGT GAT GCA GCT CG-3'
TPK1_rv	5'-GCG GCC GCA CCT TTG AAT CTG AGA CGT GGT-3'
AKIN10 - sf 1,3 5'	5'- GGGCCCATGGATGGATCAGGCACAGGCAGTA - 3'
AKIN10 - sf 2 5'	5'-GGGCCCATGTTCAAACGAGTAGATGA-3'
AKIN10 - sf 1,2,3 3'	5'-GCGGCCGCAGAGGACTCGGAGCTGAGCAA-3'
AKIN11 - sf 1,2,3 5'	5'-GGGCCCATGGATCATTCATCAAATAG-3'
AKIN11 - sf 1,2 3'	5'-GCGGCCGCAGATCACACGAAGCTCTGTAA-3'
AKIN11 - sf 3 3'	5'-GCGGCCGCAGGTGTGCGCATAGGATTGGA-3'
SNF1 activator 5'	5'-GGGCCCATGTTTGGTTCTACATTGGA-3'
SNF1 activator 3'	5'-GCGGCCGCAAAGACCGAGCAGGAATTGGAA-3'
CKA1 5'	5'-GGG CCC ATG ATA GAT ACG CTT TTC TTC-3'
CKA2 5'	5'-GGG CCC ATG CAC CTA ATC TTC TTC TTC TCC-3'
CKB1 5'	5'-GGG CCC ATG TAT AGA GAC AGA GGA ACG-3'
CKA1 3' frame	5'-GCG GCC GCA TTG ACT TCT CAT TCT GCT GG-3'
CKA2 3' frame	5'-GCG GCC GCA TTG AGT CCT CAT TCT GCT GC-3'
CKB1 3' frame	5'-GCG GCC GCA CGG TTT GTG TAA TTT GAA CC-3'
NIA2-Nt	5'-TTG GGC CCA TGG CGG CCT CTG TAG ATA ATC GC-3'
NIA2-Ct	5'-TTG CGG CCG CTC AAG AAA TCC TCC TTG ATG TTA TAT TGC-3'
	primers for point mutations
Nia2 K530toA	5'-cctcctagtctaaaggcctctgtctcgacgc-3'
Nia2 K531toA	5'-cctcctagtctagctaagtctgtctcgacgc-3'
Nia2pointrev	5'-CGCGTCAGCCGATTTTTCG-3'
TPK1 K35,39 A fw	5'-cttcaagaaaagcaagattgcgcgcctctagaagtgctcc-3'
TPK1 K35,39 A rev	5'-AAGAAGTTCTTGAGTTCAGG-3'
TPK1 K36,38 A fw	5'-cttcaagaaaacgagcattggcgcgctctagaagtgctcc-3'
TPK1 K36,38 A rev	5'-AAGAAGTTCTTGAGTTCAGG-3'
	primers for RT PCR
bZIP63 RT-fwd	5'-CTC CGA CGA AGA AAT CTC CGG TAA CC-3'
bZIP63 RT-rev	5'-CTT TAA CAG CTA CTG ATC CCC AAC GC-3'
NIA2 RT-fwd	5'-CCG ACG AAG AAG GTT GGT GG-3'
NIA2 RT-rev	5'-CCA GGA AGC GTT GGA TGC TC-3'
At4g34590 RT 5' (bzip11)	5'-GTT CGA ACC CTC TGG TTG GT-3'

At4g34590 RT 3' (bzip11)	5'-TCT TTG GAC ATG TCT CTA AAT CGG-3'
At5g49450 RT 5' (bzip1)	5'-ACG ATT CAT GAG ATC TCC AGT C-3'
At5g49450 RT 3' (bzip1)	5'-GTC TTA AAG GAC GCC ATT GGT T-3'
bZIP63.2+3 RT fw	5'-GGA ACT TTC ATC AAA CCT CAG G-3'
bZIP63.1 RT fw	5'-CGC CAT GAA AAG GGA TAC TTC TGG-3'
bZIP63.1+2 RT rev	5'-CAG CCA TTT TCA CCT TTG CTC G-3'
bZIP63.3 RT rev neu	5'-GCGAGTTTTGGTAGACAGAGAG-3'
bZIP63.2+3 RT rev	5'-CCT GAG GTT TGA TGA AAG TTC C-3'
act3 5'	5'-ATA TGA TGA GTC AGG CCC GT-3'
act3 3'	5'-TGT CTT AGG CCA GAA TCT GAA AAT-3'
CPK3-fwd	5'-AGA TGT TCG CCG TGA AGT CC-3'
CPK3-rev	5'-ACG GAT GAT TTA GCA CTT CCG-3'

5. References

1 Sanders, D., C. Brownlee, et al. (1999). "Communicating with calcium." Plant Cell **11**(4): 691-706.

2 Dodd, A. N., J. Kudla, et al. (2010). "The language of calcium signaling." Annu Rev Plant Biol **61**: 593-620.

3 Kudla, J., O. Batistic, et al. (2010). "Calcium signals: the lead currency of plant information processing." Plant Cell **22**(3): 541-63.

4 Kim, T. H., M. Bohmer, et al. (2010). "Guard cell signal transduction network: advances in understanding abscisic acid, CO2, and Ca2+ signaling." Annu Rev Plant Biol **61**: 561-91.

5 Gao, D., M. R. Knight, et al. (2004). "Self-reporting Arabidopsis expressing pH and [Ca2+] indicators unveil ion dynamics in the cytosol and in the apoplast under abiotic stress." Plant Physiol **134**(3): 898-908.

6 Arimura, G. and M. E. Maffei (2010). "Calcium and secondary CPK signaling in plants in response to herbivore attack." Biochem Biophys Res Commun **400**(4): 455-60.

7 Chin, D. and A. R. Means (2000). "Calmodulin: a prototypical calcium sensor." Trends Cell Biol **10**(8): 322-8.

8 McCormack, E., Y. C. Tsai, et al. (2005). "Handling calcium signaling: Arabidopsis CaMs and CMLs." Trends Plant Sci **10**(8): 383-9.

9 Bouche, N., A. Yellin, et al. (2005). "Plant-specific calmodulin-binding proteins." Annu Rev Plant Biol **56**: 435-66.

10 Kushwaha, R., A. Singh, et al. (2008). "Calmodulin7 plays an important role as transcriptional regulator in Arabidopsis seedling development." Plant Cell **20**(7): 1747-59.

11 Luan, S. (2009). "The CBL-CIPK network in plant calcium signaling." Trends Plant Sci **14**(1): 37-42.

12 Batistic, O. and J. Kudla (2009). "Plant calcineurin B-like proteins and their interacting protein kinases." Biochim Biophys Acta **1793**(6): 985-92.

13 Ohta, M., Y. Guo, et al. (2003). "A novel domain in the protein kinase SOS2 mediates interaction with the protein phosphatase 2C ABI2." Proc Natl Acad Sci U S A **100**(20): 11771-6.

14 Albrecht, V., O. Ritz, et al. (2001). "The NAF domain defines a novel protein-protein interaction module conserved in Ca2+-regulated kinases." Embo J **20**(5): 1051-63.

15 Hrabak, E. M., C. W. Chan, et al. (2003). "The Arabidopsis CDPK-SnRK superfamily of protein kinases." Plant Physiol **132**(2): 666-80.

16 Pandey, G. K., Y. H. Cheong, et al. (2004). "The calcium sensor calcineurin B-like 9 modulates abscisic acid sensitivity and biosynthesis in Arabidopsis." Plant Cell **16**(7): 1912-24.

17 Pandey, G. K., J. J. Grant, et al. (2008). "Calcineurin-B-like protein CBL9 interacts with target kinase CIPK3 in the regulation of ABA response in seed germination." Mol Plant **1**(2): 238-48.

18 D'Angelo, C., S. Weinl, et al. (2006). "Alternative complex formation of the Ca-regulated protein kinase CIPK1 controls abscisic acid-dependent and independent stress responses in Arabidopsis." Plant J **48**(6): 857-72.

19 Xu, J., H. D. Li, et al. (2006). "A protein kinase, interacting with two calcineurin B-like proteins, regulates K+ transporter AKT1 in Arabidopsis." Cell **125**(7): 1347-60.

20 Cheong, Y. H., G. K. Pandey, et al. (2007). "Two calcineurin B-like calcium sensors, interacting with protein kinase CIPK23, regulate leaf transpiration and root potassium uptake in Arabidopsis." Plant J **52**(2): 223-39.

21 Ho, C. H., S. H. Lin, et al. (2009). "CHL1 functions as a nitrate sensor in plants." Cell **138**(6): 1184-94.

22 Billker, O., S. Dechamps, et al. (2004). "Calcium and a calcium-dependent protein kinase regulate gamete formation and mosquito transmission in a malaria parasite." Cell **117**(4): 503-14.

23 Green, J. L., R. R. Rees-Channer, et al. (2008). "The motor complex of Plasmodium falciparum: phosphorylation by a calcium-dependent protein kinase." J Biol Chem **283**(45): 30980-9.

24 Cheng, S. H., M. R. Willmann, et al. (2002). "Calcium signaling through protein kinases. The Arabidopsis calcium-dependent protein kinase gene family." Plant Physiol **129**(2): 469-85.

25 Wernimont, A. K., J. D. Artz, et al. (2010). "Structures of apicomplexan calcium-dependent protein kinases reveal mechanism of activation by calcium." Nat Struct Mol Biol **17**(5): 596-601.

26 Geiger, D., S. Scherzer, et al. (2010). "Guard cell anion channel SLAC1 is regulated by CDPK protein kinases with distinct Ca2+ affinities." Proc Natl Acad Sci U S A **107**(17): 8023-8.

27 Ranjan, R., A. Ahmed, et al. (2009). "Dissection of mechanisms involved in the regulation of Plasmodium falciparum calcium-dependent protein kinase 4." J Biol Chem **284**(22): 15267-76.
28 Harmon, A. C., M. Gribskov, et al. (2000). "CDPKs - a kinase for every Ca2+ signal?" Trends Plant Sci **5**(4): 154-9.
29 Mehlmer, N., B. Wurzinger, et al. (2010). "The Ca(2+)-dependent protein kinase CPK3 is required for MAPK-independent salt-stress acclimation in Arabidopsis." Plant J.
30 Benetka, W., N. Mehlmer, et al. (2008). "Experimental testing of predicted myristoylation targets involved in asymmetric cell division and calcium-dependent signalling." Cell Cycle **7**(23): 3709-19.
31 Martin, M. L. and L. Busconi (2000). "Membrane localization of a rice calcium-dependent protein kinase (CDPK) is mediated by myristoylation and palmitoylation." Plant J **24**(4): 429-35.
32 Ito, T., M. Nakata, et al. (2010). "Alteration of substrate specificity: the variable N-terminal domain of tobacco Ca(2+)-dependent protein kinase is important for substrate recognition." Plant Cell **22**(5): 1592-604.
33 Ludwig, A. A., T. Romeis, et al. (2004). "CDPK-mediated signalling pathways: specificity and cross-talk." J Exp Bot **55**(395): 181-8.
34 Fujii, H., V. Chinnusamy, et al. (2009). "In vitro reconstitution of an abscisic acid signalling pathway." Nature **462**(7273): 660-4.
35 Zhu, S. Y., X. C. Yu, et al. (2007). "Two calcium-dependent protein kinases, CPK4 and CPK11, regulate abscisic acid signal transduction in Arabidopsis." Plant Cell **19**(10): 3019-36.
36 Mori, I. C., Y. Murata, et al. (2006). "CDPKs CPK6 and CPK3 function in ABA regulation of guard cell S-type anion- and Ca(2+)-permeable channels and stomatal closure." PLoS Biol **4**(10): e327.
37 Choi, H. I., H. J. Park, et al. (2005). "Arabidopsis calcium-dependent protein kinase AtCPK32 interacts with ABF4, a transcriptional regulator of abscisic acid-responsive gene expression, and modulates its activity." Plant Physiol **139**(4): 1750-61.
38 Ma, S. Y. and W. H. Wu (2007). "AtCPK23 functions in Arabidopsis responses to drought and salt stresses." Plant Mol Biol **65**(4): 511-8.
39 Romeis, T., A. A. Ludwig, et al. (2001). "Calcium-dependent protein kinases play an essential role in a plant defence response." Embo J **20**(20): 5556-67.
40 Romeis, T., P. Piedras, et al. (2000). "Resistance gene-dependent activation of a calcium-dependent protein kinase in the plant defense response." Plant Cell **12**(5): 803-16.
41 Ludwig, A. A., H. Saitoh, et al. (2005). "Ethylene-mediated cross-talk between calcium-dependent protein kinase and MAPK signaling controls stress responses in plants." Proc Natl Acad Sci U S A **102**(30): 10736-41.
42 Boudsocq, M., M. R. Willmann, et al. (2010). "Differential innate immune signalling via Ca(2+) sensor protein kinases." Nature **464**(7287): 418-22.
43 Kanchiswamy, C. N., H. Takahashi, et al. (2010). "Regulation of Arabidopsis defense responses against Spodoptera littoralis by CPK-mediated calcium signaling." BMC Plant Biol **10**: 97.
44 Kobayashi, M., I. Ohura, et al. (2007). "Calcium-dependent protein kinases regulate the production of reactive oxygen species by potato NADPH oxidase." Plant Cell **19**(3): 1065-80.
45 Myers, C., S. M. Romanowsky, et al. (2009). "Calcium-dependent protein kinases regulate polarized tip growth in pollen tubes." Plant J **59**(4): 528-39.
46 Bohmer, M. and T. Romeis (2007). "A chemical-genetic approach to elucidate protein kinase function in planta." Plant Mol Biol **65**(6): 817-27.
47 Ivashuta, S., J. Liu, et al. (2005). "RNA interference identifies a calcium-dependent protein kinase involved in Medicago truncatula root development." Plant Cell **17**(11): 2911-21.
48 Gargantini, P. R., S. Gonzalez-Rizzo, et al. (2006). "A CDPK isoform participates in the regulation of nodule number in Medicago truncatula." Plant J **48**(6): 843-56.
49 Douglas, P., N. Morrice, et al. (1995). "Identification of a regulatory phosphorylation site in the hinge 1 region of nitrate reductase from spinach (Spinacea oleracea) leaves." FEBS Lett **377**(2): 113-7.
50 Douglas, P., G. Moorhead, et al. (1998). "Purification of a nitrate reductase kinase from Spinacea oleracea leaves, and its identification as a calmodulin-domain protein kinase." Planta **206**(3): 435-42.
51 Bachmann, M., N. Shiraishi, et al. (1996). "Identification of Ser-543 as the major regulatory phosphorylation site in spinach leaf nitrate reductase." Plant Cell **8**(3): 505-17.
52 Su, W., S. C. Huber, et al. (1996). "Identification in vitro of a post-translational regulatory site in the hinge 1 region of Arabidopsis nitrate reductase." Plant Cell **8**(3): 519-27.

53 Lambeck, I., J. C. Chi, et al. (2010). "Kinetic analysis of 14-3-3-inhibited Arabidopsis thaliana nitrate reductase." Biochemistry **49**(37): 8177-86.
54 Loog, M., R. Toomik, et al. (2000). "Peptide phosphorylation by calcium-dependent protein kinase from maize seedlings." Eur J Biochem **267**(2): 337-43.
55 Zhang, X. Q., A. A. Lund, et al. (1999). "Soybean nodule sucrose synthase (nodulin-100): further analysis of its phosphorylation using recombinant and authentic root-nodule enzymes." Arch Biochem Biophys **371**(1): 70-82.
56 Takezawa, D., S. Ramachandiran, et al. (1996). "Dual regulation of a chimeric plant serine/threonine kinase by calcium and calcium/calmodulin." J Biol Chem **271**(14): 8126-32.
57 Mitra, R. M., C. A. Gleason, et al. (2004). "A Ca2+/calmodulin-dependent protein kinase required for symbiotic nodule development: Gene identification by transcript-based cloning." Proc Natl Acad Sci U S A **101**(13): 4701-5.
58 Chen, C., M. Gao, et al. (2007). "Fungal symbiosis in rice requires an ortholog of a legume common symbiosis gene encoding a Ca2+/calmodulin-dependent protein kinase." Plant Physiol **145**(4): 1619-28.
59 Levy, J., C. Bres, et al. (2004). "A putative Ca2+ and calmodulin-dependent protein kinase required for bacterial and fungal symbioses." Science **303**(5662): 1361-4.
60 Tirichine, L., H. Imaizumi-Anraku, et al. (2006). "Deregulation of a Ca2+/calmodulin-dependent kinase leads to spontaneous nodule development." Nature **441**(7097): 1153-6.
61 Godfroy, O., F. Debelle, et al. (2006). "A rice calcium- and calmodulin-dependent protein kinase restores nodulation to a legume mutant." Mol Plant Microbe Interact **19**(5): 495-501.
62 Coca, M. and B. San Segundo (2010). "AtCPK1 calcium-dependent protein kinase mediates pathogen resistance in Arabidopsis." Plant J.
63 Batistic, O., R. Waadt, et al. (2010). "CBL-mediated targeting of CIPKs facilitates the decoding of calcium signals emanating from distinct cellular stores." Plant J **61**(2): 211-22.
64 Batistic, O., N. Sorek, et al. (2008). "Dual fatty acyl modification determines the localization and plasma membrane targeting of CBL/CIPK Ca2+ signaling complexes in Arabidopsis." Plant Cell **20**(5): 1346-62.
65 Waadt, R., L. K. Schmidt, et al. (2008). "Multicolor bimolecular fluorescence complementation reveals simultaneous formation of alternative CBL/CIPK complexes in planta." Plant J **56**(3): 505-16.
66 Dammann, C., A. Ichida, et al. (2003). "Subcellular targeting of nine calcium-dependent protein kinase isoforms from Arabidopsis." Plant Physiol **132**(4): 1840-8.
67 Munns, R. and M. Tester (2008). "Mechanisms of salinity tolerance." Annu Rev Plant Biol **59**: 651-81.
68 Shabala, S. and T. A. Cuin (2008). "Potassium transport and plant salt tolerance." Physiol Plant **133**(4): 651-69.
69 Munnik, T. and J. E. Vermeer (2010). "Osmotic stress-induced phosphoinositide and inositol phosphate signalling in plants." Plant Cell Environ **33**(4): 655-69.
70 Sengupta, S., B. Patra, et al. (2008). "Inositol methyl tranferase from a halophytic wild rice, Porteresia coarctata Roxb. (Tateoka): regulation of pinitol synthesis under abiotic stress." Plant Cell Environ **31**(10): 1442-59.
71 Nishizawa, A., Y. Yabuta, et al. (2008). "Galactinol and raffinose constitute a novel function to protect plants from oxidative damage." Plant Physiol **147**(3): 1251-63.
72 Santner, A. and M. Estelle (2009). "Recent advances and emerging trends in plant hormone signalling." Nature **459**(7250): 1071-8.
73 Tan, X., L. I. Calderon-Villalobos, et al. (2007). "Mechanism of auxin perception by the TIR1 ubiquitin ligase." Nature **446**(7136): 640-5.
74 Lemtiri-Chlieh, F., E. A. MacRobbie, et al. (2003). "Inositol hexakisphosphate mobilizes an endomembrane store of calcium in guard cells." Proc Natl Acad Sci U S A **100**(17): 10091-5.
75 Fricke, W., G. Akhiyarova, et al. (2004). "Rapid and tissue-specific changes in ABA and in growth rate in response to salinity in barley leaves." J Exp Bot **55**(399): 1115-23.
76 Jiang, F. and W. Hartung (2008). "Long-distance signalling of abscisic acid (ABA): the factors regulating the intensity of the ABA signal." J Exp Bot **59**(1): 37-43.
77 Craig Plett, D. and I. S. Moller (2010). "Na(+) transport in glycophytic plants: what we know and would like to know." Plant Cell Environ **33**(4): 612-26.
78 Dinneny, J. R. (2009). "Analysis of the salt-stress response at cell-type resolution." Plant Cell Environ **33**(4): 543-51.

79 Guo, K. M., O. Babourina, et al. (2008). "The cyclic nucleotide-gated channel, AtCNGC10, influences salt tolerance in Arabidopsis." Physiol Plant **134**(3): 499-507.
80 Gobert, A., G. Park, et al. (2006). "Arabidopsis thaliana cyclic nucleotide gated channel 3 forms a non-selective ion transporter involved in germination and cation transport." J Exp Bot **57**(4): 791-800.
81 Haro, R., M. A. Banuelos, et al. (2005). "HKT1 mediates sodium uniport in roots. Pitfalls in the expression of HKT1 in yeast." Plant Physiol **139**(3): 1495-506.
82 Lauchli, A., R. A. James, et al. (2008). "Cell-specific localization of Na+ in roots of durum wheat and possible control points for salt exclusion." Plant Cell Environ **31**(11): 1565-74.
83 Munns, R. (2002). "Comparative physiology of salt and water stress." Plant Cell Environ **25**(2): 239-250.
84 DeFalco, T. A., K. W. Bender, et al. (2010). "Breaking the code: Ca2+ sensors in plant signalling." Biochem J **425**(1): 27-40.
85 Zhu, J. K. (2003). "Regulation of ion homeostasis under salt stress." Curr Opin Plant Biol **6**(5): 441-5.
86 Gobert, A., S. Isayenkov, et al. (2007). "The two-pore channel TPK1 gene encodes the vacuolar K+ conductance and plays a role in K+ homeostasis." Proc Natl Acad Sci U S A **104**(25): 10726-31.
87 Sirichandra, C., A. Wasilewska, et al. (2009). "The guard cell as a single-cell model towards understanding drought tolerance and abscisic acid action." J Exp Bot **60**(5): 1439-63.
88 Marschner, H. (1995). "The Mineral Nutrition of Higher Plants." Academic Press, London
89 Shabala, S. N. and R. R. Lew (2002). "Turgor regulation in osmotically stressed Arabidopsis epidermal root cells. Direct support for the role of inorganic ion uptake as revealed by concurrent flux and cell turgor measurements." Plant Physiol **129**(1): 290-9.
90 Gierth, M. and P. Maser (2007). "Potassium transporters in plants--involvement in K+ acquisition, redistribution and homeostasis." FEBS Lett **581**(12): 2348-56.
91 Kiegle, E., C. A. Moore, et al. (2000). "Cell-type-specific calcium responses to drought, salt and cold in the Arabidopsis root." Plant J **23**(2): 267-78.
92 Kadera, M., S. Lindbergb, et al. (2007). "Sodium sensing induces different changes in free cytosolic calcium concentration and pH in salt-tolerant and -sensitive rice (Oryza sativa) cultivars." Physiol Plant **130**(1): 99-111.
93 D'Onofrio, C. and S. Lindberg (2009). "Sodium induces simultaneous changes in cytosolic calcium and pH in salt-tolerant quince protoplasts." J Plant Physiol **166**(16): 1755-63.
94 Liu, J. and J. K. Zhu (1998). "A calcium sensor homolog required for plant salt tolerance." Science **280**(5371): 1943-5.
95 Liu, J., M. Ishitani, et al. (2000). "The Arabidopsis thaliana SOS2 gene encodes a protein kinase that is required for salt tolerance." Proc Natl Acad Sci U S A **97**(7): 3730-4.
96 Qiu, Q. S., Y. Guo, et al. (2002). "Regulation of SOS1, a plasma membrane Na+/H+ exchanger in Arabidopsis thaliana, by SOS2 and SOS3." Proc Natl Acad Sci U S A **99**(12): 8436-41.
97 Halfter, U., M. Ishitani, et al. (2000). "The Arabidopsis SOS2 protein kinase physically interacts with and is activated by the calcium-binding protein SOS3." Proc Natl Acad Sci U S A **97**(7): 3735-40.
98 Kim, B. G., R. Waadt, et al. (2007). "The calcium sensor CBL10 mediates salt tolerance by regulating ion homeostasis in Arabidopsis." Plant J **52**(3): 473-84.
99 Quan, R., H. Lin, et al. (2007). "SCABP8/CBL10, a putative calcium sensor, interacts with the protein kinase SOS2 to protect Arabidopsis shoots from salt stress." Plant Cell **19**(4): 1415-31.
100 Cheong, Y. H., K. N. Kim, et al. (2003). "CBL1, a calcium sensor that differentially regulates salt, drought, and cold responses in Arabidopsis." Plant Cell **15**(8): 1833-45.
101 Li, L., B. G. Kim, et al. (2006). "A Ca(2)+ signaling pathway regulates a K(+) channel for low-K response in Arabidopsis." Proc Natl Acad Sci U S A **103**(33): 12625-30.
102 Fuglsang, A. T., Y. Guo, et al. (2007). "Arabidopsis protein kinase PKS5 inhibits the plasma membrane H+ -ATPase by preventing interaction with 14-3-3 protein." Plant Cell **19**(5): 1617-34.
103 Milla, M. A., J. Townsend, et al. (2006). "The Arabidopsis AtDi19 gene family encodes a novel type of Cys2/His2 zinc-finger protein implicated in ABA-independent dehydration, high-salinity stress and light signaling pathways." Plant Mol Biol **61**(1-2): 13-30.
104 Xu, J., Y. S. Tian, et al. (2010). "AtCPK6, a functionally redundant and positive regulator involved in salt/drought stress tolerance in Arabidopsis." Planta **231**(6): 1251-60.
105 Jiang, X., E. O. Leidi, et al. (2010). "How do vacuolar NHX exchangers function in plant salt tolerance?" Plant Signal Behav **5**(7).

106 Yokoi, S., F. J. Quintero, et al. (2002). "Differential expression and function of Arabidopsis thaliana NHX Na+/H+ antiporters in the salt stress response." Plant J **30**(5): 529-39.
107 Rodriguez-Rosales, M. P., F. J. Galvez, et al. (2009). "Plant NHX cation/proton antiporters." Plant Signal Behav **4**(4): 265-76.
108 Blumwald, E. (2000). "Sodium transport and salt tolerance in plants." Curr Opin Cell Biol **12**(4): 431-4.
109 Brini, F., M. Hanin, et al. (2007). "Overexpression of wheat Na+/H+ antiporter TNHX1 and H+-pyrophosphatase TVP1 improve salt- and drought-stress tolerance in Arabidopsis thaliana plants." J Exp Bot **58**(2): 301-8.
110 Shi, H., M. Ishitani, et al. (2000). "The Arabidopsis thaliana salt tolerance gene SOS1 encodes a putative Na+/H+ antiporter." Proc Natl Acad Sci U S A **97**(12): 6896-901.
111 Alonso, J. M., A. N. Stepanova, et al. (2003). "Genome-wide insertional mutagenesis of Arabidopsis thaliana." Science **301**(5633): 653-7.
112 Home page for checking A.thaliana T-DNA insertion lines; http://signal.salk.edu/cgi-bin/tdnaexpress
113 Pfister, B. (2010) "Subcellular localization and function of the calcium-dependent protein kinase CPK3 in *Arabidopsis thaliana*" Diploma thesis
114 Heazlewood, J. L., P. Durek, et al. (2008). "PhosPhAt: a database of phosphorylation sites in Arabidopsis thaliana and a plant-specific phosphorylation site predictor." Nucleic Acids Res **36**(Database issue): D1015-21.
115 Durek, P., R. Schmidt, et al. (2010). "PhosPhAt: the Arabidopsis thaliana phosphorylation site database. An update." Nucleic Acids Res **38**(Database issue): D828-34.
116 Jakoby, M., B. Weisshaar, et al. (2002). "bZIP transcription factors in Arabidopsis." Trends Plant Sci **7**(3): 106-11.
117 Baena-Gonzalez, E., F. Rolland, et al. (2007). "A central integrator of transcription networks in plant stress and energy signalling." Nature **448**(7156): 938-42.
118 Latz, A., D. Becker, et al. (2007). "TPK1, a Ca(2+)-regulated Arabidopsis vacuole two-pore K(+) channel is activated by 14-3-3 proteins." Plant J **52**(3): 449-59.
119 Vaughn, K. C. and W. H. Campbell (1988). "Immunogold localization of nitrate reductase in maize leaves." Plant Physiol **88**(4): 1354-7.
120 Petersen, B., T. N. Petersen, et al. (2009). "A generic method for assignment of reliability scores applied to solvent accessibility predictions." BMC Struct Biol **9**: 51.
121 Cole, C., J. D. Barber, et al. (2008). "The Jpred 3 secondary structure prediction server." Nucleic Acids Res **36**(Web Server issue): W197-201.
122 Phytozome v6.0 a joint venture by Joint Genome Institute and the Center for Integrative Genomics (http://www.phytozome.net/)
123 Seiler, M., A. Mehrle, et al. (2006). "The 3of5 web application for complex and comprehensive pattern matching in protein sequences." BMC Bioinformatics **7**: 144.
124 Campbell, W. H. (2001). "Structure and function of eukaryotic NAD(P)H:nitrate reductase." Cell Mol Life Sci **58**(2): 194-204.
125 Kokame, K., Y. Fukada, et al. (1992). "Lipid modification at the N terminus of photoreceptor G-protein alpha-subunit." Nature **359**(6397): 749-52.
126 Hemsley, P. A. and C. S. Grierson (2008). "Multiple roles for protein palmitoylation in plants." Trends Plant Sci **13**(6): 295-302.
127 Resh, M. D. (1996). "Regulation of cellular signalling by fatty acid acylation and prenylation of signal transduction proteins." Cell Signal **8**(6): 403-12.
128 Price, J., A. Laxmi, et al. (2004). "Global transcription profiling reveals multiple sugar signal transduction mechanisms in Arabidopsis." Plant Cell **16**(8): 2128-50.
129 Niefind, K., B. Guerra, et al. (2001). "Crystal structure of human protein kinase CK2: insights into basic properties of the CK2 holoenzyme." Embo J **20**(19): 5320-31.
130 Pinna, L. A. and F. Meggio (1997). "Protein kinase CK2 ("casein kinase-2") and its implication in cell division and proliferation." Prog Cell Cycle Res **3**: 77-97.
131 Ogiso, E., Y. Takahashi, et al. (2010). "The role of casein kinase II in flowering time regulation has diversified during evolution." Plant Physiol **152**(2): 808-20.
132 Portoles, S. and P. Mas (2007). "Altered oscillator function affects clock resonance and is responsible for the reduced day-length sensitivity of CKB4 overexpressing plants." Plant J **51**(6): 966-77.
133 Mizoguchi, T., J. Putterill, et al. (2006). "Kinase and phosphatase: the cog and spring of the circadian clock." Int Rev Cytol **250**: 47-72.
134 Hardie, D. G. (2007). "AMP-activated/SNF1 protein kinases: conserved guardians of cellular energy." Nat Rev Mol Cell Biol **8**(10): 774-85.

135 Polge, C., M. Jossier, et al. (2008). "Beta-subunits of the SnRK1 complexes share a common ancestral function together with expression and function specificities; physical interaction with nitrate reductase specifically occurs via AKINbeta1-subunit." Plant Physiol **148**(3): 1570-82.
136 Bhat, R. A., T. Lahaye, et al. (2006). "The visible touch: in planta visualization of protein-protein interactions by fluorophore-based methods." Plant Methods **2**: 12.
137 Nunes-Nesi, A., A. R. Fernie, et al. (2010). "Metabolic and signaling aspects underpinning the regulation of plant carbon nitrogen interactions." Mol Plant **3**(6): 973-96.
138 Lillo, C. (2008). "Signalling cascades integrating light-enhanced nitrate metabolism." Biochem J **415**(1): 11-9.
139 Scheible, W. R., A. Gonzalez-Fontes, et al. (1997). "Tobacco mutants with a decreased number of functional nia genes compensate by modifying the diurnal regulation of transcription, post-translational modification and turnover of nitrate reductase." Planta **203**(3): 304-19.
140 McMichael, R. W., Jr., M. Bachmann, et al. (1995). "Spinach Leaf Sucrose-Phosphate Synthase and Nitrate Reductase Are Phosphorylated/Inactivated by Multiple Protein Kinases in Vitro." Plant Physiol **108**(3): 1077-1082.
141 Lillo, C., U. S. Lea, et al. (2003). "Mutation of the regulatory phosphorylation site of tobacco nitrate reductase results in constitutive activation of the enzyme in vivo and nitrite accumulation." Plant J **35**(5): 566-73.
142 Ikeda, Y., N. Koizumi, et al. (2000). "Specific binding of a 14-3-3 protein to autophosphorylated WPK4, an SNF1-related wheat protein kinase, and to WPK4-phosphorylated nitrate reductase." J Biol Chem **275**(41): 31695-700.
143 Sugden, C., P. G. Donaghy, et al. (1999). "Two SNF1-related protein kinases from spinach leaf phosphorylate and inactivate 3-hydroxy-3-methylglutaryl-coenzyme A reductase, nitrate reductase, and sucrose phosphate synthase in vitro." Plant Physiol **120**(1): 257-74.
144 Lea, U. S., M. T. Leydecker, et al. (2006). "Posttranslational regulation of nitrate reductase strongly affects the levels of free amino acids and nitrate, whereas transcriptional regulation has only minor influence." Plant Physiol **140**(3): 1085-94.
145 Mueller, C., W. R. Scheible, et al. (2001). "Influence of malate and 2-oxoglutarate on the NIA transcript level and nitrate reductase activity in tobacco leaves." Plant Cell Environ **24**: 191-203.
146 Gutierrez, R. A., M. L. Gifford, et al. (2007). "Insights into the genomic nitrate response using genetics and the Sungear Software System." J Exp Bot **58**(9): 2359-67.
147 Krouk, G., N. M. Crawford, et al. (2010). "Nitrate signaling: adaptation to fluctuating environments." Curr Opin Plant Biol **13**(3): 266-73.
148 Sulpice, R., S. Trenkamp, et al. (2010). "Network analysis of enzyme activities and metabolite levels and their relationship to biomass in a large panel of Arabidopsis accessions." Plant Cell **22**(8): 2872-93.
149 Sanchez, D. H., M. R. Siahpoosh, et al. (2008). "Plant metabolomics reveals conserved and divergent metabolic responses to salinity." Physiol Plant **132**(2): 209-19.
150 Bright, J., R. Desikan, et al. (2006). "ABA-induced NO generation and stomatal closure in Arabidopsis are dependent on H2O2 synthesis." Plant J **45**(1): 113-22.
151 Wang, P., Y. Du, et al. (2010). "Hydrogen peroxide-mediated activation of MAP kinase 6 modulates nitric oxide biosynthesis and signal transduction in Arabidopsis." Plant Cell **22**(9): 2981-98.
152 Libourel, I. G., P. C. Bethke, et al. (2006). "Nitric oxide gas stimulates germination of dormant Arabidopsis seeds: use of a flow-through apparatus for delivery of nitric oxide." Planta **223**(4): 813-20.
153 Lanteri, M. L., G. C. Pagnussat, et al. (2006). "Calcium and calcium-dependent protein kinases are involved in nitric oxide- and auxin-induced adventitious root formation in cucumber." J Exp Bot **57**(6): 1341-51.
152 Lombardo, M. C., M. Graziano, et al. (2006). "Nitric oxide functions as a positive regulator of root hair development." Plant Signal Behav **1**(1): 28-33.
154 Neill, S., R. Barros, et al. (2008). "Nitric oxide, stomatal closure, and abiotic stress." J Exp Bot **59**(2): 165-76.
155 Besson-Bard, A., C. Courtois, et al. (2008). "Nitric oxide in plants: production and cross-talk with Ca2+ signaling." Mol Plant **1**(2): 218-28.
156 Gavaghan, C. L., J. V. Li, et al. (2010). "Application of NMR-based metabolomics to the investigation of salt stress in maize (Zea mays)." Phytochem Anal.
157 Kim, J. K., T. Bamba, et al. (2007). "Time-course metabolic profiling in Arabidopsis thaliana cell cultures after salt stress treatment." J Exp Bot **58**(3): 415-24.

158 Zhu, J. K. (2002). "Salt and drought stress signal transduction in plants." Annu Rev Plant Biol **53**: 247-73.
159 Palenchar, P. M., A. Kouranov, et al. (2004). "Genome-wide patterns of carbon and nitrogen regulation of gene expression validate the combined carbon and nitrogen (CN)-signaling hypothesis in plants." Genome Biol **5**(11): R91.
160 Lamb, C. and R. A. Dixon (1997). "The Oxidative Burst in Plant Disease Resistance." Annu Rev Plant Physiol Plant Mol Biol **48**: 251-275.
161 Knight, H., A. J. Trewavas, et al. (1997). "Calcium signalling in Arabidopsis thaliana responding to drought and salinity." Plant J **12**(5): 1067-78.
162 Saijo, Y., S. Hata, et al. (2000). "Over-expression of a single Ca2+-dependent protein kinase confers both cold and salt/drought tolerance on rice plants." Plant J **23**(3): 319-27.
163 Zimmermann, P., L. Hennig, et al. (2005). "Gene-expression analysis and network discovery using Genevestigator." Trends Plant Sci **10**(9): 407-9.
164 Udvardi, M. K., T. Czechowski, et al. (2008). "Eleven golden rules of quantitative RT-PCR." Plant Cell **20**(7): 1736-7.
165 Fling SP, Gregerson DS (1986) Peptide and protein molecular weight determination by electrophoresis using a high-molarity tris buffer system without urea. Anal Biochem **155:** 83-88
166 Clough, S. J. and A. F. Bent (1998). "Floral dip: a simplified method for Agrobacterium-mediated transformation of Arabidopsis thaliana." Plant J **16**(6): 735-43.
167 Tocquin, P., L. Corbesier, et al. (2003). "A novel high efficiency, low maintenance, hydroponic system for synchronous growth and flowering of Arabidopsis thaliana." BMC Plant Biol **3**: 2.
168 Shaul, Y. and R. Seger (2006). "The detection of MAPK signaling." Curr Protoc Mol Biol **Chapter 18**: Unit 18 12.
169 Keller, A., A. I. Nesvizhskii, et al. (2002). "Empirical statistical model to estimate the accuracy of peptide identifications made by MS/MS and database search." Anal Chem **74**(20): 5383-92.
170 Nesvizhskii, A. I., A. Keller, et al. (2003). "A statistical model for identifying proteins by tandem mass spectrometry." Anal Chem **75**(17): 4646-58.
171 Kopka, J., N. Schauer, et al. (2005). "GMD@CSB.DB: the Golm Metabolome Database." Bioinformatics **21**(8): 1635-8.
172 Ausloos, P., C. L. Clifton, et al. (1999). "The critical evaluation of a comprehensive mass spectral library." J Am Soc Mass Spectrom **10**(4): 287-99.
173 Weckwerth, W., K. Wenzel, et al. (2004). "Process for the integrated extraction, identification and quantification of metabolites, proteins and RNA to reveal their co-regulation in biochemical networks." Proteomics **4**(1): 78-83.

6. Appendix

6.1. Supplementary data

6.1.1. FigureS1

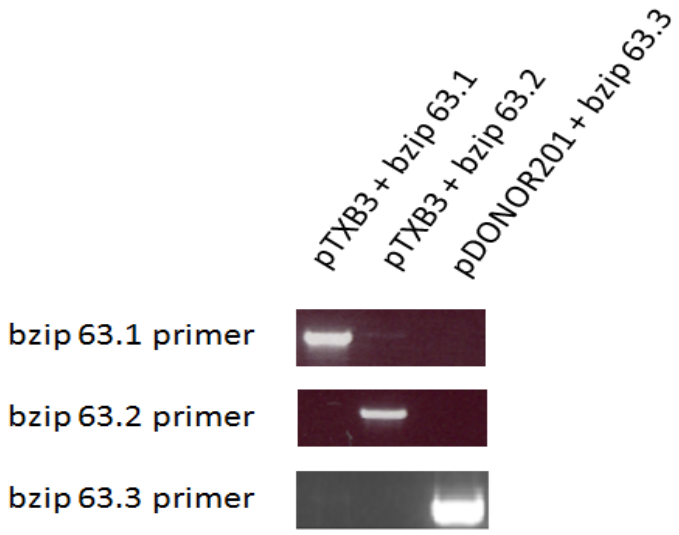

FigS1. Test of primer specificity on different bZIP63 splicing forms. Three different primer pairs were used in a PCR reaction containing equimolar ratios of plasmids each carrying a distinct bZIP63 splicing form.

6.1.2. FigureS2

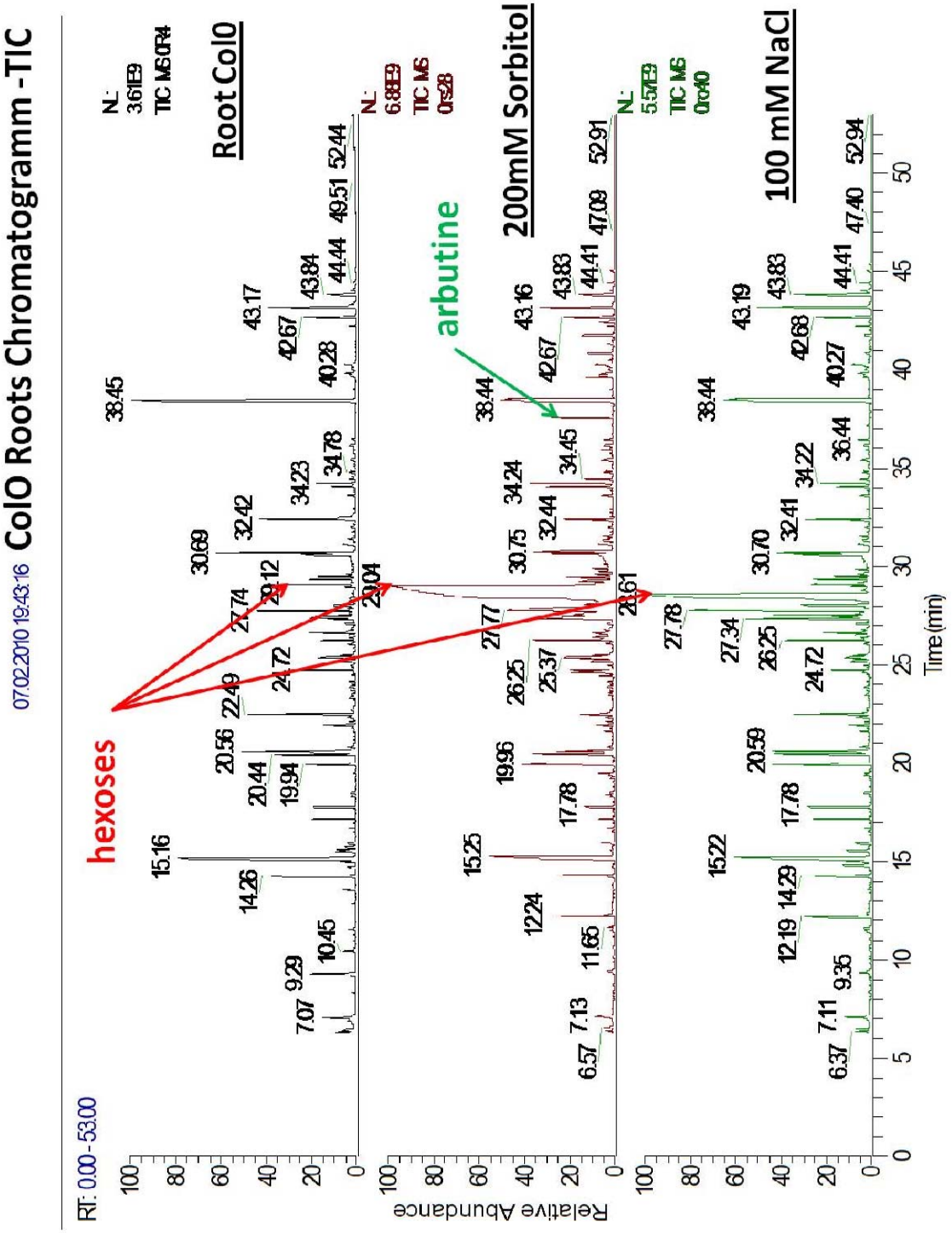

FigS2. GC Chromatograms of Col0 soluble root metabolites extracted from control, NaCl, sorbitol treated plants. Chromatograms represent the total ion counts detected by MS after metabolite separation by GC and ionisation. The peaks of the hexoses are highlighted by red arrows. The peak for arbutin is marked by a green arrow.

6.1.3. FigureS3

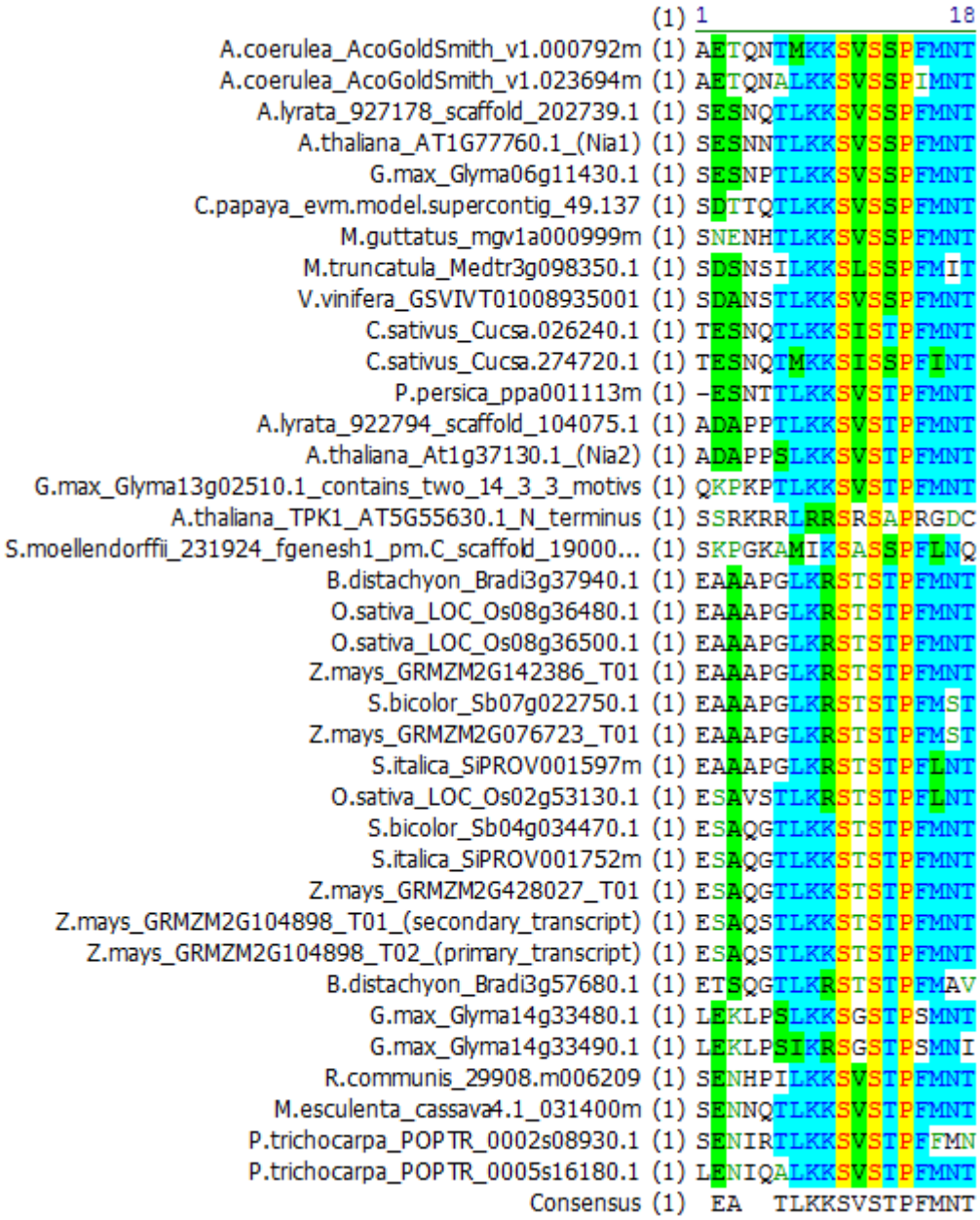

FigS3. Sequence alignment of a conserved stretch around the nitrate reductase 14-3-3 motive. The TPK1 14-3-3 was included as a distantly related sequence. Colour scheme: yellow background, residue is identical in all sequences; cyan background, a conservative residue; green background, a block of similar residues.

6.1.4. FigureS4

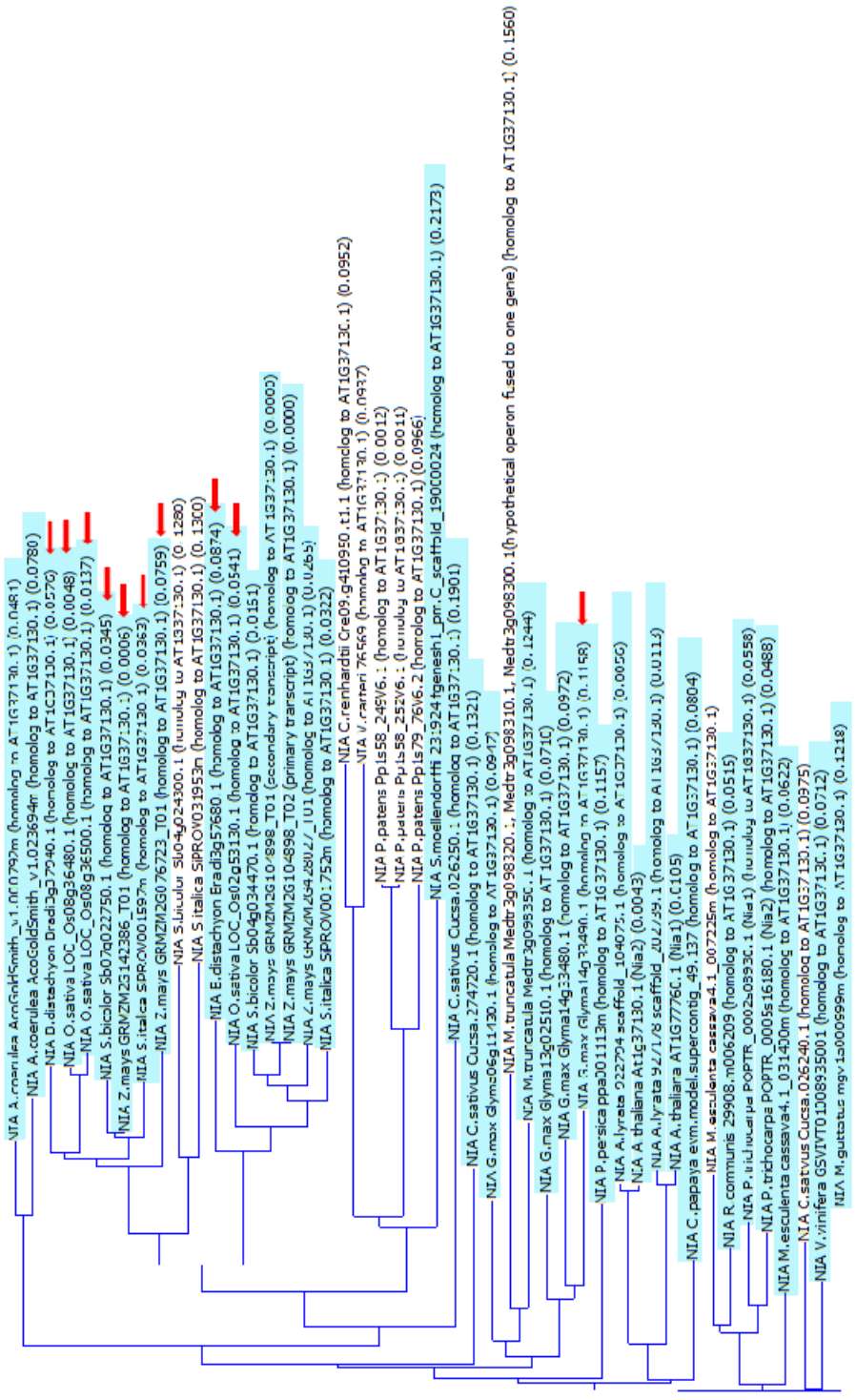

FigS4. unrooted tree obtained after multiple sequnce alignment with clustal W.
Nitrate reductases marked with cyan background contain a 14-3-3 motive. Red arrows indicate an arginine in position -4 instead of an lysine.

6.1.5. ListS1

sf … splicing form
>AT3G50000.1 - CASEIN KINASE II, ALPHA CHAIN 2
MHLIFFFSYFLRRYLLLLCAILILRAPLAHSLIPPLTCVNTGTVESDVTGIRFDRCLDTDSLAKISLSTVMSKARVYTDVNVI
RPKDYWDYESLNVQWGEQDDYEVVRKVGRGKYSEVFEGINMNNNEKCIIKILKPVKKKKIRREIKILQNLCGGPNIVKLLDVV
RDQHSKTPSLIFEYVNSTDFKVLYPTLTDYDIRYYIYELLKALDFCHSQGIMHRDVKPHNVMIDHELRKLRLIDWGLAEFYHP
GKEYNVRVASRYFKGPELLVDLQDYDYSLDMWSLGCMFAGMIFRKEPFFYGHDNQDQLVKIAKVLGTDELNAYLNKYQLELDT
QLEALVGRHSRKPWSKFINADNRHLVSPEAIDYLDKLLRYDHQDRLTAKEAMAHPYFAQVRAAESSRMRTQ
Unique hits

ILQNLCGGPNIVK	Specifc for AT3G50000 AT5G67380 sf 1 and 2 and AT2G23070 sf 1
VLGTDELNAYLNK	Specifc for AT3G50000 AT5G67380 sf 1 and 2 and AT2G23070 sf 1
VYTDVNVIRPK	Specific for gene and splicingform
EAMAHPYFAQVR	Specific for gene and splicingform
HLVSPEAIDYLDK	Specific for gene and splicingform
ALDFCHSQGIMHR	Specifc for AT3G50000; AT5G67380 sf 1,2
DVKPHNVMIDHELR	Specifc for AT3G50000; AT5G67380 sf 1,2
YSEVFEGINMNNNEK	Specific for gene and splicingform

>AT5G67380.1 - casein kinase II catalytic subunit alpha
MIDTLFFLFFLFFDSPLRRLLLLCAVLALRAPTAHSPILRSSIVTPTARAVSEVSGCTTIDPDFLVEISDSNQTRAMSKARVY
TEVNVIRPKDYWDYESLIVQWGEQDDYEVVRKVGRGKYSEVFEGINVNSKEKCIIKILKPVKKKKIRREIKILQNLCGGPNIV
KLLDVVRDQHSKTPSLIFEYVNSTDFKVLYPTLTDYDIRYYIYELLKALDFCHSQGIMHRDVKPHNVMIDHELRKLRLIDWGL
AEFYHPGKEYNVRVASRYFKGPELLVDLQDYDYSLDMWSLGCMFAGMIFRKEPFFYGHDNQDQLVKIAKVLGTDELNAYLNKY
QLELDPQLEALVGRHSRKPWSKFINADNQHLVSPEAIDFLDKLLRYDHQDRLTAKEAMAHAYFAQVRAAETSRMRSQ
Unique hits

ILQNLCGGPNIVK	Specifc for AT3G50000 AT5G67380 sf 1 and 2 and AT2G23070 sf 1
VLGTDELNAYLNK	Specifc for AT3G50000 AT5G67380 sf 1 and 2 and AT2G23070 sf 1
ALDFCHSQGIMHR	Specifc for AT3G50000; AT5G67380 sf 1,2
DVKPHNVMIDHELR	Specifc for AT3G50000; AT5G67380 sf 1,2
VYTEVNVIRPK	Specific for gene
EAMAHAYFAQVR	Specific for gene
YSEVFEGINVNSK	Specific for gene and splicing form
AMSKARVYTEVNVIRPK	Specific for gene

>AT5G67380.2 - casein kinase II catalytic subunit alpha
MIDTLFFLFFLFFDSPLRRLLLLCAVLALRAPTAHSPILRSSIVTPTARAVSEVSGCTTIDPDFLVEISDSNQTRAMSKARVY
TEVNVIRPKDYWDYESLIVQWGEQDDYEVVRKIRREIKILQNLCGGPNIVKLLDVVRDQHSKTPSLIFEYVNSTDFKVLYPTL
TDYDIRYYIYELLKALDFCHSQGIMHRDVKPHNVMIDHELRKLRLIDWGLAEFYHPGKEYNVRVASRYFKGPELLVDLQDYDY
SLDMWSLGCMFAGMIFRKEPFFYGHDNQDQLVKIAKVLGTDELNAYLNKYQLELDPQLEALVGRHSRKPWSKFINADNQHLVS
PEAIDFLDKLLRYDHQDRLTAKEAMAHAYFAQVRAAETSRMRSQ
Unique hits

ILQNLCGGPNIVK	Specifc for AT3G50000 AT5G67380 sf 1 and 2 and AT2G23070 sf 1
VLGTDELNAYLNK	Specifc for AT3G50000 AT5G67380 sf 1 and 2 and AT2G23070 sf 1
ALDFCHSQGIMHR	Specifc for AT3G50000; AT5G67380 sf 1,2
DVKPHNVMIDHELR	Specifc for AT3G50000; AT5G67380 sf 1,2
VYTEVNVIRPK	Specific for gene
EAMAHAYFAQVR	Specific for gene
AMSKARVYTEVNVIRPK	Specific for gene

>AT5G47080.1 - CASEIN KINASE II BETA SUBUNIT CKB1
MYRDRGTVNSRPEVVDRKRINDALERPSPSTSRQVNGKGKGTVTAATTTANLIGKQQSNNINHRDSRSASLSKNNTVSDDESD
TDSEESDVSGSDGEDTSWISWFCNLRGNEFFCEVDDDYIQDDFNLCGLSSLVPYYEYALDLILDVESSQGEMFTEEQNELIES
AAEMLYGLIHARYILTSKGLAAMLDKYKNYDFGRCPRVYCCGQPCLPVGQSDLPRSSTVKIYCPKCEDIYYPRSKYQGNIDGA
YFGTTFPHLFLMTYGHLKPAKATQNYVQRVFGFKLHKP
Unique hits

CEDIYYPR	Specifc for gene
GTVTAATTTANLIGK	Specifc for gene
INDALERPSPSTSR	Specifc for gene
GKGTVTAATTTANLIGK	Specifc for gene

ATQNYVQR	Specifc for gene and splicingform
QVNGKGKGTVTAATTTANLIGK	Specifc for gene

>AT5G47080.2 - CASEIN KINASE II BETA SUBUNIT CKB1
MYRDRGTVNSRPEVVDRKRINDALERPSPSTSRQVNGKGKGTVTAATTTANLIGKQQSNNINHRDSRSASLSKNNTVSDDESD
TDSEESDVSGSDGEDTSWISWFCNLRGNEFFCEVDDDYIQDDFNLCGLSSLVPYYEYALDLILDVESSQGEMFTEEQNELIES
AAEMLYGLIHARYILTSKGLAAMLDKYKNYDFGRCPRVYCCGQPCLPVGQSDLPRSSTVKIYCPKCEDIYYPRSKYQGSILFS
TVSLLLI
Unique hits

CEDIYYPR	Specifc for gene
GTVTAATTTANLIGK	Specifc for gene
INDALERPSPSTSR	Specifc for gene
GKGTVTAATTTANLIGK	Specifc for gene
QVNGKGKGTVTAATTTANLIGK	Specifc for gene

>AT5G47080.3 - CASEIN KINASE II BETA SUBUNIT CKB1
MYRDRGTVNSRPEVVDRKRINDALERPSPSTSRQVNGKGKGTVTAATTTANLIGKQQSNNINHRDSRSASLSKNNTVSDDTDS
EESDVSGSDGEDTSWISWFCNLRGNEFFCEVDDDYIQDDFNLCGLSSLVPYYEYALDLILDVESSQGEMFTEEQNELIESAAE
MLYGLIHARYILTSKGLAAMLDKYKNYDFGRCPRVYCCGQPCLPVGQSDLPRSSTVKIYCPKCEDIYYPRSKYQGSILFSTVS
LLLI
Unique hits

CEDIYYPR	Specifc for gene
GTVTAATTTANLIGK	Specifc for gene
INDALERPSPSTSR	Specifc for gene
GKGTVTAATTTANLIGK	Specifc for gene
QVNGKGKGTVTAATTTANLIGK	Specifc for gene

>AT2G23070.1 - casein kinase II alpha chain, putative;
MALRPCTGFTISSLRNASAANNNLFSLLSFSSSSPAKRNLLLSSLQDNLRRFASSASLYRQHLRNQQQQHQQQQQSRVKEKSE
TLAQKIGKSIRRAGAPSKARVYADVNVVRPKDYWDYESLAVQWGVQDDYEVVRKVGRGKYSEVFEGIHATDNEKCVIKILKPV
KKKKIKREIKILQNLCGGPNIVKLLDIVRDQQSKTPSLIFEHVNNKDFKVLYPTLSDYDVRYYIFELLKALDFCHSRGIMHRD
VKPHNVMIDHEQRKLRLIDWGLAEFYHPGKEYNVRVASRYFKGPELLVDLQDYDYSLDLWSLGCMFAGMIFRKEPFFYGHDNY
DQLVKIAKVLGTDELNAYLNKYRIELDPNLTSLVGRHSRKPWTKFINSENQHLAVPEAVDFVDKLLRYDHQERPTAKEAMAHP
YFYPIRNAESSRTPRSQ
Unique hits

ILQNLCGGPNIVK	Specifc for AT3G50000 AT5G67380 sf 1 and 2 and AT2G23070 sf 1
VLGTDELNAYLNK	Specifc for AT3G50000 AT5G67380 sf 1 and 2 and AT2G23070 sf 1
VYADVNVVRPK	Specific for gene and splicingform
TPSLIFEHVNNK	Specific for gene and splicingform

>AT1G72710.1 - CKL2 CASEIN KINASE 1-LIKE PROTEIN 2
MEPRVGNKFRLGRKIGGGSFGEIYLGTNIQTNEEVAIKLENVKTKHPQLLYESKLYKVLQGGTGVPNVKWYGVEGDYNVLVID
LLGPSLEDLFNFCSRKLSLKTVLMLADQMINRIEFVHQKSFLHRDIKPDNFLMGLGRRANQVYVIDFGLAKKYRDSNHQHIPY
RENKNLTGTARYASMNTHLGIEQSRRDDLESLGFVLMYFLKGSLPWQGLKAGNKKQKYEKISEKKVSTSIEALCRGYPSEFAS
YFHYCRSLRFDDKPDYAYLKRLFRDLFIREGFQFDYVFDWTILKYQQSQISTPPPRHHGPVVGPSSALPPAITSAERPSGGDE
ARPSGWSSGIPRRNSGQIFNSGSLAKQKAPVSSDPAISKDVVLSSSSFLRATGSSRRAAVSSSREAAVLGTDSEPSNPQIVEA
GSGSNSKIPVSRNSPIVSSEINKLSSPSRATTSVMKNYEANLKGIESLHF
Unique hits

IEFVHQK	Specifc for gene and splicing-form
APVSSDPAISK	Specifc for gene and splicing-form
HPQLLYESK	Specifc for gene and splicing-form
VSTSIEALCR	Specifc for gene and splicing-form
VLQGGTGVPNVK	Specifc for gene and splicing-form
NSPIVSSEINK	Specifc for gene and splicing-form
DVVLSSSSFLR	Specifc for gene and splicing-form
NSGQIFNSGSLAK	Specifc for gene and splicing-form
QKAPVSSDPAISK	Specifc for gene and splicing-form
TKHPQLLYESK	Specifc for gene and splicing-form
FDDKPDYAYLK	Specifc for gene and splicing-form
YQQSQISTPPPR	Specifc for gene and splicing-form
TVLMLADQMINR	Specifc for gene and splicing-form
ANQVYVIDFGLAK	Specifc for gene and splicing-form
DIKPDNFLMGLGR	Specifc for gene and splicing-form
RANQVYVIDFGLAK	Specifc for gene and splicing-form

YASMNTHLGIEQSR	Specifc for gene and splicing-form
EAAVLGTDSEPSNPQIVEAGSGSNSK	Specifc for gene and splicing-form

>AT3G29160.1 - AKIN11 Arabidopsis SNF1 kinase homolog 11
MDHSSNRFGNNGVESILPNYKLGKTLGIGSFGKVKIAEHVVTGHKVAIKILNRRKIKNMEMEEKVRREIKILRLFMHPHIIRQ
YEVIETTSDIYVVMEYVKSGELFDYIVEKGRLQEDEARNFFQQIISGVEYCHRNMVVHRDLKPENLLLDSRCNIKIADFGLSN
VMRDGHFLKTSCGSPNYAAPEVISGKLYAGPEVDVWSCGVILYALLCGTLPFDDENIPNLFKKIKGGIYTLPSHLSSEARDLI
PRMLIVDPVKRITIPEIRQHRWFQTHLPRYLAVSPPDTVEQAKKINEEIVQEVVNMGFDRNQVLESLRNRTQNDATVTYYLLL
DNRFRVPSGYLESEFQETTDSGSNPMRTPEAGASPVGHWIPAHVDHYGLGARSQVPVDRKWALGLQSHAHPREIMNEVLKALQ
ELNVCWKKIGHYNMKCRWVPGLADGQNTMVNNQLHFRDESSIIEDDCAMTSPTVIKFELQLYKAREEKYLLDIQRVNGPQFLF
LDLCAAFLTELRVI
Unique hits

YLLDIQR	Specifc for gene and sf 1,2
WFQTHLPR	Specifc for gene
IAEHVVTGHK	Specifc for gene
LFMHPHIIR	Specific for AKIN10 and 11
IADFGLSNVMR	Specifc for gene
SGELFDYIVEK	Specific for AKIN10 and 11
DLKPENLLLDSR	Specifc for gene
YLAVSPPDTVEQAK	Specifc for gene
FGNNGVESILPNYK	Specifc for gene
GGIYTLPSHLSSEAR	Specifc for gene
NQVLESLR	Specifc for gene
MLIVDPVKR	Specifc for gene
FELQLYK	Specifc for gene and sf 1,2
KIGHYNMK	AKIN10 sf 1,2,3 and AKIN 11 sf 1,2
ALQELNVCWK	Specifc for gene and sf 1,2

>AT3G29160.2 - AKIN11 Arabidopsis SNF1 kinase homolog 11
MDHSSNRFGNNGVESILPNYKLGKTLGIGSFGKVKIAEHVVTGHKVAIKILNRRKIKNMEMEEKVRREIKILRLFMHPHIIRQ
YEVIETTSDIYVVMEYVKSGELFDYIVEKGRLQEDEARNFFQQIISGVEYCHRNMVVHRDLKPENLLLDSRCNIKIADFGLSN
VMRDGHFLKTSCGSPNYAAPEVISGKLYAGPEVDVWSCGVILYALLCGTLPFDDENIPNLFKKIKGGIYTLPSHLSSEARDLI
PRMLIVDPVKRITIPEIRQHRWFQTHLPRYLAVSPPDTVEQAKKINEEIVQEVVNMGFDRNQVLESLRNRTQNDATVTYYLLL
DNRFRVPSGYLESEFQETTDSGSNPMRTPEAGASPVGHWIPAHVDHYGLGARSQVPVDRKWALGLQSHAHPREIMNEVLKALQ
ELNVCWKKIGHYNMKCRWVPGLADGQNTMVNNQLHFRDESSIIEDDCAMTSPTVIKFELQLYKAREEKYLLDIQRVNGPQFLF
LDLCAAFLTELRVI
Unique hits

YLLDIQR	Specifc for gene and sf 1,2
WFQTHLPR	Specifc for gene
IAEHVVTGHK	Specifc for gene
LFMHPHIIR	Specific for AKIN10 and 11
IADFGLSNVMR	Specifc for gene
SGELFDYIVEK	Specific for AKIN10 and 11
DLKPENLLLDSR	Specifc for gene
YLAVSPPDTVEQAK	Specifc for gene
FGNNGVESILPNYK	Specifc for gene
GGIYTLPSHLSSEAR	Specifc for gene
NQVLESLR	Specifc for gene
MLIVDPVKR	Specifc for gene
FELQLYK	Specifc for gene and sf 1,2
KIGHYNMK	AKIN10 sf 1,2,3 and AKIN 11 sf 1,2
ALQELNVCWK	Specifc for gene and sf 1,2

>AT3G29160.3 - AKIN11 Arabidopsis SNF1 kinase homolog 11
MDHSSNRFGNNGVESILPNYKLGKTLGIGSFGKVKIAEHVVTGHKVAIKILNRRKIKNMEMEEKVRREIKILRLFMHPHIIRQ
YEVIETTSDIYVVMEYVKSGELFDYIVEKGRLQEDEARNFFQQIISGVEYCHRNMVVHRDLKPENLLLDSRCNIKIADFGLSN
VMRDGHFLKTSCGSPNYAAPEVISGKLYAGPEVDVWSCGVILYALLCGTLPFDDENIPNLFKKIKGGIYTLPSHLSSEARDLI
PRMLIVDPVKRITIPEIRQHRWFQTHLPRYLAVSPPDTVEQAKKINEEIVQEVVNMGFDRNQVLESLRNRTQNDATVTYYLLL
DNRFRVPSGYLESEFQETTWFQSYAHT
Unique hits

WFQTHLPR	Specifc for gene
IAEHVVTGHK	Specifc for gene
LFMHPHIIR	Specific for AKIN10 and 11
IADFGLSNVMR	Specifc for gene
SGELFDYIVEK	Specific for AKIN10 and 11
DLKPENLLLDSR	Specifc for gene

YLAVSPPDTVEQAK	Specifc for gene
FGNNGVESILPNYK	Specifc for gene
GGIYTLPSHLSSEAR	Specifc for gene
NQVLESLR	Specifc for gene
MLIVDPVKR	Specifc for gene

>AT3G01090.1 – AKIN10
MDGSGTGSRSGVESILPNYKLGRTLGIGSFGRVKIAEHALTGHKVAIKILNRRKIKNMEMEEKVRREIKILRLFMHPHIIRLY
EVIETPTDIYLVMEYVNSGELFDYIVEKGRLQEDEARNFFQQIISGVEYCHRNMVVHRDLKPENLLLDSKCNVKIADFGLSNI
MRDGHFLKTSCGSPNYAAPEVISGKLYAGPEVDVWSCGVILYALLCGTLPFDDENIPNLFKKIKGGIYTLPSHLSPGARDLIP
RMLVVDPMKRVTIPEIRQHPWFQAHLPRYLAVPPPDTVQQAKKIDEEILQEVINMGFDRNHLIESLRNRTQNDGTVTYYLILD
NRFRASSGYLGAEFQETMEGTPRMHPAESVASPVSHRLPGLMEYQGVGLRSQYPVERKWALGLQSRAHPREIMTEVLKALQDL
NVCWKKIGHYNMKCRWVPNSSADGMLSNSMHDNNYFGDESSIIENEAAVKSPNVVKFEIQLYKTRDDKYLLDLQRVQGPQFLF
LDLCAAFLAQLRVL
Unique hits

LFMHPHIIR	Specific for AKIN10 and 11
SGELFDYIVEK	Specific for AKIN10 and 11
YLLDLQR	Specific for gene
IAEHALTGHK	Specific for gene
IADFGLSNIMR	Specific for gene
LPGLMEYQGVGLR	Specific for gene
GGIYTLPSHLSPGAR	Specific for gene
FEIQLYK	Specific for gene
ALQDLNVCWK	Specific for gene
DDKYLLDLQR	Specific for gene
MHPAESVASPVSHR	Specific for gene
IKGGIYTLPSHLSPGAR	Specific for gene
TQNDGTVTYYLILDNR	Specific for gene
DLKPENLLLDSK	Specific for gene
TLGIGSFGR	Specific for gene
KIGHYNMK	AKIN10 sf 1,2,3 and AKIN 11 sf 1,2
SGVESILPNYK	Specific for gene

>AT3G01090.2 – AKIN10
MFKRVDEFNLVSSTIDHRIFKSRMDGSGTGSRSGVESILPNYKLGRTLGIGSFGRVKIAEHALTGHKVAIKILNRRKIKNMEM
EEKVRREIKILRLFMHPHIIRLYEVIETPTDIYLVMEYVNSGELFDYIVEKGRLQEDEARNFFQQIISGVEYCHRNMVVHRDL
KPENLLLDSKCNVKIADFGLSNIMRDGHFLKTSCGSPNYAAPEVISGKLYAGPEVDVWSCGVILYALLCGTLPFDDENIPNLF
KKIKGGIYTLPSHLSPGARDLIPRMLVVDPMKRVTIPEIRQHPWFQAHLPRYLAVPPPDTVQQAKKIDEEILQEVINMGFDRN
HLIESLRNRTQNDGTVTYYLILDNRFRASSGYLGAEFQETMEGTPRMHPAESVASPVSHRLPGLMEYQGVGLRSQYPVERKWA
LGLQSRAHPREIMTEVLKALQDLNVCWKKIGHYNMKCRWVPNSSADGMLSNSMHDNNYFGDESSIIENEAAVKSPNVVKFEIQ
LYKTRDDKYLLDLQRVQGPQFLFLDLCAAFLAQLRVL
Unique hits

LFMHPHIIR	Specific for AKIN10 and 11
SGELFDYIVEK	Specific for AKIN10 and 11
YLLDLQR	Specific for gene
IAEHALTGHK	Specific for gene
IADFGLSNIMR	Specific for gene
LPGLMEYQGVGLR	Specific for gene
GGIYTLPSHLSPGAR	Specific for gene
FEIQLYK	Specific for gene
ALQDLNVCWK	Specific for gene
DDKYLLDLQR	Specific for gene
MHPAESVASPVSHR	Specific for gene
IKGGIYTLPSHLSPGAR	Specific for gene
TQNDGTVTYYLILDNR	Specific for gene
DLKPENLLLDSK	Specific for gene
TLGIGSFGR	Specific for gene
KIGHYNMK	AKIN10 sf 1,2,3 and AKIN 11 sf 1,2
SGVESILPNYK	Specific for gene

>AT3G01090.3 – AKIN10
MDGSGTGSRSGVESILPNYKLGRTLGIGSFGRVKIAEHALTGHKVAIKILNRRKIKNMEMEEKVRREIKILRLFMHPHIIRLY
EVIETPTDIYLVMEYVNSGELFDYIVEKGRLQEDEARNFFQQIISGVEYCHRNMVVHRDLKPENLLLDSKCNVKIADFGLSNI
MRDGHFLKTSCGSPNYAAPEVISGKLYAGPEVDVWSCGVILYALLCGTLPFDDENIPNLFKKIKGGIYTLPSHLSPGARDLIP
RMLVVDPMKRVTIPEIRQHPWFQAHLPRYLAVPPPDTVQQAKKIDEEILQEVINMGFDRNHLIESLRNRTQNDGTVTYYLILD
NRFRASSGYLGAEFQETMEGTPRMHPAESVASPVSHRLPGLMEYQGVGLRSQYPVERKWALGLQSRAHPREIMTEVLKALQDL

NVCWKKIGHYNMKCRWVPNSSADGMLSNSMHDNNYFGDESSIIENEAAVKSPNVVKFEIQLYKTRDDKYLLDLQRVQGPQFLF
LDLCAAFLAQLRVL
Unique hits

LFMHPHIIR	Specific for AKIN10 and 11
SGELFDYIVEK	Specific for AKIN10 and 11
YLLDLQR	Specific for gene
IAEHALTGHK	Specific for gene
IADFGLSNIMR	Specific for gene
LPGLMEYQGVGLR	Specific for gene
GGIYTLPSHLSPGAR	Specific for gene
FEIQLYK	Specific for gene
ALQDLNVCWK	Specific for gene
DDKYLLDLQR	Specific for gene
MHPAESVASPVSHR	Specific for gene
IKGGIYTLPSHLSPGAR	Specific for gene
TQNDGTVTYYLILDNR	Specific for gene
DLKPENLLLDSK	Specific for gene
TLGIGSFGR	Specific for gene
KIGHYNMK	AKIN10 sf 1,2,3 and AKIN 11 sf 1,2
SGVESILPNYK	Specific for gene

>AT1G09020.1 - SNF4 (Sucrose NonFermenting 4)
MFGSTLDSSRGNSAASGQLLTPTRFVWPYGGRRVFLSGSFTRWTEHVPMSPLEGCPTVFQVICNLTPGYHQYKFFVDGEWRHD
EHQPFVSGNGGVVNTIFITGPDMVPAGFSPETLGRSNMDVDDVFLRTADPSQEAVPRMSGVDLELSRHRISVLLSTRTAYELL
PESGKVIALDVNLPVKQAFHILYEQGIPLAPLWDFGKGQFVGVLGPLDFILILRELGTHGSNLTEEELETHTIAAWKEGKAHI
SRQYDGSGRPYPRPLVQVGPYDNLKDVALKILQNKVAAVPVIYSSLQDGSYPQLLHLASLSGILKCICRYFRHSSSSLPILQQ
PICSIPLGTWVPRIGESSSKPLATLRPHASLGSALALLVQAEVSSIPVVDDNDSLIDIYSRSDITALAKDKAYAQIHLDDMTV
HQALQLGQDASPPYGIFNGQRCHMCLRSDSLVKVMERLANPGVRRLVIVEAGSKRVEGIISLSDVFQFLLGL
Unique hits

VFLSGSFTR	Specifc for gene and splicing-form
RLVIVEAGSK	Specifc for gene and splicing-form
MSGVDLELSR	Specifc for gene and splicing-form
VIALDVNLPVK	Specifc for gene and splicing-form
TAYELLPESGK	Specifc for gene and splicing-form
SNMDVDDVFLR	Specifc for gene and splicing-form
GNSAASGQLLTPTR	Specifc for gene and splicing-form
RVFLSGSFTR	Specifc for gene and splicing-form
TADPSQEAVPR	Specifc for gene and splicing-form

6.2.1. Summary of thesis in English

In order to successfully grow, plants have to adapt to their continuously changing environment. Many of these environmental stimuli like salt and drought stress or pathogen attack, lead to distinct Ca^{2+} signals in the plant cell. So called "Ca^{2+} sensors" are then involved in translating these Ca^{2+} signals into a physiological response by either directly or indirectly changing the transcriptional state of the cell, or regulating enzymes on a post translational level. CPKs (calcium dependent protein kinases), which were found to be present in plants and some protozoa only, are one versatile group of Ca^{2+} activated protein kinases acting as Ca^{2+} sensors. Through reverse genetic experiments CPKs were found to be involved in abiotic as well as in biotic stress signalling. However, at the time starting this thesis, little was known about specific substrates for CPKs and the physiological consequences of regulation of these substrates by CPKs.

The aim of this thesis was to determine a physiological function of *At*CPK3 and identify specific substrates of *At*CPK3 in *A.thaliana*.

In screens, testing *cpk3* knock out, *cpk3* over expresser and *wild type* plants under different growth conditions, a positive correlation between CPK3 protein amount and the germination rate of the respective seeds was observed, indicating that CPK3 is involved in acclimation to salt stress.

In different unbiased approaches, like *in vivo* cross-linking or kinase assays on total membrane fractions, targets of CPK3 were identified. In parallel potential targets of CPK3, which had been identified earlier in *in vitro* assays, were tested for specificity in *in vivo* interaction assays. For TPK1, a vacuolar K^+ channel, specific interaction with CPK3 via two positively charged arginines adjacent to the regulatory 14-3-3 consensus site of TPK1 was determined in quantitative BIFC assays. In biochemical fractionation assays, a fraction of endogenous CPK3 was found to localize at the vacuolar membrane. Similar phenotypes between *tpk1* and *cpk3* mutant lines were observed in germination assays under salt stress. Together with the observation that binding of 14-3-3 proteins to the phosphorylated 14-3-3 consensus sequence of TPK1 activates the K^+ channel (Dirk Becker, University of Würzburg), these data indicate a role of CPK3 in regulating the cellular ion homeostasis, which can, explain the role of CPK3 in salt stress acclimation.

Furthermore CPK3 was demonstrated to specifically interact with nitrate reductase, in a similar way as with TPK1. The two positively charged lysines adjacent to the regulatory 14-3-3 site of nitrate reductase were found to stabilise the interaction between CPK3 and nitrate reductase. Comparison of nitrate reductase sequences revealed that regulation of nitrate reductase by 14-3-3 proteins binding to phosphorylated 14-3-3 consensus sequences seems to be restricted to vascular plants.

In addition, the protein kinases AKIN10/11 and CK2 (casein kinase 2) were identified as the kinases phosphorylating the transcription factor *At*bZIP63 in a novel approach combining in-gel kinase assays with mass spectrometry for protein identification. Interaction between the kinases and *At*bZIP63 was furthermore confirmed in vivo, using BIFC and yeast two hybrid assays.

6.2.2. Zusammenfassung der Dissertation in Deutsch

Pflanzen müssen sich an ständig ändernde Umweltverhältnisse anpassen um erfolgreich wachsen zu können. Viele Umwelteinflüsse wie zum Beispiel Salzstress, Trockenstress oder durch Pathogene hervorgerufener Stress führen zu spezifischen Änderungen in der intrazellulären Konzentration freier Ca^{2+} Ionen. Verschiedene "Kalziumsensoren" dekodieren diese Kalziumsignale entweder durch post-translationale Modifikation von Enzymen oder führen zur Änderung des Transkriptionsmusters der einzelnen Pflanzenzellen, was schließlich eine physiologische Anpassung der ganzen Pflanze an die geänderten Umweltbedingungen zur Folge hat. Kalzium abhängige Proteinkinasen (CPKs) sind eine Gruppe von Proteinkinasen die durch Bindung von Ca^{2+} Ionen aktiviert werden. Die bisherigen Daten aus Genomsequenzierungen legen nahe, dass CPKs nur in Genomen von Pflanzen und einigen Protozoen kodiert sind. Für einzelne CPKs konnte durch reverse Genetik eine Rolle in der abiotischen oder in der biotischen Stressantwort nachgewiesen werden. Zum Beginn dieser Dissertation war jedoch wenig über spezifische Substrate und die Regulation jener durch CPKs bekannt.
Ziel dieser Arbeit war es *A.thaliana* CPK3 eine physiologische Funktion zuzuordnen und etwaige Substrate von *At*CPK3 zu identifizieren.
Verschiedene *cpk3* knock out, Überexpressor und wild Typ Allele wurden unter unterschiedlichen Wachstumsbedingungen getestet. Es wurde beobachtet dass die CPK3 Proteinkonzentration positiv mit der Keimungsrate von *A.thaliana* Samen unter Salzstressbedingungen korreliert was zur Annahme führte, dass CPK3 eine Rolle in der Akklimatisierung von *A.thaliana* an Salzstress zu tun hat.
In Experimenten, wie zum Beispiel *in vivo* Crosslinking und Kinase Essays mit rekombinanter CPK3 und mikrosomalen Membranfraktionen wurden "global" Substrate von CPK3 identifiziert. Parallel dazu wurden potentielle Substrate von CPK3 die zuvor in *in vitro* Experimenten identifiziert wurden auch in *in vivo* Interaktionsessays getestet. Des Weiteren konnte gezeigt mit Hilfe von BIFC werden, dass TPK1, ein vakuolärer Kalium Kanal, spezifisch mit CPK3 *in vivo* interagiert, und das für die Interaktion zwei positiv geladene Arginine neben der regulatorischen 14-3-3 Konsensussequenz von TPK1 wichtig sind. Biochemische Fraktionierung der subzellulären Kompartimente einer Pflanzenzelle und der anschließende Nachweis von CPK3 ergab, dass ein Teil des CPK3 Proteins in Blättern an der vakuolären Membrane assoziiert ist. Zusätzlich verhielten sich die entsprechenden *cpk3* und *tpk1* Mutanten in Keimungsessays unter Salzstress ähnlich. Berücksichtigt man außerdem, dass die Bindung von 14-3-3 Proteinen an die phosphorylierte 14-3-3 Konsensussequenz von TPK1 zu einer Aktivierung des Kaliumkanals führt (Dirk Becker, Universität Würzburg), erlauben es die Daten ein Model zu erstellen, welches die Rolle von CPK3 in der Akklimatisierung an Salzstress durch Regulation der intrazellulären Ionenhomöostase beschreibt.
Außerdem konnte gezeigt werden, dass CPK3 spezifisch mit der Nitratreduktase aus A.thaliana interagiert. Ähnlich wie im Fall der Interaktion zwischen CPK3 und TPK1, stabilisieren auch zwei positiv geladene Lysine die Interaktion zwischen CPK3 und TPK1. Ein Vergleich aller Nitratreduktasesequenzen in 22 unterschiedlichen Pflanzenspezies ergab dass 14-3-3 Konsensussequenzen, welche zur posttraslationalen Regulation durch 14-3-3 Proteine nötig sind, nur in Nitratreduktasesequenzen der Gefäß pflanzen vorhanden sind.
Zusätzlich wurden noch in einem neuen Ansatz, welcher In-gel Kinaseessays mit Massenspektrometrie zur Identifikation von Proteinen verbindet, die Proteinkinase AKIN10/11 und CK2 (Casein Kinase 2) als Interaktionspartner des Transkriptionsfaktors *At*bZIP63 identifiziert werden. Diese Interaktionen konnten ebenfalls *in vivo* in BIFC-Essays bestätigt werden.

6.3. Curriculum Vitae

personal information

name	Bernhard Wurzinger
date of birth	30. March 1981
place of birth	Klosterneuburg, Austria

education

2007 - 2011	doctoral thesis "The role of Ca^{2+} Dependent Protein Kinase 3 in *Arabidopsis thaliana* during salt stress acclimation" at the University of Vienna, department of Biochemistry under supervision of Prof. Markus Teige
2005 - 2006	master thesis "Respiratory Terminal Oxidases In Filamentous Cyanobacteria" at the University of Vienna, depratment of physical chemistry under supervision of Prof. Georg Schmetterer
2001 - 2006	studies of biology with emphasis on molecular genetics and microbiology at the University of Vienna
1995 - 2000	commercial college (HAK Tulln)

professional activities

2009 - 2011	lectureship for the student practical course "Biochemisches Praktikum für Chemiker“
2005 - 2006	tutorship for the student practical course "Molekularbiologie der Cyanobakterien"

6.4. List of publications

Wurzinger, B.,A. Mair, et al. (2011). "Cross-talk of calcium-dependent protein . kinase and MAP kinase signalling." Plant Signal Behav.

Mehlmer, N., B. Wurzinger, et al. (2010). "The Ca(2+)-dependent protein kinase CPK3 is required for MAPK-independent salt-stress acclimation in Arabidopsis." Plant J.

Latz, A., Mehlmer, N., Müller, T., Zapf, S., Csaszar, E., Hedrich, R., Teige, M., Becker, D. "Salt stress triggers CDPK dependent phosphorylation of the Arabidopsis vacuolar K^+ channel TPK1." Plant Cell (In revision; The author list will include my name after revision)

6.5. Acknowledgements

Many thanks to the Supervisor of this thesis, Markus Teige who made it possible for me to work on an interesting topic using a broad range of molecular and genetics techniques. He was very helpful at any stage of this work and offered me excellent working conditions in his laboratory.

Also many, many thanks go to my colleagues Barbara, Andrea, Roman, Simon, Norbert, Prabha, Karolin, Andrea, Konstantin, Gudrun, Helga, Sylvia who were always good and helping company throughout the stay in Markus Teiges laboratory, making the laboratory an enjoyable spot.

Exceptional thanks go to Erna and Harald, who did a marvellous job in minimizing bureaucracy to an enjoyable (non-existing) level when it came to legal contracts and logistics, which allowed to fully concentrate on the experimental work.

Further thanks go to the cooperation partners; Lena Fragner and Wolfram Weckwerth who worked wonders on the GC MS system when it came to metabolite analysis; Dorothea Anrather, Edina Csaszar, Sonja Frosch and Rainer Gith who helped in obtaining and interpreting MS data on proteins; Günther Schwarz und Katrin Schrader (former Fischer) for expressing nitrate reductase.

Die Hand voller Asse, doch die Welt spielt Schach
(unknown, for all who sometimes feel unlucky)